THESIS APPROVAL

GRADUATE SCHOOL, KASETSART UNIVERSITY

Master of Engineering (Environmental Engineering)

DEGREE

Environmental Engineering	Environmental Engineering
FIELD	**DEPARTMENT**

TITLE: Formulation of Flood Routing Model Using Finite Element Method with Application to the Upper Ping River Basin

NAME: Miss Atchara Komsai

THIS THESIS HAS BEEN ACCEPTED BY

.... **THESIS ADVISOR**

(Associate Professor Winai Liengcharernsit, D.Eng.)

.... **THESIS CO-ADVISOR**

(Miss Pathchraporn Ittisukananth, D.Eng.)

.... **DEPARTMENT HEAD**

(Associate Professor Chart Chiemchaisri, D.Eng.)

APPROVED BY THE GRADUATE SCHOOL ON ....

.... **DEAN**

(Associate Professor Gunjana Theeragool, D.Agr.)

THESIS

FORMULATION OF FLOOD ROUTING MODEL USING FINITE ELEMENT METHOD WITH APPLICATION TO THE UPPER PING RIVER BASIN

ATCHARA KOMSAI

A Thesis Submitted in Partial Fulfillment of
the Requirements for the Degree of
Master of Engineering (Environmental Engineering)
Graduate School, Kasetsart University
2012

Atchara Komsai 2012: Formulation of Flood Routing Model Using Finite Element Method with Application to the Upper Ping River Basin. Master of Engineering (Environmental Engineering), Major Field: Environmental Engineering, Department of Environmental Engineering. Thesis Advisor: Associate Professor Winai Liengcharernsit, D.Eng. 142 pages

This study is aimed at formulating the flood routing in the Upper Ping river basin, Northern Thailand. Several models are developed including overland flow model, kinematic stream flow model, detention basin model, and hydraulic model. The finite element method is used in model development. These models are applied to various parts of the Upper Ping river basin, depending on the hydrologic features of the stream/water body. The model simulation was conducted by computing flood hydrograph in July – September 2010, during which rainfall with high intensity occurred in the upstream sub-basins. Water levels and stream flow rates in various sections of the main streams in the study area at various times were computed. The observed data from 11 runoff stations between P.75 and P.73 stations along the Ping river and its tributaries were used to calibrate with the results from the developed flood forecast models. The values of correlation coefficient r, efficiency index (EI), and root-mean-square-error (RMSE) were computed to determine the accuracy of the developed models. It was found that most of the results obtained from the models were in the acceptable level, though the results at some river sections were rather different from the observed data. This might be due to errors in rainfall data and values of roughness coefficient.

_______________________ ______________________ ____ / ____ /____ .

Student's signature Thesis Advisor's signature

ACKNOWLEDGMENTS

I would like to gratefully thank and deeply indebted to Assoc. Prof. Winai Liengcharernsit my thesis advisor for help, encouragement and valuable suggestion for completely writing of thesis. I am most grateful for his teaching and advice, not only the research methodologies but also many other methodologies in life. I would not have achieved this thesis without all the support that I have always received from him. I would sincerely like to thank Dr. Patchraporn Ittisukananth my co-advisor for suggestion and all her help.

I would like to sincerely thank the Royal Irrigation Department (RID) and the Thai Meteorological Department (TMD) for the useful data for this research.

I gratefully appreciate financial support this research by the Faculty of Engineering, Kasetsart University, the National Research Council of Thailand (NRCT) and the Japan Society for the Promotion of Science (JSPS).

Finally, I am especially appreciated my parents, my family and my colleagues for their continuing encouragements and supporting me throughout all my studies.

Atchara Komsai

May 2012

TABLE OF CONTENTS

Page

LIST OF TABLES

LIST OF TABLES (Continued)

Appendix Table **Page**

LIST OF TABLES (Continued)

Appendix Table **Page**

LIST OF FIGURES

LIST OF FIGURES (Continued)

Figure **Page**

LIST OF ABBREVIATIONS

A	=	cross-sectional area
b_η	=	channel width at water surface
C_h	=	Chezy's coefficient
FP	=	the Flood-Plain simulation model
DHI	=	Danish Hydraulic Institute
EFAS	=	the European Flood Alert System
f	=	infiltration area
FEM	=	The Finite-Element Method
FS	=	the Flood simulation model
GCMs	=	General Circulation Models
GIS	=	Geographic Information System
h	=	mean depth of overland flow
HEC	=	Hydrologic Engineering Centre
i	=	the rate of gross rainfall
i_e	=	an excess rainfall
I	=	number of rain gauges
n_o	=	an effective roughness parameter for overland flow
N	=	total number of rain gauges
ONEP	=	Office of Natural Resources and Environmental Policy and Planning
P_a	=	atmospheric pressure
$\overline{P}$	=	spatial average of precipitation
P_i	=	rain gauge precipitation value
q	=	discharge per unit width
Q	=	river flow rate
$Q_{in}(t)$	=	inflow into the basin as a function of time *(t),*

LIST OF ABBREVIATIONS (Continued)

$Q_{out}(H)$	=	outflow from a detention basin as a function of head (H) in the basin.
R	=	hydraulic radius
RID	=	Royal Irrigation Department
S	=	overland flow slope
SHE	=	The Système Hydrologique Européen
V	=	volume of water in the storage in the basin,
WB	=	the Water Balance model,
θ	=	an angle between the flow direction of q and the x-axis
η	=	water surface level
α	=	conveyance factor

FORMULATION OF FLOOD ROUTING MODEL USING FINITE ELEMENT METHOD WITH APPLICATION TO THE UPPER PING RIVER BASIN

INTRODUCTION

Rapid population growth and urbanization in Thailand in the past century have created high demand of land resources for agriculture, commercial and residential purposes. So, deforestation was practiced in many parts of the country. In addition, increased population also raise water demand for domestic consumptions, agriculture, industries, transportation, recreation and energy production. Water activities from human are a reason of disequilibrium in water ecosystem. As a result, changes in rainfall and stream flow patterns have occurred in various regions. Flash flood and drought occur very often nowadays which might be caused by climate change. In the past few years, big flooding occurred in many regions of Thailand for prolonged period which caused lot of damage to lives and economy. One way to reduce the damage is to develop a flood warning system. In order to do this, it is necessary to have reliable data on flood magnitudes in various rivers which flow through dense population areas.

The Ping river is one of the main rivers originating in the mountainous areas in the northern part of Thailand. Its catchment area covers about 33,896 km^2. It flows southward passing several cities before merging with Wang, Yom, and Nan rivers to form the Chao Phraya river which is the most important water resource of Thailand. The Upper Ping river is the portion of the Ping river which extends from its upstream watershed to the point where it merges with the Wang river.

In the past few decades, flooding has occurred in the Upper Ping river basin for several times. The main causes of flooding include 1) the reduction in river cross-sections caused by some intrusive building structures or land embankment, especially along the river sections which pass through dense population areas; 2) heavy rainfall in the upstream watershed; 3) deforestation in the mountainous upstream areas; and 4) poor water resource management.

This study is aimed at developing numerical models for flood routing in the Upper Ping river basin. The finite element method is used to develop the flood forecast models. MATLAB programming language is employed in program development. The main objective is to develop a tool to determine flood magnitudes in various reaches of the Upper Ping river, so as to provide reliable data for flood warning purpose.

OBJECTIVES

This study is aimed at developing numerical models for flood routing in the Upper Ping river basin. The main objective is to develop a tool to determine flood magnitudes in various rivers in the Upper Ping river basin, so as to provide reliable data for flood warning purpose.

Scope of work

1. To develop a mathematical model for computing two dimensional overland flow from the catchment of the study area. The variables in the model are water depth and discharge per unit width in the x- and y-directions.

2. To develop mathematical models for computing one dimensional flow in a channel. The variables in the model are cross-sectional flow area and stream flow rate.

3. MATLAB is used to develop the computer programs.

4. The developed models are applied to the Upper Ping river basin which covers the upstream watersheds to the confluence of the Ping and the Wang rivers.

LITERATURE REVIEW

1. The Upper Ping River Basin

The Ping River, approximately 650 km length, is one of the most important rivers in Thailand and is the largest of the eight river basins that together form the Chao Phraya river. The Ping River Basin covers about 22 percent of the larger Chao Phraya river system within which it is nested, and contributes about 24 percent of the system's average annual runoff (ONEP, 2005; Pfotenhauer, 1994). People situated along this river use water for many purposes, such as domestic consumption, agriculture, industry, transportation and recreation. Water quality in the Ping river in the recent years is deteriorated because of human activities, farming activities, and domestic waste discharging.

The Ping river is one of the four 'upper' tributary rivers that merge together to form the well-known Chao Phraya river at Nakhon Sawan. These four tributary rivers contribute more than 70 percent of the total average annual runoff that feeds the entire Chao Phraya river system. Its highly complex system of downstream barrages and irrigation canals has become the integral part of Siamese civilization and the Thai nation state. Thus, from the centers of political and economic power in the lower Chao Phraya river basin, the four 'upper' river basins are viewed as areas to be protected from any activities that would threaten the downstream water consuming processes. The 'lower' portions of the Ping river basin below the Bhumibol dam are located near the western margin of the 'lower north' region in Nakhon Sawan, Kamphaengphet and Tak provinces. While the Ping basin covers substantial portions of Tak and Kamphaengphet provinces, it includes only a quite small portion of Nakhon Sawan province. Areas within the Ping river basin are quite strategically important, however, and it is worth noting that provincial capital cities are all located within or near the boundary of Ping basin lands (ONEP, 2005).

For centuries the Upper Ping was the central artery of the separate Lanna Kingdom with Chiang Mai as its capital and a key trading town in other periods when under Burmese rule. Royalty and elites have built canals and made rules about water, labor and taxes on harvests that extend back more than 700 years. Throughout this time and up to the present locally built and managed irrigation systems have persisted as another infrastructural and institutional layer (Cohen and Pearson, 1998). Over the last five decades (1960–2009) water and land use in the Upper Ping has been transformed by the expansion and intensification of agriculture, urban–industrial (Lebel *et al*., 2009)

Within the ‘upper’ portion of the Ping River Basin further to the north, lowlands of the inter-montane Chiang Mai – Lamphun Valley are home for a major center of people and economic activity that has evolved from the Lanna empire, for which it was the center of power before its ‘merger’ with Siam as part of Thailand’s nation-building process that began during the late 19th Century. As with the Siamese further downstream, dominant Tai cultures in the Chiang Mai – Lamphun Valley have strong roots and traditions based in lowland irrigated paddy agriculture, water management, and river bank life. Major lowland valley areas have been integrated into Thailand’s economic and social development infrastructure and programs, as symbolized by the emergence of Chiang Mai City as the second largest city in Thailand (albeit still more than an order of magnitude smaller than Bangkok). Boundaries of Chiang Mai and Lamphun provinces provide a close, but not quite perfect fit with natural boundaries of ‘upper’ portions of the Ping River Basin.

In the Upper Ping basin, the Mae Taeng Project was constructed to solve the problem of ‘water shortages’ for agriculture (Figure 1). In the Third National Economic and Social Development Plan (1972–76), major large-scale dams in the Upper Ping basin – the Mae Ngad and Mae Kuang Dam project – began construction (Figure 1). In the Fourth National Economic and Social Development Plan (1977–81) the Royal Irrigation Department (RID) accelerated the replacement with permanent concrete structures on traditional irrigation and established the Northern Industrial Estate in Lamphun Province. There are now four major water infrastructure projects in the upper Ping basin: Mae Faek Weir; Mae Taeng Weir; Mae Ngad Dam and Mae Kuang Dam (Figure 1) (Lebel *et al*., 2009). The cumulative area irrigable in the wet season rose between 1972 and 2005 from about 50,000 to 214 000 hectares. The Bhumipol Dam, constructed in 1964, marks the lower end of the Upper Ping and is still the largest storage dam and hydropower source within Thailand. Dams on the main tributaries of the Chao Phraya River were built and operated to produce electricity for urban–industrial development and regulate monsoonal-varying flows for flood protection and irrigation of the surrounding central plains.

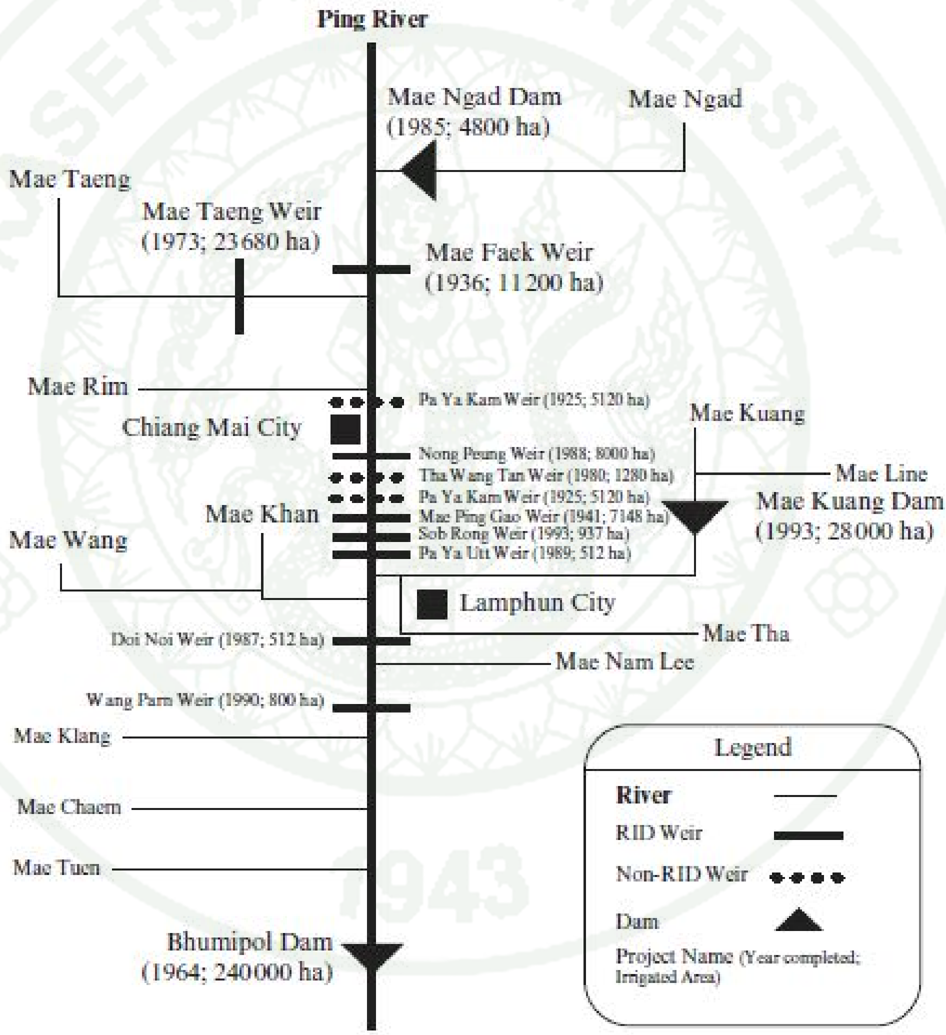

Figure 1 Schematic representation of water infrastructure in the Upper Ping river basin

1.1 Location and topography of the Upper Ping river basin

The Upper Ping river basin is located in the north of Thailand, the most areas in two provinces, Chiang Mai and Lamphun. The basin is along with the north-south of Thailand.

The north and the west connect to the Salawin river basin and the south is next to the Lower Ping river basin and the East also connect with the Wang river basin (Figure 2). The important watershed in the Upper Ping river is separated to 14 sub-basins as follow in Figure 3;

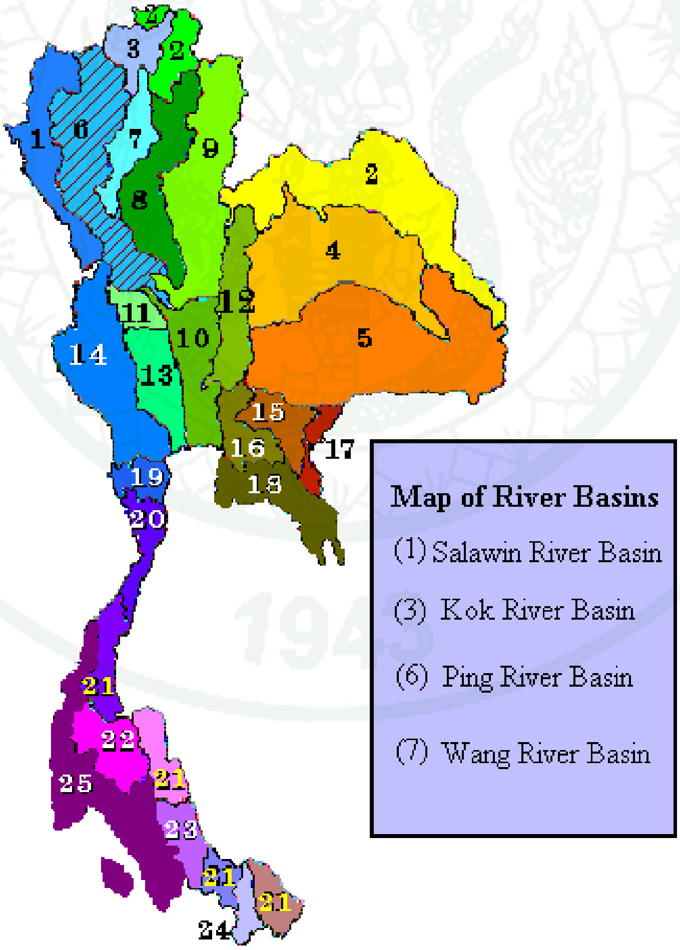

Figure 2 Location of the Ping river basin in a map of river basins

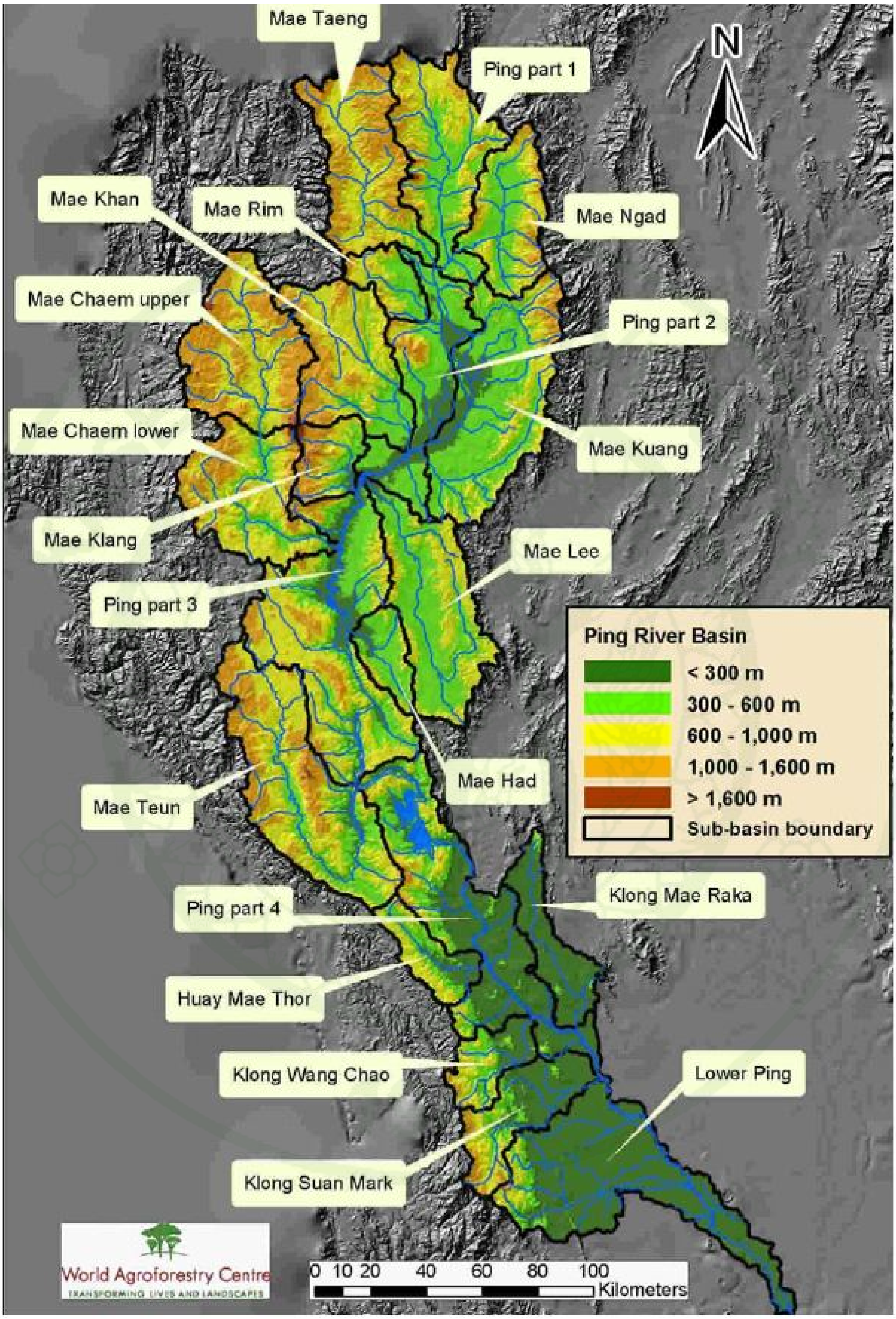

Figure 3 Altitude zone map of the Ping river basin

1.1.1 The Ping river

The Ping river basin is a large rainfall area which extends for a long distance. The Ping river originates in a watershed on the west of Chiang Dao district and then flows through several districts in Chiang Mai and Lamphun provinces. The Ping river basin can be separated into 3 parts. The first part is the watershed area on the Chiang Dao mountain covering about 1,974 km^2. The tributaries on the west side are Mae Ngad river, Mae Kuang river, Mae Lee river and Mae Had river, and on the east side are Mae Taeng river, Mae Rim river, Mae Chaem river, Mae Klang river and Mae Tuen river. The second part of the Ping river basin which is about 1,616 km^2 is the area covering the center of Chiang Mai province and suburban of Lamphun province. The third part is the area connected to the second part which covers the watershed of Doi Tao lake, a portion of the Bhumibol reservoir.

1.1.2 Mae Taeng river basin

It is a tributary of the Ping river. Watershed area is of rectangle shape with 80 km long in the north-south direction and 40 km wide along the east-west direction. The northern boundary is connected with Thailand - Myanmar border. The Mae Taeng river joined the Ping river at Sob Taeng which is about 2 km from the Mae Taeng district office. The upstream tributaries are from Dan Lao mountain range which is about 151 km long and covers about 1,957 km^2.

1.1.3 Mae Rim river basin

The Mae rim river is a tributary of the Ping river that flows through the Mae Rim district. It is 49 km long and joins the Ping river in the Mae Teang district. The catchment area is around 508 km^2.

1.1.4 Mae Ngad river basin

The Mae Ngad river originates from the north of the western Pee Pun Nam range in Phrao district. It flows into the Mae Ngad reservoir and joins with the Ping river in Mae Taeng district. The length is 95 km and the catchment area is 1,285 km^2.

1.1.5 Mae Chaem river basin

The Mae Chaem river is located on the west of Chiang Mai. It joins the Ping river in Mae Chaem district. Most area is located in Mae Chaem district, Chiang Mai. The remaining is in Mae La Noi district, Maehongson, and Hod district, Chiang Mai. The Mae Chaem river basin is separated to upper and lower parts. The whole catchment area is 3,895 km^2 and the length is 170 km.

1.1.6 Mae Kuang river basin

It is the major tributary of the Ping river. It originates in Sansai and Doi Saket districts, Chiang Mai, and Muang district, Lamphun. It flows into the Ping river at Ban Sob Ta Pha Sang district, Lamphun. The total length is 115 km from upstream to the Mae Ping River.

1.1.7 Mae Lee river basin

The original of water is from Doi Term in Khuntan range and Phamaung mountain. The flow direction looks like a horseshoe and the channel is in a narrow and deep valley. It joins the Ping river at Ban Hong district, Lamphun. The catchment area is 2,081 km^2 and the length is 126 km.

1.1.8 Mae Teun river basin

Mae Teun river basin has catchment area around 2,896 km^2. It originates from the mountain range between Om Koi district, Chiang Mai, and Mae Sariang district, Maehongson. It joins the Ping river at Sam Ngao district, Tak. The length is 164 km.

1.1.9 Mae Klang river basin

The river originates from the eastern Doi Inthanon mountain and joins with the Ping river at Chom Thong district, Chiang Mai. The catchment area is 616 km^2 and the length is 32 km.

1.1.10 Mae Khan river basin

Mae Khan river originates from the range of mountain in Samoeng district. The length is 35 km and the catchment area is 1,833 km^2.

1.2 Climate

The general climate information of the Ping river basin in 30 years (2504-2533) at Chiang Mai station can be summarized as follow:

Temperature: The average temperature is 25.4 ^{o}c. The average maximum temperature is 41.4 ^{o}c in May and the average minimum temperature is 3.7 ^{o}c in January.

Relative humidity: The average monthly relative humidity is between 47-85 percent. The annual average relative humidity in Chiang Mai is 72 percent.

Evaporation rate: The monthly evaporation rate is related to relative humidity and temperature. When the relative humidity is low and the temperature is high, the evaporation rate will increase. The minimum evaporation rate is 93.6 mm in December and maximum is 194.4 mm in April.

Wind: the monthly average wind speed is in the range of 1.4-3.3 knots.

Rainfall: the southwest monsoon and the northeast monsoon create distinct seasons. The southwest monsoon usually arrives from India at the end of May and lasts until November. Rainfall is generally heaviest in September with an average precipitation of 212.6 mm for that month alone. The northeast monsoon lasts from mid-November until early May and brings cool air from northern Vietnam/China but no rain for Northern and Central Thailand. The monthly average precipitation in each station is not much different. The least amount of precipitation is approximately 6.9 mm occurring in February.

1.3 Land use

Watershed land use in the north of Thailand consists of mountains and complex hills. That mountains or hills are very huge area in the top of northern area and is smaller in the southern area. The catchment area is divided as follows (Figure 4):

Within the agriculture sector, we can also anticipate continuing strong incentives for movement into crops offering higher value per worker. A number of constraints, however, are likely to limit the rate and extent to which this occurs. In terms of current agricultural production, the following distributional aspects are particularly noteworthy (ONEP, 2005):

Paddy field: It might do rice farming regularly, once a year during the rainy season or twice a year or do not have to do farm but the area still as a paddy field. This area is located in the valley plains. In mountainous areas of Tak and the Upper Ping provinces, much smaller pockets of paddy land are found in small valleys and areas where terrain allows, and especially main season paddy crops are often planted and also do in dry season are assisted by weir and canal structures long managed by traditional water management organizations. Irrigated areas also occur in the more limited lowlands of Tak, and expand again in the large inter-montane valley in Upper Ping Basin provinces, where traditional irrigation facilities have been reworked with 'modern' structures. The rivers or streams flow through the field.

Short-season Field Crops: The most extensively planted short field crop in the Ping River Basin is maize, most of which is sold for use in producing animal feed. There are also substantial areas planted to various legumes, especially soybean, mungbean and groundnut. Various upland areas planted to legumes have been displaced by maize during recent years.

Long-season Field Crops: the Lower Ping Basin Provinces have extensive areas planted to long-season industrial crops, especially sugarcane and cassava. While sugarcane extends a bit into Tak Province, these crops become very rare in inter-montane valley and mountain areas of the Upper Ping Basin. While a bit of cotton appears in Tak, the main long-season field crop in mountain areas is upland rice, which occurs in areas where terrain does not allow establishment of paddy fields. Especially in inter-montane valley areas, tobacco has also been an important crop, In Upper Basin provinces, mountain areas of Chiang Mai also include some plantings of coffee and tea, including both Chinese types of tea and 'miang' tea gardens that are traditionally planted into natural forests.

Fruits: Although a variety of fruits are grown in home gardens throughout the Ping Basin, commercial production at significant scales are first seen in terms of citrus production in Kamphaengphet. But it is not until the Upper Ping Basin provinces that fruit tree production becomes a major enterprise. The largest is the major longan industry in the inter-montane Chiang Mai-Lamphun Valley, but there are also extensive plantings of mango, lychee, and a range of other crops often planted in mixed orchards. A substantial citrus industry has also begun in the far northwest corner of the Ping Basin, and it has been expanding during recent years.

Strawberry production has also become important at higher elevation, and a range of subtropical and temperate fruits have expanded in some mountain areas with assistance from opium crop substitution and highland development programs.

Forest: The forest areas are found in mountain, hillside and complex mountain range. That has the tropical rain forest such as, rain forest, dry evergreen forest and pine forest and the deciduous forest such as mixed forest and deciduous dipterocarp forest. There also has a substantial range of herbals, medicinals, mushrooms, dyes, and various other types of from natural forest sources.

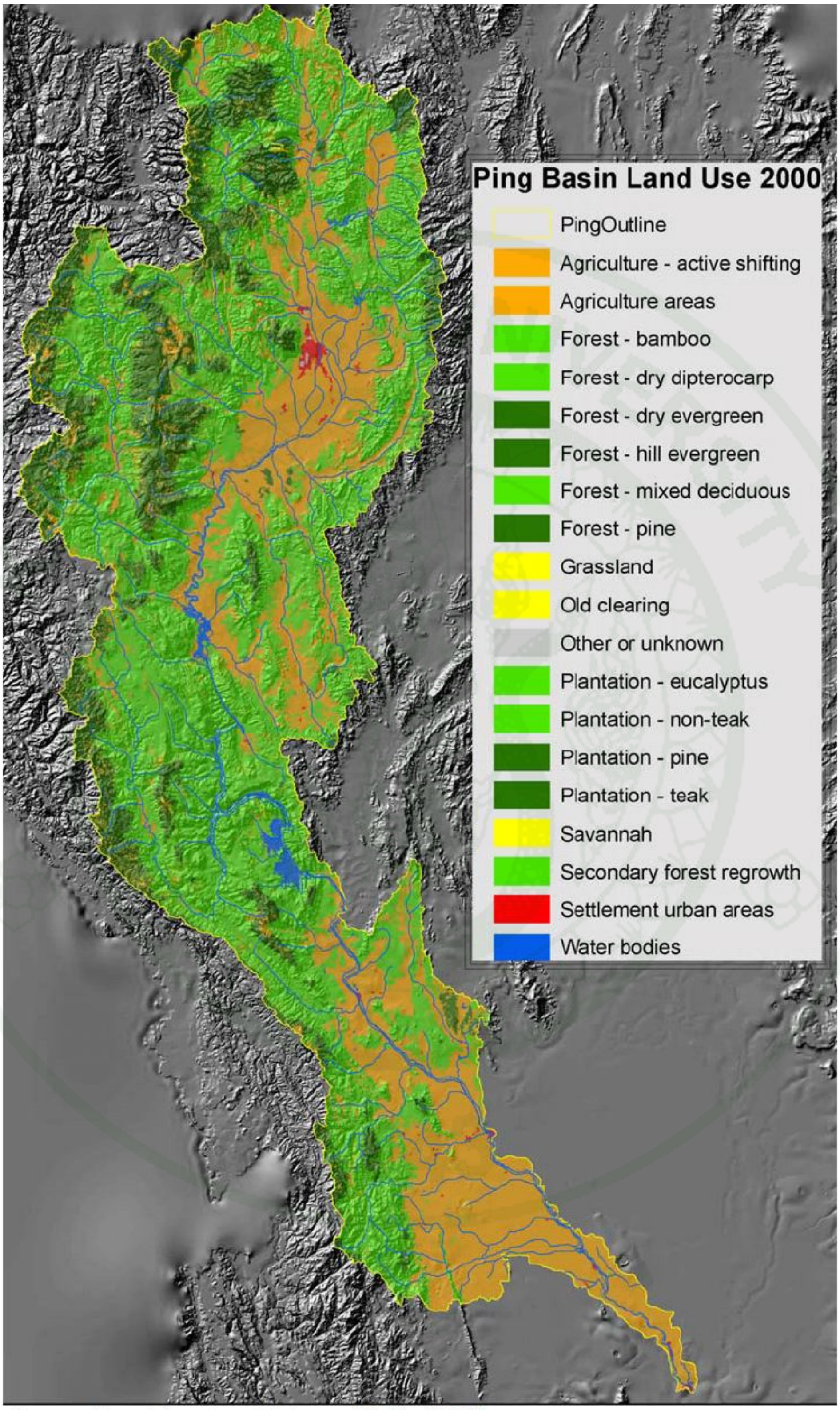

Source: Forest department data provided by ONEP

Figure 4 Ping basin land use

2. Environmental Concerns

2.1 Water management

ONEP concerns about watershed management, however, are not limited to forest cover and quality issues, and they are not the exclusive domain of environmental activists and foresters. Indeed, public environmental awareness and concern about land use in upper watershed areas has been fed by a range of trends, events and perceived risks that can strongly affect people in their everyday lives. In terms of water flow regimes, major issues include (ONEP, 2005):

Flash floods and landslides: News media have reported a series of incidents involving relatively localized flash floods and landslides that have resulted in serious agricultural and property damage, and sometimes substantial loss of lives. Sites within the Ping river basin have been included, and they are usually located in upper tributary valleys at the foot of steeply sloping small mountain stream valleys.

Main channel floods: Damage caused by major floods along the main channel of the Ping river and its major tributaries have also been featured in mass media, and there is a general impression that they are increasing in frequency and magnitude. The most recent example is the series of floods that hit Chiang Mai City during 2005, which have been described as the most serious floods in 40 years. And given the level of riverside and floodplain development during that period, the level of their damage is unprecedented.

Dry season agricultural water shortages: Rising demand for reliable year-round water supplies for irrigated agriculture at downstream locations has increased sensitivity to, and competition for water during the dry season. Thus, many have been taking an increasingly critical look at uses of both land and water at upstream locations.

Inadequate village and urban water supplies: Similarly, efforts to improve supplies of water for drinking and domestic use in villages and urban areas alike have added an additional element of competition for water resources, which reaches a peak during dry seasons and during El Nino years.

Diminishing ground water supplies: A growing number of communities have invested in shallow and deep wells to help provide access to water for agricultural, domestic and even industrial uses. In some areas, such as parts of the Chiang Mai Valley, many are now reporting receding groundwater tables that are causing increasing alarm.

2.2 Background problem

Impacts of natural disasters are major concerns both among the general public and in the public policy arena. Floods and landslides make headlines in the media, and have provided major trigger events for revoking logging concessions in national forests (the “logging ban”), launching many emergency assistance programs, and driving new programs for prevention and early warning systems. The recent tsunami disaster is likely to help further intensify such concerns. Thus, the specific sub-criterion focusing on natural hazards is (ONEP, 2005):

There are two types of floods that can have very important negative impacts on people and their assets in the Ping river basin.

Main channel floods: This type of flood occurs when levels of major streams and rivers rise beyond their usual channels to inundate adjacent flood plains and/or other low-lying areas. They are usually associated with fairly sustained and reasonably high rainfall patterns that occur during a similar period of time over a large portion of tributaries feeding catchments that approach the scale of sub-basins or river basins. Individual upper tributaries may be less directly affected, but the cumulative additions of flow from numerous upper tributaries increases the amount of inundation along more distant downstream main river channels. Thus, these types of floods are a more important concern in the Middle Ping sub-basins; impact of such flooding is minimized in some the Lower Ping sub-basins due to the river flow "buffering capacity" of the Bhumibol reservoir.

Flash floods: This type of flood tends to be associated with more localized extreme rainfall events, combined with particular physical characteristics of local catchments and their spatial terrain and drainage patterns. Especially when extreme rainfall events are preceded by rain that has already saturated soils in local catchments, flash floods can also be associated with landslides. Since such extreme events are usually rather localized, flash floods (and landslides) have their strongest impacts at scales that are smaller than most sub-basins. Except perhaps in the smallest sub-basins, this would correspond more closely with smaller sub-watersheds of tributaries that feed into the main streams and rivers of sub-basins.

Both types of floods can be disastrous for those who are in their path, and accounts in popular media often associate both types with headwater deforestation or other types of land use that are classified as "inappropriate". Although accurate historical data appears to be quite spotty and scarce, there are popular perceptions that floods and landslides are increasing in frequency.

3. Hydrology and Hydraulic Theory

3.1 Flood Routing

The movement of a flood wave down a channel or through a reservoir and the associated change in timing or attenuation of the wave constitutes an important topic in floodplain hydrology. It is essential to understand the theoretical and practical aspects of flood routing to predict the temporal and spatial variations of flood wave through a river reach or reservoir. Flood routing methods can also be used to predict the outflow hydrograph from a watershed subjected to a known amount of precipitation.

3.1.1 Hydrologic routing methods

Routing techniques may be classified in two major categories: simple hydrologic routing and more complex hydraulic routing. Hydrologic routing involves the balancing of inflow, outflow, and volume of storage through use of the continuity equation. A second relationship, the storage-discharge relation, is also required between outflow rate and storage in the system. Applications of hydrologic routing techniques to problems of flood prediction, flood control measures, reservoir design and operation, watershed simulation, and urban design are numerous. Many computer models are available that take input rainfall, convert to outflow hydrographs, and then route the hydrographs through complex river or reservoir networks using hydrologic routing methods.

3.1.1.1 Kinematic Overland Flow Routing

Overland flow is handled separately from open channel flow because of the assumptions inherent in developing the kinematic flow equation for overland flow planes. Overland flow in the model is distributed over a wide area and at very shallow average depth until it reaches a well-defined collector channel. After overland runoff is routed down the length of the overland flow strip, it is then routed along the collector system and eventually into a main channel. Runoff moves through the collector system, picking up additional lateral inflow from adjacent strips uniformly distributed along the system. Collector and main channel kinematic wave routing are similar in theory and differ only in the shape of the collector.

For the conditions of kinematic flow, with no appreciable backwater effect and a wide plane with shallow flows, the discharge can be described as a function of depth as follows (Bedient and Huber, 2002):

$$q = \alpha h^m = \frac{\sqrt{S}}{n_o} h^{5/3} \tag{3.1}$$

where q is discharge per unit width

α is conveyance factor = $\frac{\sqrt{S}}{n_o}$

S is overland flow slope

n_o is an effective roughness parameter for overland flow

h is mean depth of overland flow

m is 5/3 from Manning's equation

The continuity equation for is

$$\frac{\partial h}{\partial t} + \frac{\partial q}{\partial s} = i - f \tag{3.2}$$

where i is the rate of gross rainfall

f is infiltration area

q is flow rate per unit width

h is mean depth of overland flow

3.1.1.2 Kinematic Channel Routing

Simple cross-sectional shapes such as triangles, trapezoids, and circles are used as representative collectors or stream channels. These are completely characterized by slope, length, cross-sectional dimension, shape, and Manning's n value. The basic forms of the equations are similar to the overland flow equation.

For stream channels or collectors,

$$\frac{\partial Ac}{\partial t} + \frac{\partial Q}{\partial x} = q \tag{3.3}$$

$$Q = \alpha_c Ac^{m_c} \tag{3.4}$$

in which

Ac is cross-sectional flow area

Q is stream flow rate

q is lateral inflow per unit length

α_c , m_c are kinematic wave parameters for the particular channel

The values of α_c and m_c will be different for each differently-shaped cross section and will vary with effective Manning's 'n' and channel slope as well (Table 1). Figure 5 presents shape parameter for typical channels.

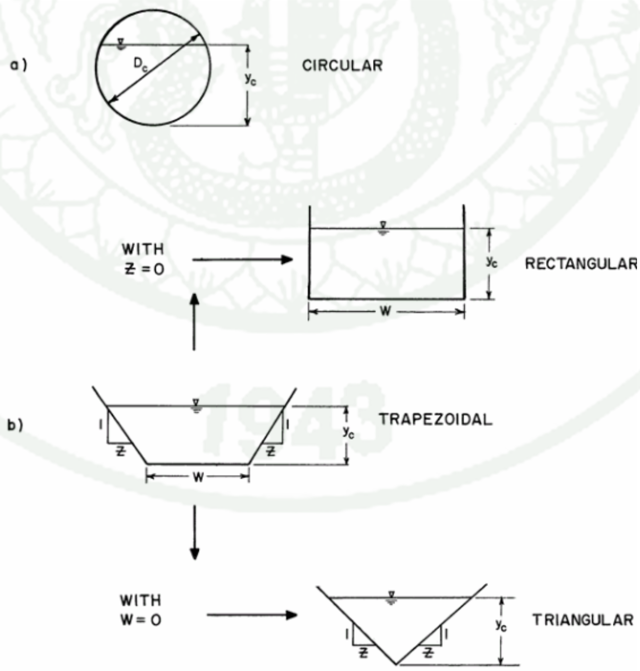

Figure 5 Basic channel shapes and their variations for kinematic wave stream routing

Table 1 Kinematic channel parameters

Channel Shape	α_c	m_c
Rectangular	$\dfrac{0.48\sqrt{S_c}}{n}$	4/3
Triangular	$\dfrac{0.63\sqrt{S_c}}{n}\left(\dfrac{z}{1+z^2}\right)^{1/3}$	4/3
Circular	$\dfrac{0.804\sqrt{S_c}}{n}(D_c)^{1/6}$	5/4
Trapezoidal	$\dfrac{\sqrt{S_c}}{n}\left(\dfrac{1}{w+zy_c\sqrt{1+z^2}}\right)^{2/3}$	5/3

3.1.1.3 Detention Basin Routing

The purpose of flood routing for detention basin design is to determine how the outflow from a detention basin and the storage in the basin vary with time for a known inflow hydrograph.

The continuity equation is expressed as

$$\frac{dV}{dt} = Q_{in}(t) - Q_{out}(H) \tag{3.5}$$

where

V is volume of water in the storage in the basin,

$Q_{in}(t)$ is inflow into the basin as a function of time (t),

$Q_{out}(H)$ is outflow from a detention basin as a function of head (H) in the basin.

3.1.2 Hydraulic routing methods

Hydraulic routing is more complex and accurate than hydrologic routing and is based on the solution of the continuity equation and momentum equation for unsteady flow in open channels. Unsteady flow in rivers, reservoirs, and estuaries is caused by motion of long waves due to tides, flood waves, storm surges, and dynamic reservoir releases.

3.2 Estimation of precipitation

One important aspect of hydrologic modeling is the estimation of the total precipitation and its distribution within a watershed. This problem is commonly referred to as "areal estimation of precipitation" and is best described as follows (HYDROEUROPE team 7, 2008):

3.2.1. Arithmetic Average Method

The advantage of Arithmetic Average Method is that it needs the simplest calculation. But it shows a big disadvantage: the method is suitable if the climate and the relief is near uniform and the regional distribution of rain gauges is homogenous. So in this instance this method have appreciable inaccuracy, therefore it was used to compare this result with the other methods results.

The arithmetic average of the rainfalls was calculated with the equation (HYDROEUROPE team 7, 2008):

$$\overline{P} = \frac{\sum_{i=1}^{N} P_i}{N} \tag{3.6}$$

where

$\overline{P}$ is spatial average of precipitation

P_i is rain gauge precipitation value at rain gauge i

i is number of rain gauges

N is total number of rain gauges

3.2.2. Thiessen Polygon Method

The Thiessen Polygon Method was also used to find the spatial distribution of rainfall. In this method the catchment was divided performed the following construction: drawing straight lines between the rain gauges and constructing perpendicular bisectors for each line. Accordingly required sub regions are obtained which areas in the catchment are closest to each rain gauge station that shows Figure 6.

Every sub region belongs to one of the rain gauge. The spatial average precipitation in each region assumed to be identical with precipitation value of the regions rain gauge. This involves determining the area of influence for each station, rather than assuming a straight-line variation. It is easier than the isohytal method but less accuracy.

The Thiessen formula was used to compute the rainfall distribution (HYDROEUROPE team 7, 2008):

$$\overline{P} = \frac{\sum_{i=1}^{N} A_i P_i}{\sum_{i=1}^{N} A_i} \tag{3.7}$$

where

$\overline{P}$ is spatial average of precipitation

A_i is area of the part of the sub-catchment belongs to the rain gauge i

P_i is rain gauge precipitation value at rain gauge i

N is total number of rain gauges

$$A = \sum_{i=1}^{N} A_i \qquad \text{total area of the sub-catchment}$$

In simpler form:

$$\overline{P} = \sum_{i=1}^{N} v_i P_i \; ; \quad \text{where } v_i = \frac{A_i}{\sum_{i=1}^{N} A_i}$$

To determine $i\ A$, use the following procedure:

1. Join adjacent station locations with straight lines
2. Take the PERPENDUCALR BISECTORS to those lines.
3. Define the polygons bounding each station and compute its area.

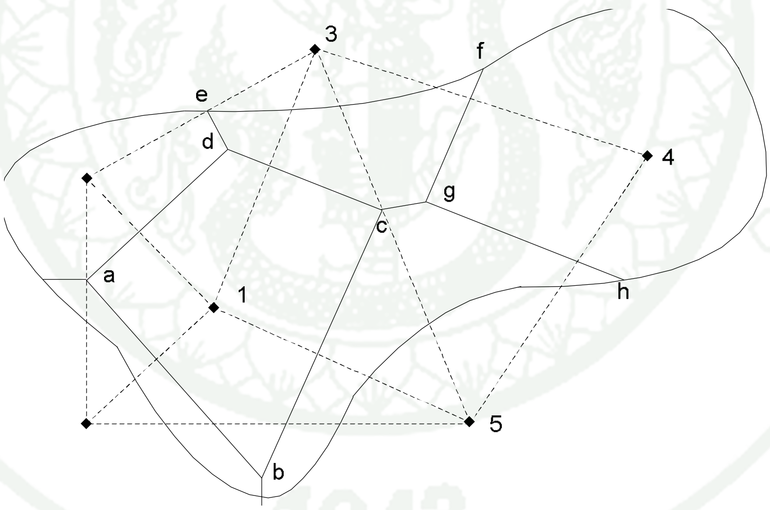

Figure 6 Rainfall estimation by using Theissen method (Liwatchanakul, 1996)

• Theissen method defines areas represented by each gauge in order to weigh the effects of non-uniform rainfall distribution.

• Adjoining lines are created between each of the rain gauges. Perpendicular bisectors are then created to form polygons around each gauge.

• The area within the polygon is assumed to be the area represented by each gauge.

• More accurate than the arithmetic method. Once the polygons have been created, it is a simple process to compute mean rainfall from other events.

• Advantage – polygons only need to be created once.

• Disadvantage – does not account for topographic influences.

3.2.3 Isohyetal Method

The most basic method of representing is the spatial distribution. This is generally the most accurate method but is also the most laborious. The Isohyetal method uses the observed precipitation data as the basic for drawing contours of equal precipitation (isohyets), and then weights the average precipitation of adjacent isohyets by the area between the isohyets. The method is suitable for large areas, especially those in which orographic effects may be present (Bethlahmy, 1976).

The Isohyetal method was calculated with the equation:

$$\overline{P} = \frac{\sum_{i=1}^{N} A_i P_i}{\sum_{i=1}^{N} A_i} \tag{3.8}$$

where

$\overline{P}$ is spatial average of precipitation

A_i is area of the part of the sub-catchment belongs to the rain gauge i

P_i is rain gauge precipitation value at rain gauge i

N is total number of rain gauges

$$A = \sum_{i=1}^{N} A_i \quad = \text{ total area of the sub-catchment}$$

The weights are defined by the contour map area as shown below and h_i is the representative contour.

Isohyets

• Considered the most accurate method for computing mean rainfall. Rainfall gauges and locations are plotted.

• Contours of equal rainfall amounts (isohyets) are then drawn.

• The area between the isohyets are treated the same as Theissen polygons areas.

• Isohyetal method takes into account topographic influence, therefore, more accurate over mountainous terrain.

• Disadvantage – new isohyets have to be made for each rainfall event.

Figure 7 Rainfall estimation by using Isohyetal method (Liwatchanakul, 1996)

4. Mathematical Models and Hydrological Models

4.1 Mathematical models

Physical phenomena are described by a set of governing equations. Numerical methods are frequently used to solve the set of governing equations. Numerical methods invariably involve the computer. The computer performs arithmetic operations upon discrete numbers in a defined sequence of steps. The sequence steps are defined in the program. A useful solution is obtained if the mathematical model accurately represents the physical phenomena, that is, the model has the correct governing equations.

Today available models are really numerous and generally it's more frequent to choose a model from a list of existing ones than to develop a new model. Although there are no clear rules for making a choice between models, some simple guidelines can be stated. Starting from the studied physical system, the first step is to define the problem and determine what information is needed and what questions need to be answered. This means that it is necessary to evaluate the required output, the hydrologic processes that need to be modelled, the availability of input data (Lastoria, 2008). Subsequently the simplest method that can provide the answer to the questions has to be chosen. In particular it's necessary to identify the simplest model that will yield adequate accuracy, bearing in mind that model complexity is not synonymous with the accuracy of the results, that the model has to be characterized by flexibility, by the possibility of making it applicable under various spatial and temporal conditions and that increased accuracy has to be worth the increased effort.

4.2 Previous Study

4.2.1 Study of Development of Mathematical Model in Hydrology

Anderson and Bates (1994) simulated a two dimensional finite element model for flood flow using varying level of data availability. This study tried to uniquely validate the entire predicted flow field derived from the model that highlighted as an essential task for all distributed hydrological and hydraulic modeling. Furthermore, Determination model parameterization uncertainties relating to the provision of boundary conditions for the numerical solution scheme was other object in this study.

Giammarco *et al.* (1996) studied the control volume finite element (CVFE) to deal more effectively with overland flow in two-dimension. The derivation of the CVFE discrete formulation was preceded by a discussion on the classical integrated finite difference (IFD) and finite element (FE) approaches. This research attempted to merge the advantages of being both conservative at local scale (as in the IFD method) and capable of representing spatial domains characterized by complex and irregular geometry (as in the FE method).

Tabuenca *et al.* (1997) used two mathematical models to simulate pollution in the Bay of Santander. Both models were formulated in two-dimensional equations. Linear triangular finite elements were used in Galerkin procedure for spatial discretization. A finite difference scheme is used for the time integration. The efficiency and accuracy of the models were tested by their application to simple illustrative example.

Gee and Tseng (1997) described development the Mississippi-Misouri UNET Forecast Model to simulate 1-D unsteady flow through a network of open channels. It included development of a graphical user interface (GUI) reflecting the unique needs of real-time forecasting. The modeling system was developed to encompass low flows, routine day-to-day forecasting needs (such as lock and dam operation), as well as the simulation and forecasting of flood events.

Zhou *et al.* (2006) studied the numerical model with the Saint-Venant equations of one dimensional unsteady flow based on the split-characteristic finite element method. The assembled finite element equations were solved with the tri-diagonal matrix algorithm. The method was used to eliminate the restriction due to the wave celerity for the computational analysis of unsteady open channel flow. The numerical method was tested to simulate one dimensional steady flow, and unsteady flow with shock wave or flood wave.

Chagas *et al.* (2010) developed and applied a mathematical model base on the Saith-Venant hydrodynamic equations to study the behavior of flood movement in natural rivers. The governing partial differential equations were solved with the aid of finite differences, and the iterative Newton-Raphson algorithm was employed for the solution of system of nonlinear algebraic equations. QUARIGUA (Risk Quantitative Analysis of Flooding in Urban Rivers) program was used to perform the simulation and to evaluate the behavior of the control variables, several scenarios for the main channel as well as for the flood wave.

4.2.3 Study of Flood Routing in the Upper Ping River Basin

Puttaraksa *et al*. (2005) developed one dimensional implicit dynamic wave model (DYMWAV) to simulate one dimensional unsteady flow situation with backwater and tidal effects. The implicit weighted four points finite difference and the Newton Raphson's method were used to solve the nonlinear equations. The DYMWAV model was applied to upper Ping river basin to investigate the model performance for flow situations affected by backwater. The performance of the DYMWAV was then compared with the performance of the MIKE 11 Hydrodynamic model.

Arumpitakpun (2006) investigated the flood characteristics of the Ping river from gauged station at Nawarat bridge by using hydrodynamic model. In this study, the InfoWorks for River System (RS) program was used to simulate rainfall-runoff model that solved with US SCS calculation. The model calibration and verification were adjusted at the same time on ungauged station along the tributaries.

In 2009, both the URBS model and Nedbor-Afstroming model (NAM) were used in simulating flood behavior in the Upper Ping river basin by

Puttaraksa and Sriwongsitanon. In this study, the relationships between the USRB model parameters and catchment characteristics were applied for flood estimation of the ungauged catchment within the catchment area of the 11 stations used in the formulation process.

Taesombat and Sriwongsitanon (2010) studied the performance of two public domain models – the IHACRES (rainfall-runoff model) and the FLDWAV (hydrodynamic model) – using in the Upper Ping river basin. Three selected flood events in 2001, 2003 and 2004 were observed in estimating flood hydrograph at ungauged location and flood properties (flow rate and water level).

4.3 Commonly used hydrological models

Listed 8 models were derived from a survey conducted within the FORALPS project, to assess the state-of-the-art of rainfall-runoff models and to identify and suggest the most useful for applications in the Alpine Space. A description of each model is provided, general information, considering their capability to describe flow conditions and to represent spatial and temporal variability. The typical sector of application and the processes of hydrological cycle that are modeled are described. Additional information regarding program features, references and availability of the software are also given (Lastoria, 2008).

Some of these water models are not only aimed at flood forecasting and flood impact analysis, but more in general at environmental impact studies, integrating quality and quantity concerns. On one hand, hydrologic processes are influenced by various factors, e.g. the spatial variability of soils, topography, land use and cover, climate, and by changes produced by human presence on territory. On the other hand, contaminants are transported by runoff to surface waters and by infiltration and deep percolation to groundwater. Therefore, models of hydrologic processes are often at the core of studies about water quality and quantity, two aspects of water resource management that are strictly interrelated.

4.3.1 HEC-HMS (Rel. 3.1.0)

The Hydrologic Modeling System HEC-HMS is a program developed by the Hydrologic Engineering Centre (HEC) of the US Army Corps of Engineers. It is the successor to and the replacement for HEC's HEC-1 program, whose characteristics are improved with additional capabilities for distributed modeling and continuous simulation. The program is designed to simulate the precipitation-runoff processes and routing processes, both natural and controlled.

HEC-HMS is designed to simulate both single events and continuous long periods. The physical representation of a watershed is accomplished with a basin model, where hydrologic elements (sub-basin, reach, junction, reservoir, diversion, source, and sink) are connected in a dendritic network to simulate runoff processes. However, spatially distributed runoff can be computed with the quasi-distributed linear transform (ModClark) of cell-based precipitation and infiltration.

HMS is applicable in a wide range of geographic areas for solving the widest possible range of problems. These include water supply in large river basins, flood hydrology, and small urban or natural watershed runoff. HMS uses a separate model to represent each component of the runoff process, as illustrated in Figure 8. Thus it includes separate models to compute runoff volume, direct runoff (overland flow and interflow), base-flow and channel flow.

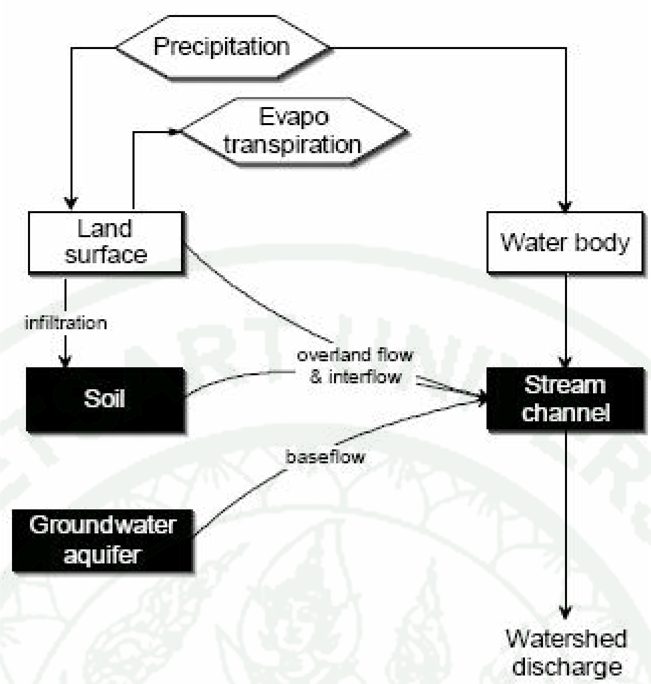

Figure 8 Typical HEC-HMS representation of watershed runoff

HMS is a public domain software. Free download of software and documentation can be performed from the website: http://www.hec.usace.army.mil.

4.3.2 WATFLOOD

WATFLOOD was developed for the Surveys and Information Branch of the Ecosystem Science and Evaluation Directorate of Environment Canada by Nicholas Kouwen of the Department of Civil Engineering at the University of Waterloo (Canada). The WATFLOOD programs are mostly a set of FORTRAN programs for DOS, compiled in Visual Fortran Ver. 6. It is a Visual Basic program that is used for data input and output and calls the DOS programs in a shell.

WATFLOOD is a distributed hydrologic model. It has been used with grid sizes from 1 to 25 km and for watershed areas from 15 to 1,700,000 km^2.

This integrated set of computer programs has been applied to forecast flood flows for watershed having response times ranging from one hour to several weeks

The model is aimed at flood forecasting, climate change and environmental impact studies. It was designed for distributed modeling using remotely sensed data, particularly from remotely sensed land cover maps and weather radar.

WATFLOOD is a commercial software package. However a simplified and limited version of WATFLOOD, WATFLOOD LITE is available for student use with no key requirement. The documentation and the software can be downloaded from the website: http://www.civil.uwaterloo.ca/Watflood/index.htm.

4.3.3 TOPMODEL

The development of TOPMODEL was initiated by Kirkby at the School of Geography, University of Leeds. The model was further developed by Keith Beven at the Lancaster. Since 1974 there have been many variants of TOPMODEL, but never a definitive version.

TOPMODEL is a semi-distributed and partly physically based model. It is a topography based hydrological program and allows single or multiple sub-catchment calculations with average rainfall and potential evapotranspiration inputs to the whole catchment. The topographic index of TOPMODEL is scale dependent so that parameter values and consequent results are strictly dependent and sensitive to grid size or DEM resolution. For this reason the model requires a high quality DEM, without sinks. The recommended resolution of the grid size is not greater than 50m.

TOPMODEL is mainly used to simulate humid or dry catchment responses, predict flood frequency, analyze land surface to atmospheric interactions and predict geochemical characteristics.

A demonstration version of TOPMODEL for Windows developed from versions used for teaching purposes over a number of years in the Environmental Science degree course at Lancaster University can be downloaded from the web site: http://www.es.lancs.ac.uk/hfdg/freeware/hfdg_freeware_top.htm.

4.3.4 ARNO

The ARNO rainfall-runoff model was originally developed as part of a real time flood forecasting system for River Arno (Italy). Input data required by ARNO model are: topographic data (hill-slope and channel slopes), precipitation, temperature and river levels at several stations within the catchment, soil type and land use data and rating curves for hydrometric stations where the discharge is to be simulated. Some of the parameters can be determined from the above data, but most of them have to be determined by trial and error. However, this is a relatively straightforward process since the model parameters have clearly defined effects on catchment response.

The ARNO modeling system is widely used for real-time flood forecasting but is also employed in land-surface-atmosphere process research and as a tool for investigating land use changes. The main physical phenomena represented in the model are: the water balance in the soil, the water losses through evapotranspiration, snow melt, overland flow, groundwater flow and channel flow routing. These processes have been developed into the model as inter-linked modules. ARNO is a commercial software package.

4.3.5 SHE

The Système Hydrologique Européen (SHE) was produced jointly by the Danish Hydraulic Institute (DHI), the British Institute of Hydrology, and the French consulting company SOGREAH, with the financial support of the Commission of European Communities. It has been developed as a fully modular system for the mathematical description of the land phase of the hydrological cycle.

SHE is a physically-based, distributed model. The spatial distribution of catchment parameters, precipitation input and hydrological response is achieved in the horizontal through representation of the catchment by an orthogonal grid network and in the vertical by a column of horizontal layers at each grid square.

Fields of application are: irrigation, land-use change, water developments, groundwater contamination, erosion/sediment transfer, flood prediction. The physical processes considered in the SHE are schematized in Figure 9. Each of the major hydrological processes of water movement is considered and is modelled either by finite difference representations of partial differential equations of mass and energy conservation or by empirical equations derived from independent experimental research. The model is based on a modular scheme where each component representing different hydrological processes can be modified or omitted depending on the hydrological conditions and availability of data, and it is relatively simple to add further components. SHE is a commercial software package.

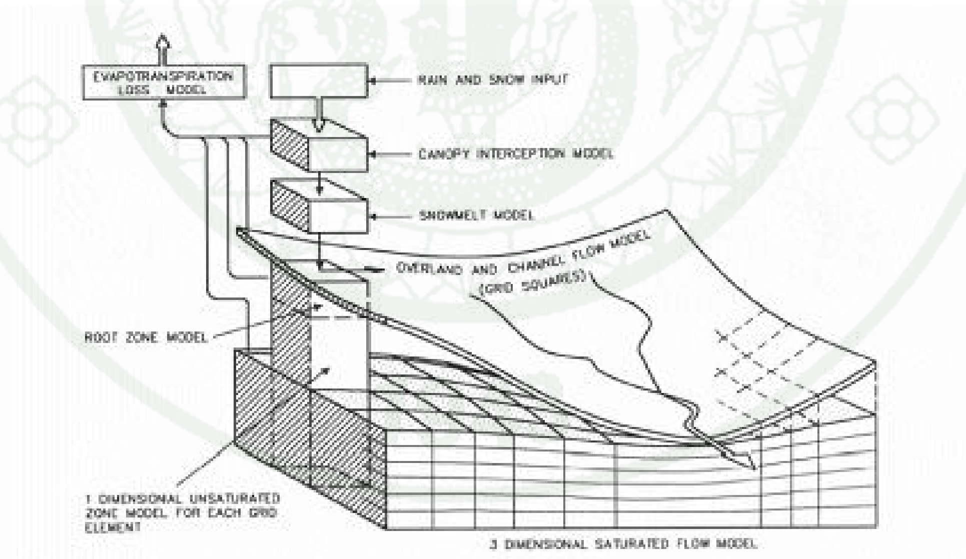

Figure 9 Schematic representation of the SHE system structure

4.3.6 MIKE 11/MIKE SHE

The MIKE SHE model is the subsequent enhancement of SHE model. The most recent model enhancement was the development of an integrated surface water and ground water model by linking the water movement module of MIKE SHE with the channel simulation component of MIKE 11. The MIKE SHE modeling system consists of a water movement module and several water quality modules. The water movement module simulates the hydrological components including evapotranspiration, soil water movement, overland flow, channel flow, and ground water flow. The related water quality modules are: 1) advection-dispersion, 2) particle tracking, 3) sorption and degradation, 4) geochemistry, 5) biodegradation, and 6) crop yield and nitrogen consumption.

MIKE SHE can be used for the analysis, planning, and management of a wide range of water resources and environmental problems related to surface water and groundwater. The MIKE SHE modeling system simulates most major hydrological processes of water movement, including canopy and land surface interception after precipitation, snowmelt, evapotranspiration, overland flow, channel flow, unsaturated subsurface flow, and saturated ground water flow.

MIKE SHE and MIKE 11 are proprietary software, owned and distributed by DHI. DHI’s web site is at http://www.dhigroup.com/Software/WaterResources/MIKESHE.aspx where are also proposed several papers and articles in the section “Reference”. MIKE SHE can be linked to ESRI’s ArcView for advanced Geographic Information System (GIS) applications, and however most data preparation and model set-up can be completed using GIS software, ArcView, or MIKE SHE’s built-in graphic pre-processor.

4.3.7 LISFLOOD

The LISFLOOD is a physically-based model specifically developed at the EC Joint Research Centre to simulate floods in large European drainage basins. LISFLOOD name derives from a soil erosion model made by De Roo for the province of Limburg and then modified for flood scenario modeling. The model was built using the PCRaster Dynamic Modeling Language a GIS capable of dynamic modeling. This model takes into account the influence of topography, precipitation amounts and intensities, antecedent soil moisture content, land use type and soil type.

The LISFLOOD model has been developed to investigate the causes of the flooding and the influence of land use, soil characteristics and antecedent catchment moisture conditions in large river catchments. It is used in the European Flood Alert System (EFAS) for flood forecasting. The model consists of three modules that differ mostly in time step and spatial resolution: the Water Balance (WB) model, the Flood simulation model (FS) and the Flood-Plain simulation model (FP).

The outputs of LISFLOOD consist of hydrographs at user-defined locations in the catchment, usually the locations where also measured discharge is known. Furthermore, time series of for example evapotranspiration, soil moisture content or snow depth can be created at selected locations, if validation data are available. The model produces a number of GIS maps, such as water source areas, discharge coefficient, total precipitation, total evapotranspiration, total groundwater recharge and soil moisture maps.

4.3.8 TOPKAPI

The TOPKAPI (TOPographic Kinematic APproximation and Integration) hydrological model was developed by Prof. E. Todini and the hydrology research group at the University of Bologna. It is based on the idea of combining the kinematic approach and the topography of the basin. It has been developed on the basis of a critical analysis of two popular hydrologic models, the ARNO model and the TOPMODEL model, with the purpose of realizing hydrologic model with a strong physical base and a parsimonious number of physically meaningful parameters, allowing for the application of the model at increasing spatial scale without loosing the physical meaning of the parameters, and overcoming traditional limits of distributed modeling such as small catchments, long computation times, long calibration times, etc.

TOPKAPI, widely used for real-time flood forecasting, is suitable for land-use and climate change impact assessment, for extreme flood analysis, given the possibility of its extension to un-gauged catchments, and is a promising tool for use with General Circulation Models (GCMs). The present TOPKAPI model is structured around five modules (Figure 10) that represent the evapotranspiration, snowmelt, soil water, surface water and channel water components respectively.

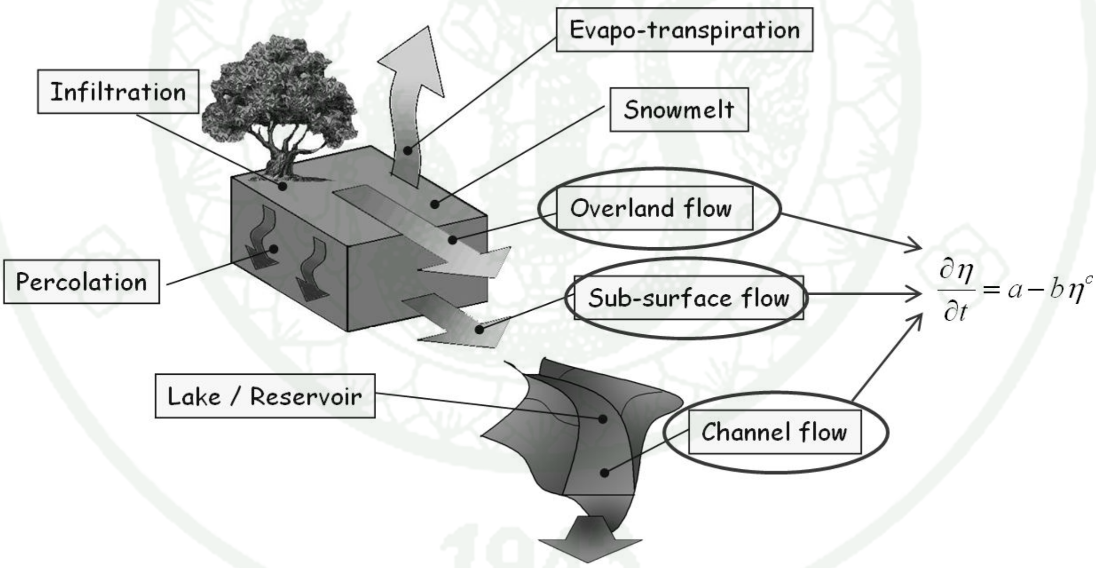

Figure 10 The basic components of the TOPKAPI model

TOPKAPI is a proprietary software, owned and distributed by PROGEA (PROtezione e GEstione Ambientale) SRL. An advantage of the TOPKAPI model is its physical basis.

Classically, hydrologic models have been optimized for point measurements, and not distributed in space and time. The most common technique in use in the US is based on the unit hydrograph approach. Practical application of the unit hydrograph methods through the development of HEC-1 and HEC-HMS have been advanced by the US Army Corps of Engineers, Hydrologic Engineering Center. These techniques often assume basin averaged or sub-basin averaged parameters and inputs giving rise to the lumped model. Derivation of the unit hydrograph for a particular watershed must come from stream gage records or from synthetic estimation techniques. Both methods assume that the rainfall is uniform over the basin and that the basin always responds to the same degree given a unit of rainfall excess. Output is proportional to the rainfall depth and not necessarily to the rainfall intensities during the storm. Lumped models can be less responsive to very intense, but short-lived rainfalls, because the accumulated depth may be small and only over a limited area of the watershed (Vieux and Vieux, 2005).

One of the most significant errors in estimating the hydrologic response of a basin is the precipitation input. When rain gauges sparsely arranged in or near a watershed were the sole means of gauging the input, severe stream flow estimation errors often result. Before the advent of radar and satellite remote sensing of the atmosphere, there was little motivation for the development of better hydrologic models. Given high-resolution spatial and temporal resolution of precipitation intensities, advanced hydrologic modeling techniques hold some promise in better hydrologic prediction. With detailed precipitation input widely available, there is more motivation to formulate a better hydrologic model.

5. Finite element method

5.1 Finite element

Developments in the field of numerical analysis during the 20th century gave rise to various methods that provided approximate solution to equations having partial derivative. Be it the finite differences method, the spectral methods, the finite volumes method or even the singularities method, it cannot be denied that the finite elements method is the most efficient one (Chaskalovic, 2008). In case of the mathematical modeling, this first stage of approximation may turn out to be disastrous.

The Finite-Element Method (FEM) has been widespread in hydro- and environmental engineering for several decades. The computational domain is subdivided in many small finite elements with nodes; in 2D general triangles or quadrilaterals are chosen. The unknown variables are generally defined at the nodes, sometimes at the center of the element or the center of the edges as well. The course of the unknowns over the elements is determined by interpolation functions. For each element, the underlying differential equation is treated by minimizing an integral formulation. Then the single equations are put together, in most cases resulting in a system of equation. Finally, the solution for the whole system is determined, taking initial and/or boundary conditions into account. Due to the possibly unstructured meshes, it is very suitable for complex boundaries and complex inner structures (see Figure 11) (Hinkelmann, 2005)

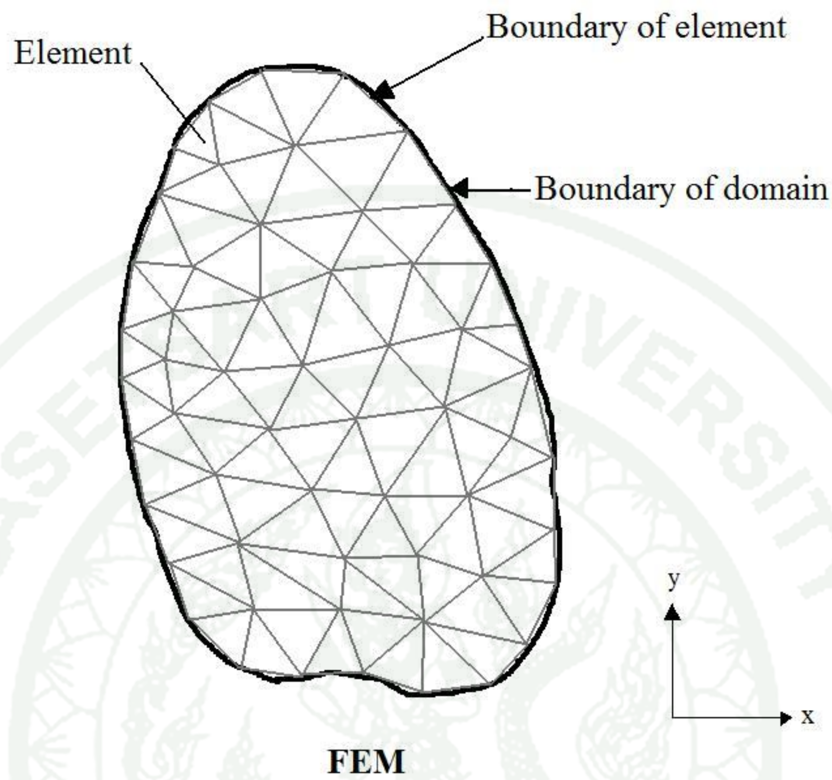

Figure 11 Finite element structure

Advantages of the finite element method (Logan, 2001)

The finite element method has been applied to numerous problems, both structural and nonstructural. This method has a number of advantages that have made it very popular. They include the ability to

5.1.1. Model irregularly shaped bodies quite easily

5.1.2. Handle general load conditions without difficulty

5.1.3. Model bodies composed of several different materials because the element equations are evaluated individually

5.1.4. Handle unlimited numbers and kinds of boundary conditions

5.1.5. Vary the size of the elements to make it possible to use small elements where necessary

5.1.6. Alter the finite element model relatively easily and cheaply

5.1.7. Include dynamic effects

5.1.8. Handle nonlinear behavior existing with large deformation and nonlinear material

5.2 Weighted Residuals methods

The methods of weighted residuals are useful for developing the element equations; particularly popular is Galerkin's method. These methods yield the same results as the energy method wherever the energy method are applicable. The weighted residual methods allow the finite element method to be applied directly to any differential equation.

The solution *u* of a differential equation can be approximated by a linear combination of the parameter *cj* and appropriate functions F*j* as shown in Eq. 5.1

$$u » u_N = \sum_{j=1}^{N} c_j \Phi_j(x) + \Phi_0 \qquad (5.1)$$

The Weighted Residual Method is illustrated on a simple one-dimensional problem. First the problem is given a general mathematical form that is relevant for any differential equation. It is assumed that a problem is governed by the differential equation

$$D(u)=q \qquad (5.2)$$

D is a linear operator here, in this case a differential operator, and *q* is some kind of outer load. If substitute the approximation u_N from Eq. 5.1 into Eq. 5.2, the initial equation is not exactly satisfied anymore, and a remainder, also called residual, is generated.

$$R=D(u_N)-q=D\left(\sum_{j=1}^{N} c_j\Phi_j + \Phi_0\right)-q=D\sum_{j=1}^{N} c_j\Phi_j + D(\Phi_0)-q \neq 0 \qquad (5.3)$$

Assuming u to be a function of only x and y (i.e. a two-dimensional, steady problem), the residual R is N also a function of x and y, but also of cj. With help of the method of weighted residuals, the parameters cj are chosen so that the residual R approaches zero. The weighted integral below has to be solved.

$$\int_\Omega \psi_i(x, y)R(x, y, cj)dx\, dy = 0 \qquad (i=1, 2, \ldots\ldots, N) \qquad (5.4)$$

Integration is over the area Ω(two-dimensional area) and ψ_I are the weighting functions, that are principally different from the approximation functions Φj. Only for the Galerkin method ψ_i and Φ_j are set equal.

Eq. 5.1 to 5.4 are strictly speaking not a finite element formulation. Eq. 5.1 has to be modified first:

$$u(x, y) \approx u^e(x, y) = \sum_{j=1}^{N} u_j^e \Psi_j^e(x, y) \qquad (5.5)$$

where $u^e(x,y)$ is an approximation of the solution ; $u(x,y)$ over the element Ω^e with the vertex count n; u_j^e is the value of the function of $u^e(x,y)$ at the vertex j of the element and $\psi_j^e(x,y)$ is the approximation function for the element. Note that the definition $\psi=\Phi$ has already been made in Eq. 5.5 according to the Galerkin method.

If Eq. 5.5 is substituted into 5.4, obtain the following general expression for the finite element form according to the method of weighted residuals:

$$\int_{\Omega^e} \Psi_i^e(x,y)\left\{D\left(\sum_{j=1}^{n} u_j^e \Psi_j^e(x,y)\right) + D(\Psi_0^e) - q\right\}dxdy = 0 \qquad (5.6)$$

5.3 Runge-Kutta method

The idea of using information about the function $y(x)$ at points other than the initial point of an interval can be generalized to produce more efficient and more accurate schemes for solving ordinary differential equations. Probably the most widely used of these are the methods of Runge and Kutta.

The second-order Runge-Kutta method is a good illustration of the approach. The general method is represented by (Homberger and Wiberg, 2005):

$$y_{i+1} = y_i + ak_1 + bk_2 \tag{5.7}$$

where

$$k_1 = f(x_i,y_i)\Delta x$$
$$k2 = f(x_i+\alpha\Delta x, y_i+\beta k_1)\Delta x$$

and a, b, α and β are constants to be selected. If we set a=l and b=0, we get the simple Euler method. If $a=b=1/2$ and $\alpha=\beta=1$, their recover the modified Euler method.

The second-order Runge-Kutta formula is obtained by setting the values of the four parameters a, b, α and β to make the expression for y_{i+1} agree with the Taylor series through the second-order in Δx. The Runge-Kutta methods are derived by rewriting k_2 in terms of the function f at $[x_i,y_i]$. This can be done using a Taylor series expansion of $f(x_i,y_i)$. The general form of a Taylor series for a function of two variables is

$$f(x+\Delta x, y+\Delta y) = f(x,y)+f_x(x,y)\ \Delta x+f_y(x,y)\ \Delta y + 1/2[f_{xx}(\Delta x)^2+2f_{xy}(\Delta x\Delta y)+f_{yy}(\Delta y)^2]+\ldots \tag{5.8}$$

where the x and y subscripts stand for partial derivatives. This allows us to approximate k_2 as

$$k_2 \cong \Delta x[fx_i, y_i] + (f_x \alpha \Delta x + f_y \beta f \Delta x)_i] \tag{5.9}$$

6. MATLAB Program

MATLAB stands for MATrix LABoratory. Dr. Cleve Molor developed the first program by using Fortran. The first version of Matlab was produced in the mid 1970s as a teaching tool. Now, C language is developed in MATLAB by MathWorks company. The vastly expanded Matlab is now used for mathematical calculations and simulation in companies and government labs ranging from aerospace, car design, signal analysis through to instrument control & financial analysis. Other similar programs are Mathematica and Maple. Mathematica is somewhat better at symbolic calculations but is slower at large numerical calculations (O'Connor, n.d.).

MATLAB is a software program for numeric computation, numerical analysis, matrix computation, signal processing and graphic. It is also a high-level technical computing language. It can solve integrals and differential equations numerically, plot a wide variety of two and three dimensional graphs and technical computing problems easier and faster than with traditional programming languages, such as C, C++, and Fortran. MATLAB also contains a programming language that is rather like Pascal. MATLAB has many functions that numerically solve large systems of linear equations, a system of ordinary differential equations, roots of transcendental equations, integral, statistical problems, optimization problems, control system problems, and many other types of problems encountered in engineering and is used in a wide range of applications for engineering. Furthermore, it is able to do dynamic link with other programs such as Word, Excel and others that work with Windows.

In this study, MATLAB is used to develop mathematical model. Then correctness and accuracy are checked and determined with developed mathematical model. Discharge per unit per width and water depth are applied for computing the amount of flood that solve hydraulic and hydrology problems and forecast a inundation.

MATERIALS AND METHODS

Materials

1. Computer and printer
2. MATLAB Program
3. Topographic map 1:50,000 (Chiang Mai and Lamphun province)

Methods

The finite element method is used for model development. The Galerkin's weighted residual technique is employed to convert the basic governing equations which are in the form of partial differential equations to sets of first-order differential equations. With given initial and boundary conditions these sets of differential equations can be solved to obtain the values of flow rates at various nodal points identified in the study areas which include watershed area and streams.

1. Formulation of Flood Routing Models

In this study, several types of flood routing methods mentioned in the previous section will be used for developing flood forecast model for the Upper Ping river basin. This is because the basin covers very large areas with different topographic features, land use and hydrologic patterns. Though most rivers in the basin flow southwards, there exist some hydraulic structures such as dams which cause backwater effect and river flows are regulated. The following routing methods will be used in this study.

1.1) Kinematic overland flow routing method for computation of overland flow due to excess rainfall on the catchment areas of each river and its tributaries.

1.2) Kinematic channel routing method for stream channels with no backwater effect.

1.3) Detention basin routing method for reservoir.

1.4) Hydraulic routing method for those rivers with backwater effect from dams.

1.1 Kinematic Overland Flow Routing Model

In the kinematic routing model, the inertial and pressure terms in the momentum equation are neglected and the weight or gravity force is approximately balanced by the resistive force of bed friction (Bedient and Huber, 2002). For an overland flow segment on a wide plane with shallow flow, the discharge per unit width can be described as a function of depth as follows:

$$q = \alpha h^m = \frac{\sqrt{S}}{n_o} h^{5/3} \tag{1}$$

in which

q is discharge per unit width

α is conveyance factor = $\frac{\sqrt{S}}{n_o}$

S is overland flow slope

n_o is an effective roughness parameter for overland flow

h is water depth

m = 5/3 from Manning's equation

The continuity equation for one-dimensional flow is

$$\frac{\partial h}{\partial t} + \frac{\partial q}{\partial s} = i_e \tag{2}$$

in which i_e is an excess rainfall

In case of two-dimensional flow, the discharge per unit width q can be separated into 2 components, q_x and q_y, , in which:

$$q_x = q \cos\theta \qquad \text{and} \qquad q_y = q \sin\theta \tag{3}$$

where θ is an angle between the flow direction of q and the x-axis.

Therefore, the continuity equation becomes

$$\frac{\partial h}{\partial t} + \frac{\partial q_x}{\partial x} + \frac{\partial q_y}{\partial y} = i_e \tag{4}$$

which can be written as

$$\frac{\partial h}{\partial t} + \frac{\partial q}{\partial x}\cos\theta + \frac{\partial q}{\partial y}\sin\theta = i_e \tag{5}$$

Replace q by αh^m, we obtain

$$\frac{\partial h}{\partial t} + \frac{\partial\left(\alpha h^m\right)}{\partial x}\cos\theta + \frac{\partial\left(\alpha h^m\right)}{\partial y}\sin\theta = i_e \tag{6}$$

which can be rearranged as

$$\frac{\partial h}{\partial t} + m\alpha h^{m-1}\left(\cos\theta\,\frac{\partial h}{\partial x} + \sin\theta\,\frac{\partial h}{\partial y}\right) - i_e = 0 \tag{7}$$

Providing value of excess rainfall, the finite element method is used to solve for *h* at various time *t*. Details are as follow:

Let the unknown variable *h* is approximated by $\hat{h}$ which is a function of water depths at nodal points identified in the study domain as follows:

$$\hat{h} = \sum_{i=1}^{n} N_i H_i = \boldsymbol{N}^{\boldsymbol{T}}\boldsymbol{H} \tag{8}$$

in which

N_i is an interpolation function

H_i is water depth at node i

N is matrix of N_i

H is matrix of H_i

Replace h in Eq.(8) with $\hat{h}$ will result in some error or residual R, in which

$$R = \frac{\partial \hat{h}}{\partial t} + m\alpha \hat{h}^{m-1}\left(\cos\theta \frac{\partial \hat{h}}{\partial x} + \sin\theta \frac{\partial \hat{h}}{\partial y} \right) - i_e \tag{9}$$

In weighted residual method, this residual is multiplied with a weighting function w and integral of the product over the whole study domain is set to zero, which results in the following weighted residual equation:

$$\iint_{\Omega} w \left\{ \frac{\partial \hat{h}}{\partial t} + m\alpha \hat{h}^{m-1}\left(\cos\theta \frac{\partial \hat{h}}{\partial x} + \sin\theta \frac{\partial \hat{h}}{\partial y} \right) - i_e \right\} dA = 0 \tag{10}$$

which can be rewritten as:

$$\iint_{\Omega} w \left\{ \frac{\partial \hat{h}}{\partial t} + m\alpha \cos\theta \hat{h}^{m-1} \frac{\partial \hat{h}}{\partial x} + m\alpha \sin\theta \hat{h}^{m-1} \frac{\partial \hat{h}}{\partial y} - i_e \right\} dA = 0 \tag{11}$$

The parameter $\alpha = \dfrac{\sqrt{S}}{n_n}$ and angle θ usually vary depending on topography and land use of the area. In this study, it is approximated that the value $\alpha \cos\theta$ and $\alpha \sin\theta$ are expressed in terms of the values at nodal points using the same interpolation function. Let $\alpha_x = \alpha \cos\theta$ and $\alpha_y = \alpha \sin\theta$ be expressed in terms of their nodal values as follow:

$$\alpha_x = \alpha \cos\theta = \sum_{i=1}^{n} N_i \alpha_{xi} = \boldsymbol{N^T \alpha_x} \tag{12}$$

and

$$\alpha_y = \alpha \sin\theta = \sum_{i=1}^{n} N_i \alpha_{yi} = \boldsymbol{N^T \alpha_y} \tag{13}$$

Substitute $\hat{h}$, $\alpha\cos\theta$ and $\alpha\sin\theta$ expressed in terms of their nodal values in Eq.(11), we obtain:

$$\iint_{\Omega} w\left\{\frac{\partial\left(\boldsymbol{N^T H}\right)}{\partial t} + m\boldsymbol{N^T \alpha_x}\left(\boldsymbol{N^T H}\right)^{m-1}\frac{\partial\left(\boldsymbol{N^T H}\right)}{\partial x}\right\}dA$$
$$+\iint_{\Omega} w\left\{m\boldsymbol{N^T \alpha_y}\left(\boldsymbol{N^T H}\right)^{m-1}\frac{\partial\left(\boldsymbol{N^T H}\right)}{\partial y} - i_e\right\}dA = 0 \tag{14}$$

In Galerkin's method, the interpolation function $N_i(i = 1,2,..., n)$ are used as the weighting function *w.* So, we obtain a set of *n* weighted residual equations, which can be written in the matrix form as follows:

$$\iint_{\Omega} \boldsymbol{N}\left\{\frac{\partial\left(\boldsymbol{N^T H}\right)}{\partial t} + m\boldsymbol{N^T \alpha_x}\left(\boldsymbol{N^T H}\right)^{m-1}\frac{\partial\left(\boldsymbol{N^T H}\right)}{\partial x}\right\}dA$$
$$+\iint_{\Omega} \boldsymbol{N}\left\{m\boldsymbol{N^T \alpha_y}\left(\boldsymbol{N^T H}\right)^{m-1}\frac{\partial\left(\boldsymbol{N^T H}\right)}{\partial y} - i_e\right\}dA = \boldsymbol{0} \tag{15}$$

which can be rearranged as

$$\iint_{\Omega} \boldsymbol{NN^T}dA\frac{\partial \boldsymbol{H}}{\partial t} + \iint_{\Omega}\left\{m\boldsymbol{NN^T \alpha_x}\left(\boldsymbol{N^T H}\right)^{m-1}\frac{\partial \boldsymbol{N^T}}{\partial x}\boldsymbol{H}\right\}dA$$
$$\iint_{\Omega}\left\{m\boldsymbol{NN^T \alpha_y}\left(\boldsymbol{N^T H}\right)^{m-1}\frac{\partial \boldsymbol{N^T}}{\partial y}\boldsymbol{H}\right\}dA - \iint_{\Omega}\boldsymbol{N}i_e dA = \boldsymbol{0} \tag{16}$$

In finite element method, the study domain is divided into a number of elements and integral over the whole study domain is equal to the sum of the integrals over these elements. That is we can obtain the integrals in Eq.(16) from:

$$\iint_{\Omega} \boldsymbol{NN^T}dA = \sum_{e=1}^{k}\iint_{A^e}\boldsymbol{N^e N^{eT}}dA \tag{17}$$

$$\iint_{\Omega} \left\{ m\boldsymbol{N}\boldsymbol{N}^{\boldsymbol{T}}\boldsymbol{\alpha}_{\boldsymbol{x}} \left(\boldsymbol{N}^{\boldsymbol{T}}\boldsymbol{H}\right)^{m-1} \frac{\partial \boldsymbol{N}^{\boldsymbol{T}}}{\partial x} \boldsymbol{H} \right\} dA = \sum_{e=1}^{k} \iint_{A^e} \left\{ m\boldsymbol{N}^{\boldsymbol{e}}\boldsymbol{N}^{\boldsymbol{eT}}\boldsymbol{\alpha}_{\boldsymbol{x}}^{\boldsymbol{e}} \left(\boldsymbol{N}^{\boldsymbol{eT}}\boldsymbol{H}^{\boldsymbol{e}}\right)^{m-1} \frac{\partial \boldsymbol{N}^{\boldsymbol{eT}}}{\partial x} \boldsymbol{H}^{\boldsymbol{e}} \right\} dA \tag{18}$$

$$\iint_{\Omega} \left\{ m\boldsymbol{N}\boldsymbol{N}^{\boldsymbol{T}}\boldsymbol{\alpha}_{\boldsymbol{y}} \left(\boldsymbol{N}^{\boldsymbol{T}}\boldsymbol{H}\right)^{m-1} \frac{\partial \boldsymbol{N}^{\boldsymbol{T}}}{\partial y} \boldsymbol{H} \right\} dA = \sum_{e=1}^{k} \iint_{A^e} \left\{ m\boldsymbol{N}^{\boldsymbol{e}}\boldsymbol{N}^{\boldsymbol{eT}}\boldsymbol{\alpha}_{\boldsymbol{y}}^{\boldsymbol{e}} \left(\boldsymbol{N}^{\boldsymbol{eT}}\boldsymbol{H}^{\boldsymbol{e}}\right)^{m-1} \frac{\partial \boldsymbol{N}^{\boldsymbol{eT}}}{\partial y} \boldsymbol{H}^{\boldsymbol{e}} \right\} dA \tag{19}$$

$$\iint_{\Omega} \boldsymbol{N} i_e dA = \sum_{e=1}^{k} \iint_{A^e} \boldsymbol{N}^{\boldsymbol{e}} i_e^e dA \tag{20}$$

In this study, a linear triangular element is used. The interpolation function N is expressed in terms of the natural coordinate system as follows (Connor and Brebbia, 1976):

$$\boldsymbol{N} = \begin{Bmatrix} N_1 \\ N_2 \\ N_3 \end{Bmatrix} = \begin{Bmatrix} \xi_1 \\ \xi_2 \\ \xi_3 \end{Bmatrix} \tag{21}$$

The relationships between natural coordinate system ξ_1, ξ_2, ξ_3 and the Cartesian coordinate system x, y are as follow:

$$\xi_1 = \frac{1}{2A}\left(c_1 + b_1 x + a_1 y\right) \tag{22}$$

$$\xi_2 = \frac{1}{2A}\left(c_2 + b_2 x + a_2 y\right) \tag{23}$$

$$\xi_3 = \frac{1}{2A}\left(c_3 + b_3 x + a_3 y\right) \tag{24}$$

in which

$$a_1 = x_3 - x_2 \;\; ; \;\; a_2 = x_1 - x_3 \;\; ; \;\; a_3 = x_2 - x_1 \tag{25}$$

$$b_1 = y_2 - y_3 \;\; ; \;\; b_2 = y_3 - y_1 \;\; ; \;\; b_3 = y_1 - y_2 \tag{26}$$

$$c_1 = \left(x_2 y_3 - x_3 y_2\right); c_2 = \left(x_3 y_1 - x_1 y_3\right); c_3 = \left(x_1 y_2 - x_2 y_1\right) \tag{27}$$

and

$$\text{A = Area of the triangle} \quad = \frac{1}{2}\left(a_2 b_1 - a_1 b_2\right) \tag{28}$$

From Eq.(22), (23) and (24), the derivatives $\frac{\partial \boldsymbol{N^{eT}}}{\partial x}$ and $\frac{\partial \boldsymbol{N^{eT}}}{\partial y}$ equal $\frac{\boldsymbol{b^T}}{2A}$ and $\frac{\boldsymbol{a^T}}{2A}$, respectively. So, Eq.(18) and (19) become:

$$\iint_{\Omega} \left\{ m\boldsymbol{N}\boldsymbol{N^T}\boldsymbol{\alpha_a}\left(\boldsymbol{N^T}\boldsymbol{H}\right)^{m-1} \frac{\partial \boldsymbol{N^T}}{\partial x} \boldsymbol{H} \right\} dA = \sum_{e=1}^{k} \iint_{A^e} \left\{ m\boldsymbol{N^e}\boldsymbol{N^{eT}}\boldsymbol{\alpha_x^e}\left(\boldsymbol{N^{eT}}\boldsymbol{H^e}\right)^{m-1} \frac{\boldsymbol{b^T}}{2A} \boldsymbol{H^e} \right\} dA \tag{29}$$

$$\iint_{\Omega} \left\{ m\boldsymbol{N}\boldsymbol{N^T}\boldsymbol{\alpha_y}\left(\boldsymbol{N^T}\boldsymbol{H}\right)^{m-1} \frac{\partial \boldsymbol{N^T}}{\partial y} \boldsymbol{H} \right\} dA = \sum_{e=1}^{k} \iint_{A^e} \left\{ m\boldsymbol{N^e}\boldsymbol{N^{eT}}\boldsymbol{\alpha_y^e}\left(\boldsymbol{N^{eT}}\boldsymbol{H^e}\right)^{m-1} \frac{\boldsymbol{a^T}}{2A} \boldsymbol{H^e} \right\} dA \tag{30}$$

The element integrals $\iint_{A^e} \boldsymbol{N^e}\boldsymbol{N^{eT}} dA$ and $\iint_{A^e} \boldsymbol{N^e} i_e^e dA$ are as follow:

$$\iint_{A^e} \boldsymbol{N^e}\boldsymbol{N^{eT}} dA \quad = \quad \frac{A^e}{12}\begin{bmatrix} 2 & 1 & 1 \\ 1 & 2 & 1 \\ 1 & 1 & 2 \end{bmatrix} \tag{31}$$

$$\iint_{A^e} \boldsymbol{N^e} i_e^e dA \quad = \quad \frac{i_e^e A^e}{3}\begin{bmatrix} 1 \\ 1 \\ 1 \end{bmatrix} \tag{32}$$

Element integrals in Eq.(29) and (30) can be obtained by using numerical integration. Once, the element integrals are computed, they are assembled to form system integrals of Eq.(17)-(20).

Eq.(16) can be written in a compact form as:

$$\boldsymbol{M}\,\frac{d\boldsymbol{H}}{dt} + \boldsymbol{M_{hx}} + \boldsymbol{M_{hy}} - \boldsymbol{M_i} \;=\; \boldsymbol{0} \tag{33}$$

In which

$$\boldsymbol{M} \;=\; \iint_{\Omega} \boldsymbol{N}\boldsymbol{N}^{\boldsymbol{T}}\,dA \tag{34}$$

$$\boldsymbol{M_{hx}} \;=\; \iint_{\Omega} \left\{ m\boldsymbol{N}\boldsymbol{N}^{\boldsymbol{T}}\boldsymbol{\alpha_x}\left(\boldsymbol{N}^{\boldsymbol{T}}\boldsymbol{H}\right)^{m-1}\frac{\partial \boldsymbol{N}^{\boldsymbol{T}}}{\partial x}\,\boldsymbol{H} \right\} dA \tag{35}$$

$$\boldsymbol{M_{hy}} \;=\; \iint_{\Omega} \left\{ m\boldsymbol{N}\boldsymbol{N}^{\boldsymbol{T}}\boldsymbol{\alpha_y}\left(\boldsymbol{N}^{\boldsymbol{T}}\boldsymbol{H}\right)^{m-1}\frac{\partial \boldsymbol{N}^{\boldsymbol{T}}}{\partial y}\,\boldsymbol{H} \right\} dA \tag{36}$$

$$\boldsymbol{M_i} \;=\; \iint_{\Omega} \boldsymbol{N} i_e\,dA \tag{37}$$

The Runge-Kutta method can be used to solve this set of first-order differential equations. Once the water depth at each nodal point H_i is known, the discharge per unit width at node *i*, q_i, can be computed from:

$$q_i = \alpha_i H_i^{\,m} = \frac{\sqrt{S_i}}{n_{oi}}\,H_i^{5/3} \tag{38}$$

1.2 Kinematic Channel Routing Model

For stream channels, the basic equations for kinematic routing include (Bedient and Huber, 2002):

Continuity equation:

$$\frac{\partial A}{\partial t} + \frac{\partial Q}{\partial x} = q \tag{39}$$

Q-A Relationship:

$$Q = \alpha_c A^{m_c} \tag{40}$$

in which

A is cross-sectional flow area

Q is stream flow rate

q is lateral inflow per unit length

α_c , m_c are kinematic wave parameters for the particular channel (Table 1).

Replace Q in Eq.(39) by $\alpha_c A^{m_c}$, we obtain:

$$\frac{\partial A}{\partial t} + \frac{\partial\left(\alpha_c A^{m_c}\right)}{\partial x} = q \tag{41}$$

or

$$\frac{\partial A}{\partial t} + m_c \alpha_c A^{m_c - 1}\frac{\partial A}{\partial x} + A^{m_c}\frac{\partial \alpha_c}{\partial x} - q = 0 \tag{42}$$

Eq.(42) is then solved for the value of A at various distance x and time t. The finite element method is used as a numerical method to solve this equation. Details are as follow:

Let the unknown variable A is approximated by $\hat{A}$ which is a function of cross-sectional areas at nodal points identified in the study domain as follows:

$$\hat{A} = \sum_{i=1}^{n} N_i A_i = \boldsymbol{N^T A} \tag{43}$$

in which

N_i is an interpolation function

A_i is cross-sectional area at node i

N is matrix of N_i

A is matrix of A_i

Replace A in Eq.(42) with $\hat{A}$ will result in some error or residual *R,* in which

$$R = \frac{\partial \hat{A}}{\partial t} + m_c \alpha_c \hat{A}^{m_c - 1} \frac{\partial A}{\partial x} + \hat{A}^{m_c} \frac{\partial \alpha_c}{\partial x} - q \tag{44}$$

In weighted residual method, this residual is multiplied with a weighting function *w* and integral of the product over the whole study domain is set to zero, which results in the following weighted residual equation:

$$\int_\Omega \mathrm{w} \left\{ \frac{\partial \hat{A}}{\partial t} + m_c \alpha_c \hat{A}^{m_c - 1} \frac{\partial A}{\partial x} + \hat{A}^{m_c} \frac{\partial \alpha_c}{\partial x} - q \right\} dx = 0 \tag{45}$$

The parameter α_c usually varies with distance along the channel. In this study, it will be expressed in terms of the nodal values using the same interpolation function as $\hat{A}$, that is

$$\alpha_c = \sum_{i=1}^{n} N_i \alpha_{ci} = \boldsymbol{N^T \alpha_c} \tag{46}$$

Substitute $\hat{A}$ and α_c in Eq.(45) by the expressions in Eq.(43) and (46), we obtain:

$$\int_\Omega \mathrm{w} \left\{ \frac{\partial (\boldsymbol{N^T A})}{\partial t} + m_c \boldsymbol{N^T \alpha_c} (\boldsymbol{N^T A})^{m_c - 1} \frac{\partial (\boldsymbol{N^T A})}{\partial x} + (\boldsymbol{N^T A})^{m_c} \frac{\partial (\boldsymbol{N^T \alpha_c})}{\partial x} - q \right\} dx = 0 \tag{47}$$

In Galerkin's method, the interpolation function $N_i (i = 1,2,..., n)$ are used as the weighting function *w.* So, we obtain a set of *n* weighted residual equations, which can be written in the matrix form as follows:

$$\int_{\Omega} \boldsymbol{N}\left\{\frac{\partial\left(\boldsymbol{N}^{T}\boldsymbol{A}\right)}{\partial t} + m_{c}\boldsymbol{N}^{T}\boldsymbol{\alpha_{c}}\left(\boldsymbol{N}^{T}\boldsymbol{A}\right)^{m_{c}-1}\frac{\partial\left(\boldsymbol{N}^{T}\boldsymbol{A}\right)}{\partial x} + \left(\boldsymbol{N}^{T}\boldsymbol{A}\right)^{m_{c}}\frac{\partial\left(\boldsymbol{N}^{T}\boldsymbol{\alpha_{c}}\right)}{\partial x} - q\right\}dx = 0 \tag{48}$$

which can be rearranged as:

$$\int_{\Omega} \boldsymbol{N}\boldsymbol{N}^{T}dx\,\frac{\partial \boldsymbol{A}}{\partial t} + \int_{\Omega} m_{c}\boldsymbol{N}\boldsymbol{N}^{T}\boldsymbol{\alpha_{c}}\left(\boldsymbol{N}^{T}\boldsymbol{A}\right)^{m_{c}-1}\frac{\partial \boldsymbol{N}^{T}}{\partial x}\boldsymbol{A}dx + \int_{\Omega} \boldsymbol{N}\left(\boldsymbol{N}^{T}\boldsymbol{A}\right)^{m_{c}}\frac{\partial \boldsymbol{N}^{T}}{\partial x}\boldsymbol{\alpha_{c}}dx - \int_{\Omega} q\boldsymbol{N}dx = 0 \tag{49}$$

In finite element method, the study domain is divided into a number of elements and integral over the whole study domain is equal to the sum of the integrals over these elements. That is we can obtain the integrals in Eq.(49) from:

$$\int_{\Omega} \boldsymbol{N}\boldsymbol{N}^{T}dx = \sum_{e=1}^{m}\int_{l_e} \boldsymbol{N}^{e}\boldsymbol{N}^{eT}dx \tag{50}$$

$$\int_{\Omega} m_{c}\boldsymbol{N}\boldsymbol{N}^{T}\boldsymbol{\alpha_{c}}\left(\boldsymbol{N}^{T}\boldsymbol{A}\right)^{m_{c}-1}\frac{\partial \boldsymbol{N}^{T}}{\partial x}\boldsymbol{A}dx = \sum_{e=1}^{m}\int_{l_e} m_{c}\boldsymbol{N}^{e}\boldsymbol{N}^{eT}\boldsymbol{\alpha_{c}^{e}}\left(\boldsymbol{N}^{eT}\boldsymbol{A}^{e}\right)^{m_{c}-1}\frac{\partial \boldsymbol{N}^{eT}}{\partial x}\boldsymbol{A}^{e}dx \tag{51}$$

$$\int_{\Omega} \boldsymbol{N}\left(\boldsymbol{N}^{T}\boldsymbol{A}\right)^{m_{c}}\frac{\partial \boldsymbol{N}^{T}}{\partial x}\boldsymbol{\alpha_{c}}dx = \sum_{e=1}^{m}\int_{l_e} \boldsymbol{N}^{e}\left(\boldsymbol{N}^{eT}\boldsymbol{A}^{e}\right)^{m_{c}}\frac{\partial \boldsymbol{N}^{eT}}{\partial x}\boldsymbol{\alpha_{c}^{e}}dx \tag{52}$$

$$\int_{\Omega} q\boldsymbol{N}dx = \sum_{e=1}^{m}\int_{l_e} q^{e}\boldsymbol{N}^{e}dx \tag{53}$$

In determining element integral, the natural coordinate system is used instead of the Cartesian coordinate system. In this study, the one-dimensional linear element with nodes at both ends of the element is used. The coordinate x is replaced by ξ in which $dx = \frac{l^{e}}{2}d\xi$. The values of ξ at nodes 1 and 2 of each element are -1 and +1, respectively. The interpolation function $\boldsymbol{N}^{e}$ is expressed by

$$\boldsymbol{N}^{e} = \begin{Bmatrix} N_1 \\ N_2 \end{Bmatrix} = \begin{Bmatrix} \dfrac{1-\xi}{2} \\ \dfrac{1+\xi}{2} \end{Bmatrix} \tag{54}$$

Derivative of $\boldsymbol{N}^e$ with respect to x is equal to

$$\frac{\partial \boldsymbol{N}^e}{\partial x} = \frac{\partial \boldsymbol{N}^e}{l^e \partial \xi / 2} = \begin{Bmatrix} \dfrac{2\partial N_1}{l^e \partial \xi} \\ \dfrac{2\partial N_2}{l^e \partial \xi} \end{Bmatrix} = \frac{1}{l^e}\begin{Bmatrix} -1 \\ +1 \end{Bmatrix} \tag{55}$$

The element integrals in Eq.(50)-(53) can be written as

$$\int_{l_e} \boldsymbol{N}^e \boldsymbol{N}^{eT} dx = \int_{-1}^{1} \boldsymbol{N}^e \boldsymbol{N}^{eT} l^e d\xi = \int_{-1}^{1} \begin{Bmatrix} \dfrac{1-\xi}{2} \\ \dfrac{1+\xi}{2} \end{Bmatrix} \begin{bmatrix} \dfrac{1-\xi}{2} & \dfrac{1+\xi}{2} \end{bmatrix} \frac{l^e}{2} d\xi$$

$$= \frac{l^e}{8} \int_{-1}^{1} \begin{bmatrix} (1-\xi)^2 & (1-\xi^2) \\ (1-\xi^2) & (1+\xi)^2 \end{bmatrix} d\xi = \frac{l^e}{6} \begin{bmatrix} 2 & 1 \\ 1 & 2 \end{bmatrix} \tag{56}$$

$$\int_{l_e} m_c \boldsymbol{N}^e \boldsymbol{N}^{eT} \boldsymbol{\alpha}_c^e \left(\boldsymbol{N}^{eT} \boldsymbol{A}^e\right)^{m_c - 1} \frac{\partial \boldsymbol{N}^{eT}}{\partial x} \boldsymbol{A}^e dx$$

$$= \int_{-1}^{1} m_c \begin{Bmatrix} \dfrac{1-\xi}{2} \\ \dfrac{1+\xi}{2} \end{Bmatrix} \begin{bmatrix} \dfrac{1-\xi}{2} & \dfrac{1+\xi}{2} \end{bmatrix} \boldsymbol{\alpha}_c^e \left(\frac{1-\xi}{2} A_1^e + \frac{1+\xi}{2} A_2^e \right)^{m_c} \frac{1}{l^e} \left(-A_1^e + A_2^e \right) \frac{l^e}{2} d\xi$$

$$= \frac{m_c \left(A_2^e - A_1^e\right)}{8} \int_{-1}^{1} \begin{Bmatrix} (1-\xi)^2 & (1-\xi^2) \\ (1-\xi^2) & (1+\xi)^2 \end{Bmatrix} \boldsymbol{\alpha}_c^e \left(\frac{1-\xi}{2} A_1^e + \frac{1+\xi}{2} A_2^e \right)^{m_c} d\xi \tag{57}$$

$$\int_{l_e} \boldsymbol{N}^e \left(\boldsymbol{N}^{eT} \boldsymbol{A}^e\right)^{m_c} \frac{\partial \boldsymbol{N}^{eT}}{\partial x} \boldsymbol{\alpha}_c^e dx = \int_{-1}^{1} \begin{Bmatrix} \dfrac{1-\xi}{2} \\ \dfrac{1+\xi}{2} \end{Bmatrix} \left(\frac{1-\xi}{2} A_1^e + \frac{1+\xi}{2} A_2^e \right)^{\boldsymbol{m_c}} \frac{1}{l^e} \left(-\boldsymbol{\alpha}_{c1}^e + \alpha_{c2}^e \right) \frac{l^e}{2} d\xi$$

$$= \frac{\alpha_{c2}^e - \alpha_{c1}^e}{4} \int_{-1}^{1} \begin{Bmatrix} 1-\xi \\ 1+\xi \end{Bmatrix} \left(\frac{1-\xi}{2} A_1^e + \frac{1+\xi}{2} A_2^e \right)^{\boldsymbol{m_c}} d\xi \tag{58}$$

$$\int_{l_e} q^e \boldsymbol{N}^e dx = \int_{-1}^{1} q^e \begin{Bmatrix} \dfrac{1-\xi}{2} \\ \dfrac{1+\xi}{2} \end{Bmatrix} \frac{l^e}{2} d\xi = \begin{Bmatrix} \dfrac{q^e l^e}{2} \\ \dfrac{q^e l^e}{2} \end{Bmatrix} \tag{59}$$

Element integrals in Eq.(57) and (58) can be obtained by numerical integration.

Eq.(49) can be written in a compact form as:

$$\boldsymbol{M}\frac{d\boldsymbol{A}}{dt} + \boldsymbol{M}_a + \boldsymbol{M}_b - \boldsymbol{M}_q = \boldsymbol{0} \tag{60}$$

in which

$$\boldsymbol{M} = \iint_{\Omega} \boldsymbol{N}\boldsymbol{N}^{\boldsymbol{T}} dA \tag{61}$$

$$\boldsymbol{M}_a = \int_{\Omega} m_c \boldsymbol{N}\boldsymbol{N}^T \boldsymbol{\alpha}_c \left(\boldsymbol{N}^T\boldsymbol{A}\right)^{m_c-1} \frac{\partial \boldsymbol{N}^T}{\partial x} \boldsymbol{A} dx \tag{62}$$

$$\boldsymbol{M}_b = \int_{\Omega} \boldsymbol{N}\left(\boldsymbol{N}^T\boldsymbol{A}\right)^{m_c} \frac{\partial \boldsymbol{N}^T}{\partial x} \boldsymbol{\alpha}_c dx \tag{63}$$

$$\boldsymbol{M}_q = \int_{\Omega} q\boldsymbol{N} dx \tag{64}$$

The Runge-Kutta method can be used to solve this set of first-order differential equations. Once the cross-sectional area at each nodal point A_i is known, the discharge at node *i*, Q_i, can be computed from:

$$Q_i = \alpha_{ci} A_i^{m_c} \tag{65}$$

1.3 Detention Basin Routing Model

The storage routing through a reservoir will generally attenuate the peak outflow and lag the time to peak for the outflow hydrograph. The rate of change of storage can be written as the continuity equation (Bedient and Huber, 2002):

$$\frac{dV}{dt} = Q_{in}(t) - Q_{out}(H) \tag{66}$$

in which

V is storage volume

$Q_{in}(t)$ is inflow as a function of time t

$Q_{out}(H)$ is outflow as a function of head H

The change in volume dV due to a change in depth dH can be expressed as:

$$dV = A(H)dH \tag{67}$$

where $A(H)$ is water surface area related to depth H. Then, the continuity equation can be expressed as:

$$\frac{dH}{dt} = \frac{Q_{in}(t) - Q_{out}(H)}{A(H)} \tag{68}$$

or in a general form as:

$$\frac{dH}{dt} = f(H, t) \tag{69}$$

The Runge-Kutta method can be used to determine the value of head H at any time t, providing that the initial value and the relationship between head H and the outflow Q_{out} are given.

1.4 Hydraulic Routing Model

The basic equations for hydraulic routing model are:

Continuity equation:

$$b_\eta \frac{\partial \eta}{\partial t} + \frac{\partial Q}{\partial x} - q = 0 \qquad (70)$$

Momentum equation:

$$\frac{\partial Q}{\partial t} + \frac{Q}{A}\frac{\partial Q}{\partial x} + \frac{A}{\rho}\frac{\partial P_a}{\partial x} + gA\frac{\partial \eta}{\partial x} + g\frac{Q|Q|}{ARC_h^2} = 0 \qquad (71)$$

in which

η is water surface level

Q is river flow rate

b_η is channel width at water surface

q is lateral inflow per unit length

A is cross-sectional area

P_a is atmospheric pressure

R is hydraulic radius

C_h is Chezy's coefficient

Boundary conditions:

$$\eta(L,t) = \eta_L^*(t) \tag{72}$$

$$Q(0,t) = Q^*(t) \tag{73}$$

In this study, the finite element method is used to determine water surface level η and river flow rate Q. Details are as follow:

Let the unknown variables η and Q in Eq. (70) and (71) are respectively replaced by approximated functions $\hat{\eta}$ and $\hat{Q}$, which are expressed in terms of their nodal values, i.e.,

$$\hat{\eta} = \sum_{i=1}^{n} N_i \eta_i = \boldsymbol{N}^T \boldsymbol{\eta} \tag{74}$$

and

$$\hat{Q} = \sum_{i=1}^{n} N_i Q_i = \boldsymbol{N}^T \boldsymbol{Q} \tag{75}$$

This will result in the following residuals:

$$R_\eta = b_\eta \frac{\partial \hat{\eta}}{\partial t} + \frac{\partial \hat{Q}}{\partial x} - q \tag{76}$$

and

$$R_Q = \frac{\partial \hat{Q}}{\partial t} + \frac{\hat{Q}}{A}\frac{\partial \hat{Q}}{\partial x} + \frac{A}{\rho}\frac{\partial P_a}{\partial x} + gA\frac{\partial \hat{\eta}}{\partial x} + g\frac{\hat{Q}\left|\hat{Q}\right|}{ARC_h^2} \tag{77}$$

These residuals are then multiplied with weighting function w and the integrals of their products over the study domain are set to zero. This results in the following weighted residual equations:

$$\int_\Omega w\left\{ b_\eta \frac{\partial \hat{\eta}}{\partial t} + \frac{\partial \hat{Q}}{\partial x} - q \right\} dx = 0 \tag{78}$$

and

$$\int_{\Omega} w\left\{\frac{\partial \hat{Q}}{\partial t}+\frac{\hat{Q}}{A}\frac{\partial \hat{Q}}{\partial x}+\frac{A}{\rho}\frac{\partial P_a}{\partial x}+gA\frac{\partial \hat{\eta}}{\partial x}+g\frac{\hat{Q}\left|\hat{Q}\right|}{ARC_h^2}\right\}dx=0 \tag{79}$$

In Galerkin technique, the interpolation functions N_i (i=1,2,..,n) are used as a weighting function. Thus, the following sets of weighted residual equations are obtained:

$$\int_{\Omega} N_i\left\{b_\eta\frac{\partial \hat{\eta}}{\partial t}+\frac{\partial \hat{Q}}{\partial x}-q\right\}dx=0 \quad (i=1,2,..,n) \tag{80}$$

and

$$\int_{\Omega} N_i\left\{\frac{\partial \hat{Q}}{\partial t}+\frac{\hat{Q}}{A}\frac{\partial \hat{Q}}{\partial x}+\frac{A}{\rho}\frac{\partial P_a}{\partial x}+gA\frac{\partial \hat{\eta}}{\partial x}+g\frac{\hat{Q}\left|\hat{Q}\right|}{ARC_h^2}\right\}dx=0 \quad (i=1,2,\ldots,n) \tag{81}$$

which can be written in the matrix form as:

$$\int_{\Omega} \boldsymbol{N}\left\{b_\eta\frac{\partial \hat{\eta}}{\partial t}+\frac{\partial \hat{Q}}{\partial x}-q\right\}dx=\mathbf{0} \tag{82}$$

and

$$\int_{\Omega} \boldsymbol{N}\left\{\frac{\partial \hat{Q}}{\partial t}+\frac{\hat{Q}}{A}\frac{\partial \hat{Q}}{\partial x}+\frac{A}{\rho}\frac{\partial P_a}{\partial x}+gA\frac{\partial \hat{\eta}}{\partial x}+g\frac{\hat{Q}\left|\hat{Q}\right|}{ARC_h^2}\right\}dx=\mathbf{0} \tag{83}$$

Besides the unknown variables $\hat{\eta}$ and $\hat{Q}$, the parameters b_η, A, P and R can be expressed in terms of their nodal values as follow:

$$b_\eta=\sum_{i=1}^{n}N_i b_{\eta_i}=\boldsymbol{N}^T\boldsymbol{b}_{\boldsymbol{\eta}} \tag{84}$$

$$A=\sum_{i=1}^{n}N_i A_i=\boldsymbol{N}^T\boldsymbol{A} \tag{85}$$

$$P = \sum_{i=1}^{n} N_i P_i \ = \boldsymbol{N}^T \boldsymbol{P} \tag{86}$$

$$R = \sum_{i=1}^{n} N_i R_i \ = \boldsymbol{N}^T \boldsymbol{R} \tag{87}$$

Substitute into Eq.(82) and (83), we obtain

$$\int_{\Omega} \boldsymbol{N} \left\{ \boldsymbol{N}^T \boldsymbol{b}_{\eta} \frac{\partial(\boldsymbol{N}^T \boldsymbol{\eta})}{\partial t} + \frac{\partial(\boldsymbol{N}^T \boldsymbol{Q})}{\partial x} - q \right\} dx = \mathbf{0} \tag{88}$$

and

$$\int_{\Omega} \boldsymbol{N} \left\{ \frac{\partial(\boldsymbol{N}^T \boldsymbol{Q})}{\partial t} + \frac{\boldsymbol{N}^T \boldsymbol{Q}}{\boldsymbol{N}^T \boldsymbol{A}} \frac{\partial(\boldsymbol{N}^T \boldsymbol{Q})}{\partial x} + \frac{\boldsymbol{N}^T \boldsymbol{A}}{\rho} \frac{\partial(\boldsymbol{N}^T \boldsymbol{P}_a)}{\partial x} + g\boldsymbol{N}^T \boldsymbol{A} \frac{\partial(\boldsymbol{N}^T \boldsymbol{\eta})}{\partial x} + g \frac{\boldsymbol{N}^T \boldsymbol{Q} \left| \boldsymbol{N}^T \boldsymbol{Q} \right|}{\boldsymbol{N}^T \boldsymbol{A} \boldsymbol{N}^T \boldsymbol{R} C_h^2} \right\} dx = \mathbf{0} \tag{89}$$

which can be rearranged as

$$\int_{\Omega} \boldsymbol{N}\boldsymbol{N}^T \boldsymbol{b}_{\eta} \boldsymbol{N}^T dx \frac{\partial \boldsymbol{\eta}}{\partial t} + \int_{\Omega} \boldsymbol{N} \frac{\partial \boldsymbol{N}^T}{\partial x} dx \boldsymbol{Q} - \int_{\Omega} \boldsymbol{N} q dx = \mathbf{0} \tag{90}$$

and

$$\int_{\Omega} \boldsymbol{N}\boldsymbol{N}^T dx \frac{\partial \boldsymbol{Q}}{\partial t} + \int_{\Omega} \frac{\boldsymbol{N}\boldsymbol{N}^T \boldsymbol{Q}}{\boldsymbol{N}^T \boldsymbol{A}} \frac{\partial(\boldsymbol{N}^T \boldsymbol{Q})}{\partial x} dx + \int_{\Omega} \frac{\boldsymbol{N}\boldsymbol{N}^T \boldsymbol{A}}{\rho} \frac{\partial \boldsymbol{N}^T}{\partial x} dx \boldsymbol{P}_a + \int_{\Omega} g\boldsymbol{N}\boldsymbol{N}^T \boldsymbol{A} \frac{\partial \boldsymbol{N}^T}{\partial x} dx \boldsymbol{\eta} + \int_{\Omega} g \frac{\boldsymbol{N}\boldsymbol{N}^T \boldsymbol{Q} \left| \boldsymbol{N}^T \boldsymbol{Q} \right|}{\boldsymbol{N}^T \boldsymbol{A} \boldsymbol{N}^T \boldsymbol{R} C_h^2} dx = \mathbf{0} \tag{91}$$

Eqs.(90) and (91) can be written in compact form as:

$$\boldsymbol{M}_{\eta} \frac{d\boldsymbol{\eta}}{dt} + \boldsymbol{M}_x \boldsymbol{Q} - \boldsymbol{M}_q \ = \mathbf{0} \tag{92}$$

and

$$\boldsymbol{M} \frac{d\boldsymbol{Q}}{dt} + \boldsymbol{M}_Q + \boldsymbol{M}_{pa} \boldsymbol{P}_a + \boldsymbol{M}_{ax} \boldsymbol{\eta} + \boldsymbol{M}_{Ch} \ = \mathbf{0} \tag{93}$$

in which

$$\boldsymbol{M}_{\eta} = \int_{\Omega} \boldsymbol{N}\boldsymbol{N}^{T}\boldsymbol{b}_{\eta}\boldsymbol{N}^{T}\,dx \tag{94}$$

$$\boldsymbol{M}_{x} = \int_{\Omega} \boldsymbol{N}\frac{\partial \boldsymbol{N}^{T}}{\partial x}\,dx \tag{95}$$

$$\boldsymbol{M}_{q} = \int_{\Omega} \boldsymbol{N}q\,dx \tag{96}$$

$$\boldsymbol{M} = \int_{\Omega} \boldsymbol{N}\boldsymbol{N}^{T}\,dx \tag{97}$$

$$\boldsymbol{M}_{Q} = \int_{\Omega} \frac{\boldsymbol{N}\boldsymbol{N}^{T}\boldsymbol{Q}}{\boldsymbol{N}^{T}\boldsymbol{A}}\frac{\partial(\boldsymbol{N}^{T}\boldsymbol{Q})}{\partial x}\,dx \tag{98}$$

$$\boldsymbol{M}_{Pa} = \int_{\Omega} \frac{\boldsymbol{N}\boldsymbol{N}^{T}\boldsymbol{A}}{\rho}\frac{\partial \boldsymbol{N}^{T}}{\partial x}\,dx \tag{99}$$

$$\boldsymbol{M}_{ax} = \int_{\Omega} g\boldsymbol{N}\boldsymbol{N}^{T}\boldsymbol{A}\frac{\partial \boldsymbol{N}^{T}}{\partial x}\,dx \tag{100}$$

$$\boldsymbol{M}_{Ch} = \int_{\Omega} g\frac{\boldsymbol{N}\boldsymbol{N}^{T}\boldsymbol{Q}\left|\boldsymbol{N}^{T}\boldsymbol{Q}\right|}{\boldsymbol{N}^{T}\boldsymbol{A}\boldsymbol{N}^{T}\boldsymbol{R}C_{h}^{2}}\,dx \tag{101}$$

In finite element method, the study domain is divided into a number of elements and integral over the whole study domain is equal to the sum of the integrals over these elements. Then, the Runge-Kutta method can be used to solve these two sets of first-order differential equations. As a result, water surface elevation η and river discharge Q at each node in the study domain are obtained.

2. Study area

The study area was in the Upper Ping River basin, which covers a catchment area of around 25,370 km^2 in the provinces of Chiang Mai and Lamphun, northern

Thailand. The Ping River originates in Chiang Dao District, north of Chiang Mai and flows to the south where it enters the Bhumibol Dam - a large dam with an active storage capacity of 9.7 billion m^3. In this study, the Upper Ping river basin was divided to 14 sub-basins in Figure 2 that show the area on Table 2.

Table 2 Sub-basin number ,catchment area and the number of element in the Upper Ping river basin

Sub-basin No.	Sub-basin	Area (km^2)	No. of Element
1	Mae Taeng	1957	1300
2	Mae Ping part 1	1974	305
3	Mae Ngad	1285	286
4	Mae Kuang	2734	467
5	Mae Rim	508	270
6	Mae Ping part 2	1616	362
7	Mae Khan	1833	527
8	Mae Klang	616	316
9	Mae Chaem upper	2061	412
10	Mae Chaem lower	1834	477
11	Mae Teun	2896	-
12	Mae Lee	2081	407
13	Mae Had	520	-
14	Mae Ping part 3	3452	75
	Total	25367	4906

In each sub basin was divided in sub-catchment. The concept is previously division area in the original of river. A boundary of each catchment is set by considering the ridge of a hill, tributaries and flow direction. In the catchment, sub-area is separated by finite element method. Then the next catchment is established follow the channel flow. So, a lot of catchments are along the main river. For example, the Mae Taeng river basin was separated to 26 sub-catchments that show in Figure 12.

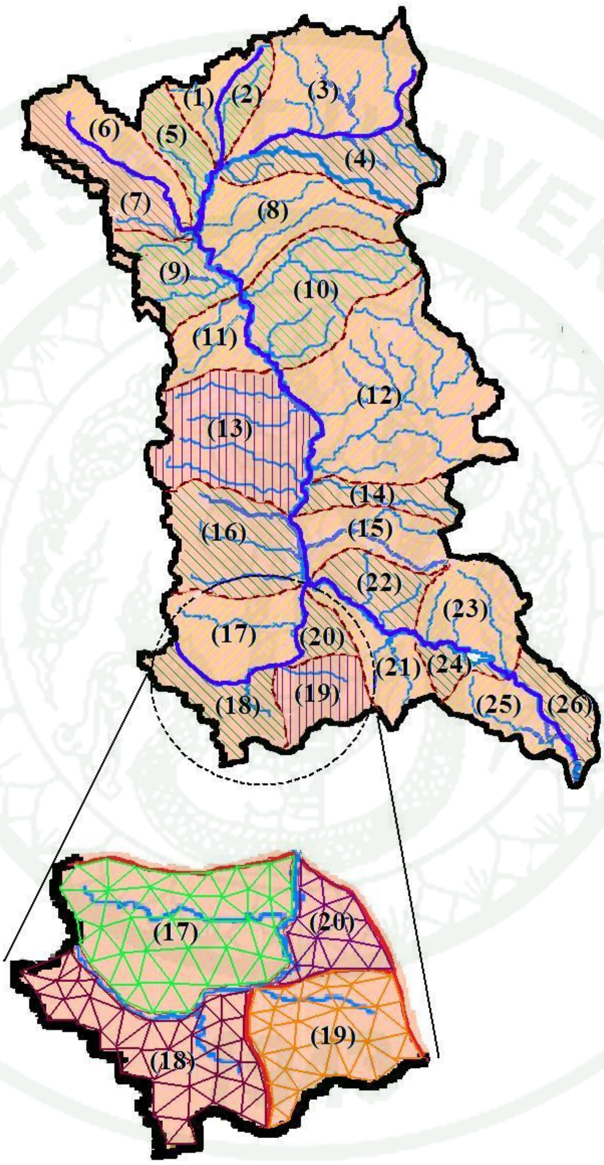

Figure 12 Division of the Mae Taeng catchment

3. Data collection

Hourly rainfall data, water level, cross-sectional area and discharge data collected by the Royal Irrigation Department (RID) and the Thai Meteorological Department (TMD) were used in this study. The rainfall data were used as the input data for the mode to simulate flow hydrographs for the catchments.

3.1 Rainfall data

In this study, 3 hours rainfall data from TMD were input to calculate water flow in the model by using finite element method. The excess rainfall data are from 8 stations in study area and locate as follow in Table 3 :

Table 3 Rain gauged station used in this study

Station	Code	Location	
		Latitude	Longitude
Chiang Mai (CM)	327501	18 47	98 59
Doi Ang Kang, CM	327202	19 57	99 09
Mae Hong Son (MHS)	300201	19 18	97 50
Mae Sariang, MHS	300202	18 10	97 56
Lamphun	329201	18 34	99 02
Lampang (LP)	328201	18 17	99 31
Tern, LP	328202	17 19	99 27
Bhumibol Dam, Tak	376203	17 14	98 52

The estimation of rainfall in each sub basin was calculated by using Thiessen method that shows the detail in Figure 13 and Table 3.

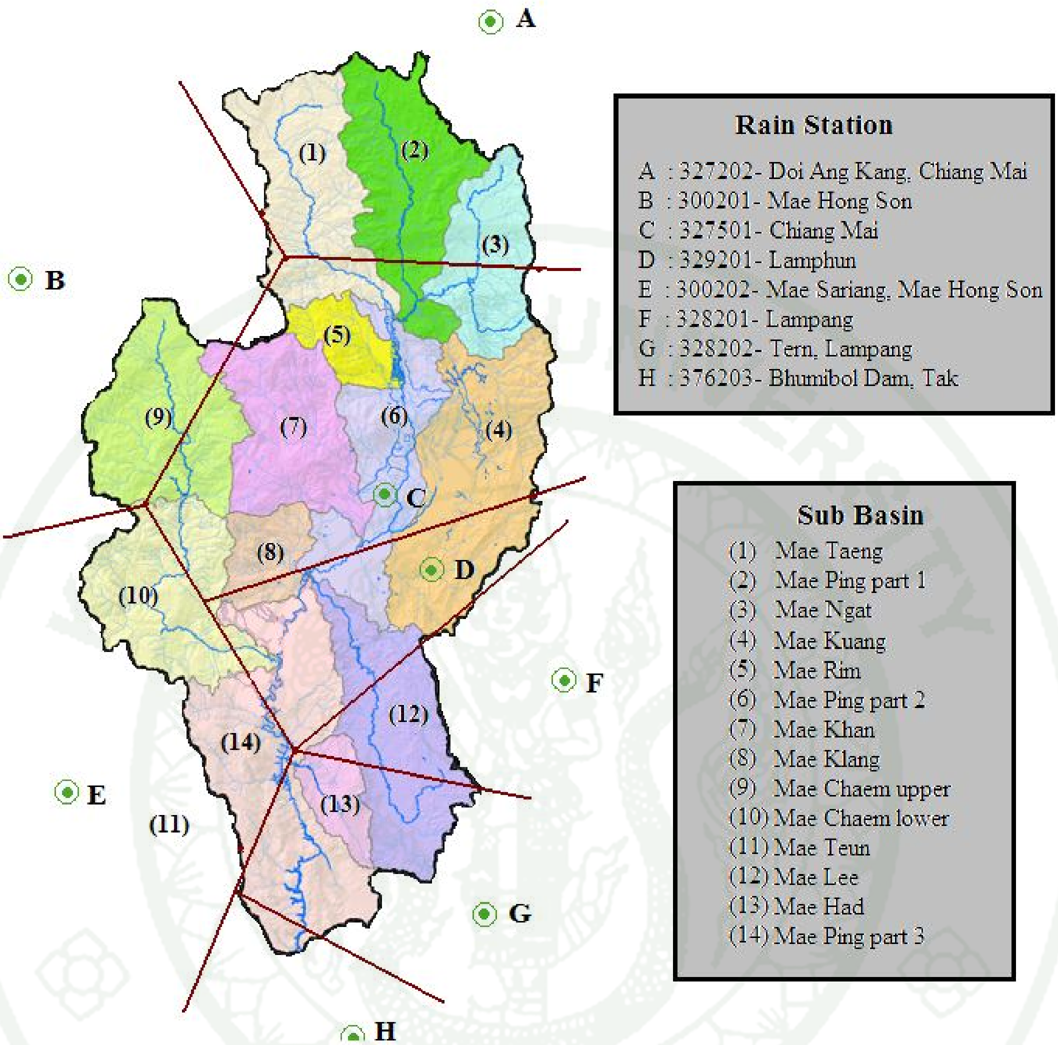

Figure 13 Division rain gauge station which influence to rainfall in sub-catchments within Upper Ping River Basin by using Theissen method

Table 4 The factor of Thiessen of sub-catchments for different rain gauges

Sub-Basin No.	Station Code							
	327501	327201	300201	300202	329201	328201	328202	376203
1	0.108	0.867	0.026	-	-	-	-	-
2	0.152	0.848	-	-	-	-	-	-
3	0.64	0.36	-	-	-	-	-	-
4	0.512	-	-	-	0.488	-	-	-
5	1.0	-	-	-	-	-	-	-
6	0.842	-	-	-	-	-	-	-
7	0.945	-	0.055	-	0.158	-	-	-
8	-	-	-	-	-	-	-	-
9	0.243	-	0.757	-	-	-	-	-
10	0.123	-	-	0.86	0.018	-	-	-
11	-	-	-	0.482	-	-	-	0.518
12	-	-	-	-	0.18	0.336	0.483	-
13	-	-	-	-	-	-	1.0	-
14	-	-	-	0.324	0.361	0.01	0.29	0.014

3.2 Runoff data

The study used daily runoff data at 11 stations and flow release from Mae Ngad Dam and Mae Kuang Dam. These data are from RID. Runoff data at the upstream and downstream were used for calibration with the simulated data. Table 5 and Figure 14 show the location of 11 runoff stations used in this study.

Table 5 Location of Runoff Stations

Code station	Location	Lat. E	Long. W
P.1	Nawarat Bridge, Muang district, Chiang Mai	18^{o}- 47' - 09"	99^{o}-00' - 29"
P.5	Tha Sing Phithak Bridge, Muang district, Chiang Mai	18^{o}- 34' - 32"	99^{o}- 00' - 44"
P.21	Ban Rim Tai, Ban Rim Tai district, Chiang Mai	18^{o}- 55' - 29"	98^{o}- 56' - 34"
P.24A	Pracha Uthit Bridge, Chom Thong district, Chiang Mai	18^{o}- 23' - 15"	98^{o}- 40' - 51"
P.67	Ban Mae Tae, San Sai district, Chiang Mai	19^{o}- 01' - 11"	98^{o}- 57' - 42"
P.71	Ban Klang, San Pa Tong district, Chiang Mai	18^{o}- 32' - 14"	98^{o}- 51' - 47"
P.73	Ban Sop Soi, Chom Thong district, Chiang Mai	18^{o}- 17' - 18"	98^{o}- 39' - 11"
P.75	Ban Cho Lae, Mae Taeng district, Chiang Mai	19^{o}- 08' - 52"	99^{o}- 00' - 36"
P.85	Ban Loiy Kaew, Ban Hong district, Lamphun	18^{o}- 21' - 49"	98^{o}- 46' - 31"
P.87	Ban Pha Sang, Pha Sang district, Lamphun	18^{o}- 31' - 04"	98^{o}- 56' - 42"
P.92	Ban Muang Keid, Mae Taeng district, Chiang Mai	19^{o}- 13' - 15"	98^{o}- 50' - 51"

3.2 Cross-sectional area data

The 11 cross-sections of channels located along the Ping river which among P.75-P.73 stations. The main river and its tributaries were used in trapezoidal shape for channel flow calculation.

3.3 Parameter from topographic map

Flow direction: The flow direction map was derived from the flow from a higher level to a lower level that was perpendicular with contours. The angel between the flow direction and the x-axis (θ) was also collected.

Slope: The slope was defined for overland and channel flow in the Manning equation. The slope was from differential in elevation divided by a horizontal distance between contours. At this point the slope map presented overland slope. The slope of channel was estimated from gauged station.

Infiltration: In this study, excess rainfall was used in calculation. So, runoff coefficient was used to determine the peak amount of runoff from a surface. It is often based on soil type, land use and rainfall intensity.

Roughness: The hydraulic roughness for overland flow can be derived from type of land use in topographic map. The channel roughness values were estimated from type of stream/channel surface.

Channels: Channels were parameterized with map defined channel bed slope from topographic map and estimated from gauged station. The channel width, channel depth and channel side slope data were from cross-sectional channel from RID.

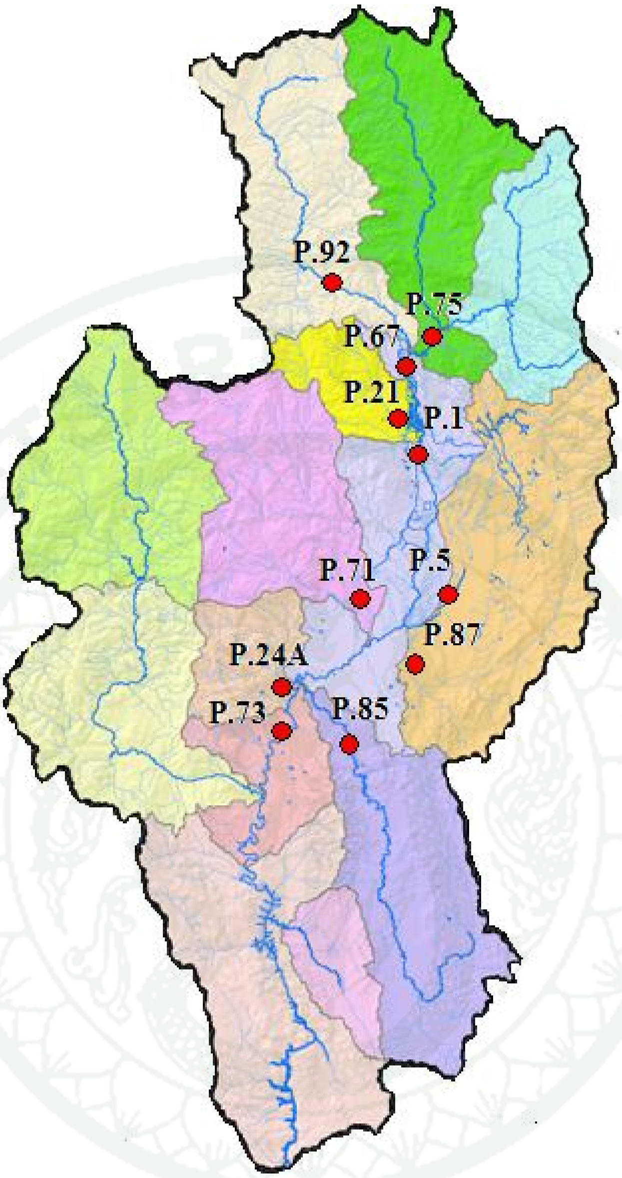

Figure 14 Location of runoff stations

4. Development of Computer Programs

Computer programs shall be written using MATLAB to help solve the formulated flood routing models. The programs shall be verified by applying to a simple study area and determine the obtained results.

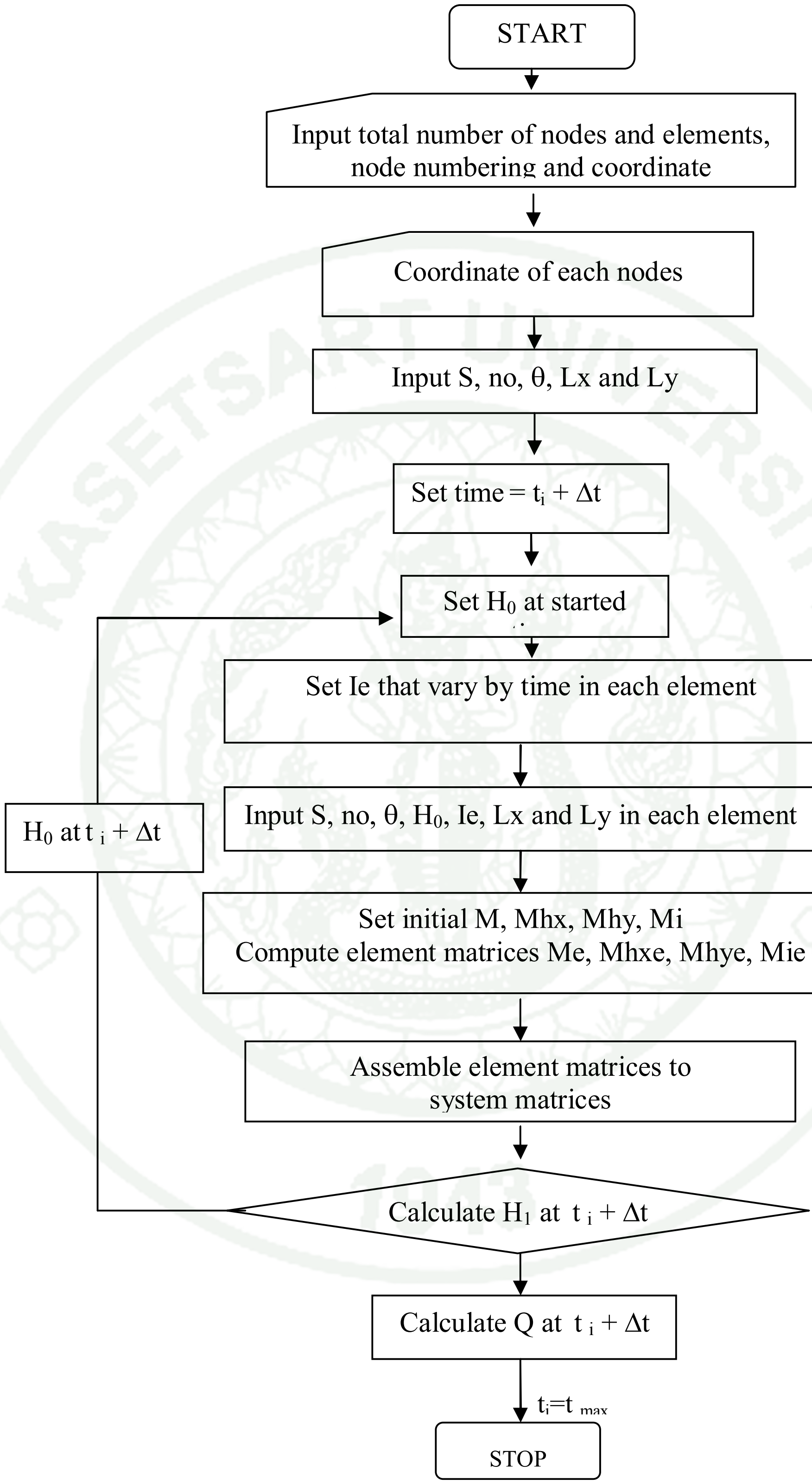

Figure 15 MATLAB diagram of calculation 2-D overland flow

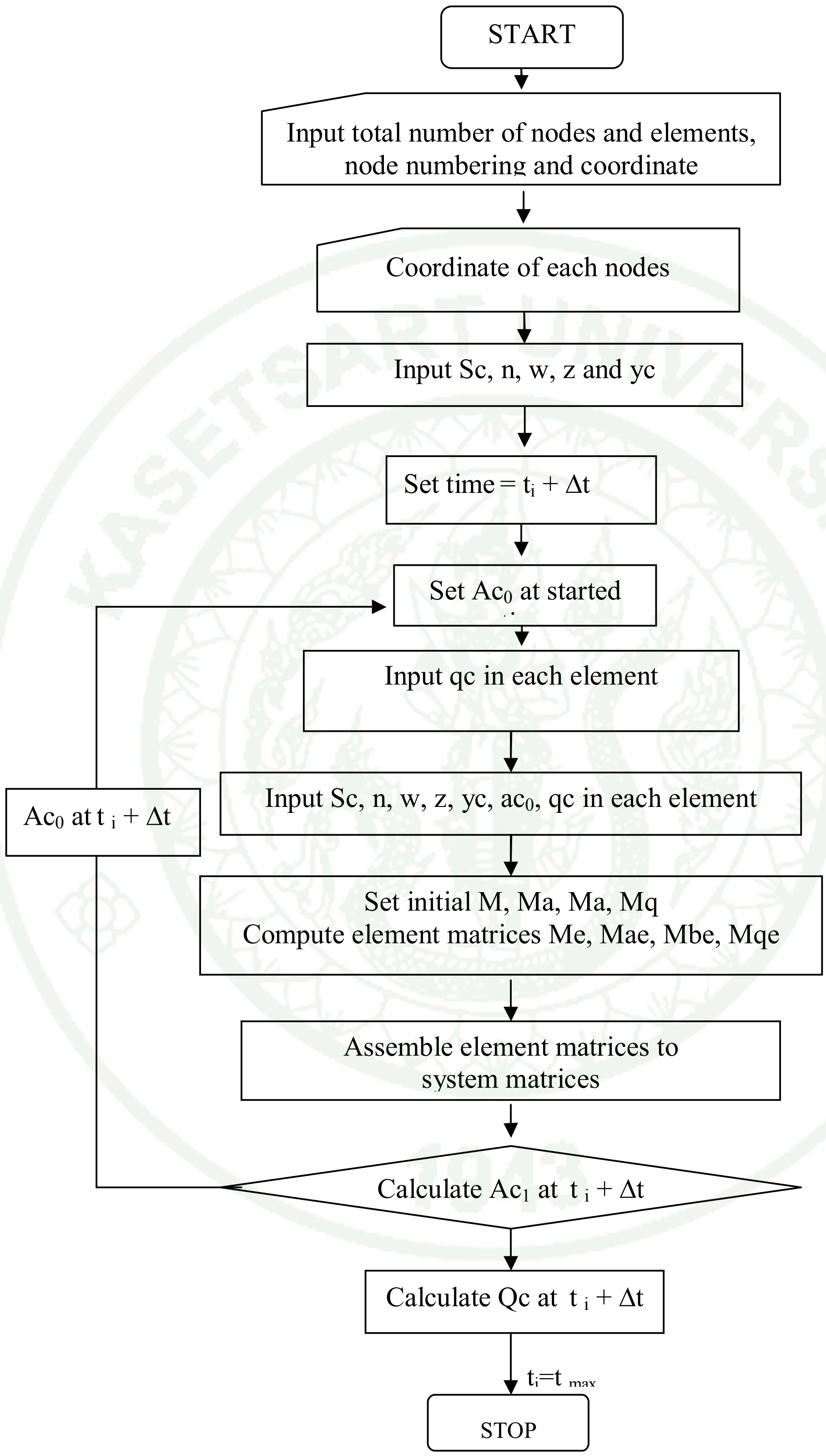

Figure 16 MATLAB diagram of calculation 1-D channel flow

5. Model Application

The above mentioned models have been applied for flood routing in the Upper Ping river basin, Northern Thailand. In order to reduce the number of equations to be solved for the rates of overland flow at nodal points, the whole watershed area of the Upper Ping river is divided into a number of sub-basins. The overland flow caused by rainfall in each sub-basin is computed separately. This results in the rates of lateral inflow into various reaches of streams which receive surface water from these sub-basins. The stream flow rate is then computed starting from the most upstream reach and the obtained results are used as upstream boundary condition for the next downstream reach. With this approach the overland flow computation in each sub-basin can be made separately over the whole simulation period, while the stream flow computation must be made reach by reach to cover the whole Upper Ping river in each time step.

6. Model calibration

Performance Statistics

The correlation coefficient (r) describes the degree of collinearity between simulated and measured data. The correlation coefficient, which ranges from −1 to 1, is an index of the degree of linear relationship between observed and simulated data. If $r = 0$, no linear relationship exists. If $r = 1$ or -1, a perfect positive or negative linear relationship exists.

The efficiency index or Nash-Sutcliff criterion is often used to measure the performance of a hydrological model. The efficiency index lies in the interval from $-\infty$ to +1. The zero value means the model performs equal to a naïve predication, that is, a prediction using an average observed value, whereas values <0.0 indicates that the mean observed value is a better predictor than the simulated value, which indicates unacceptable performance. A value of one is a perfect fit.

The root mean square error defined by Equation (6.3) measures the average error between the observed and the simulated discharges. The closer the RMSE value is to zero, the better the performance of the model. The RMSE was used to measure the agreement between the observed and simulated water balance.

The results were compared to the observed data by using three statistical indicators to evaluate the performance, the correlation coefficient (*r*) approaches 1, the root mean square error (RMSE) approaches zero, and the efficiency index (EI), that show in Equation 6.1, 6.2 and 6.3 respectively.

$$r = \frac{\sum_{i=1}^{N}\left(Q_{oi} - \overline{Q_o}\right)\times\left(Q_{ci} - \overline{Q_o}\right)}{\left[\sum_{i=1}^{N}\left(Q_{oi} - \overline{Q_o}\right)^2 \times \sum_{i=1}^{N}\left(Q_{ci} - \overline{Q_o}\right)^2\right]^{0.5}} \tag{6.1}$$

$$EI = \frac{\sum_{i=1}^{N}\left(Q_{oi} - \overline{Q_o}\right)^2 \times \sum_{i=1}^{N}\left(Q_{oi} - Q_{ci}\right)^2}{\left[\sum_{i=1}^{N}\left(Q_{oi} - \overline{Q_o}\right)^2\right]} \tag{6.2}$$

$$RMSE = \sqrt{\frac{1}{N}\sum_{i=1}^{N}\left(Q_{oi} - Q_{ci}\right)^2} \tag{6.3}$$

Where, $\overline{Q_o}$ is the averaged observed data, $\overline{Q_c}$ is the average model results, Q_{oi} is the observed data at the time I, Q_{ci} is the model result at the time I, *N* is the number of data points.

The simulated model was used to estimate flow hydrograph within 11 stations which mentioned in data collection. A flood event was selected in 2010 during July – September to be used for model calibration. On September 17th, 2010 the maximum flow rate at P.1 station was 370 m^3/s which exceeded channel capacity (350 m^3/s). The suitable Manning’s n for both overland flow and channel flow were selected by trial and error to obtain the best value between calculated and observed hydrograph at each station.

RESULTS AND DISCUSSION

Results

The model parameters used for the overland flow and channel flow computation are shown in Table 6. After applying these parameters together with the rainfall data in the model, the simulation results are compared with the observed data at 11 runoff stations as shown in Figures 17-26.

Table 6 Model parameters for the runoff stations

Runoff station	Roughness coefficient (n)		Runoff coefficient (C)	Channel shape			Channel slope
	For overland flow	For channel flow		w	z	y_c	
P.1	0.6	0.25	0.2	70	5	8	0.0015
P.5	0.6	0.25	0.4	50	2.5	7	0.0015
P.21	0.6	0.25	0.2	20	2	4	0.0076
P.24A	0.6	0.25	0.15	25	0.5	5	0.0133
P.67	0.6	0.25	0.2	45	10	8	0.0020
P.71	0.7	0.25	0.2	27	2	6	0.0050
P.73	0.6	0.25	0.2	140	2.5	7	0.0009
P.75	0.6	0.25	0.2	50	2.5	6	0.0026
P.85	0.6	0.25	0.2	30	5	6	0.0027
P.87	0.6	0.1	0.1	30	0	4	0.0030
P.92	0.6	0.25	0.6	40	5	7	0.0032

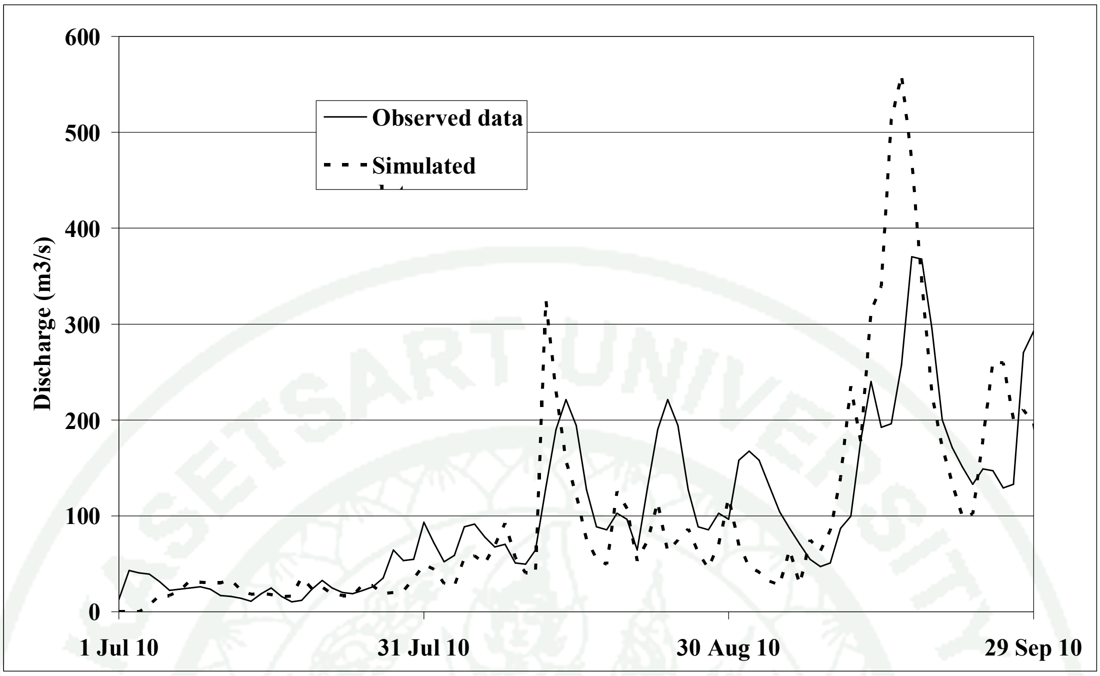

Figure 17 Simulated and observed flood hydrograph at the runoff station P.1 in 2010

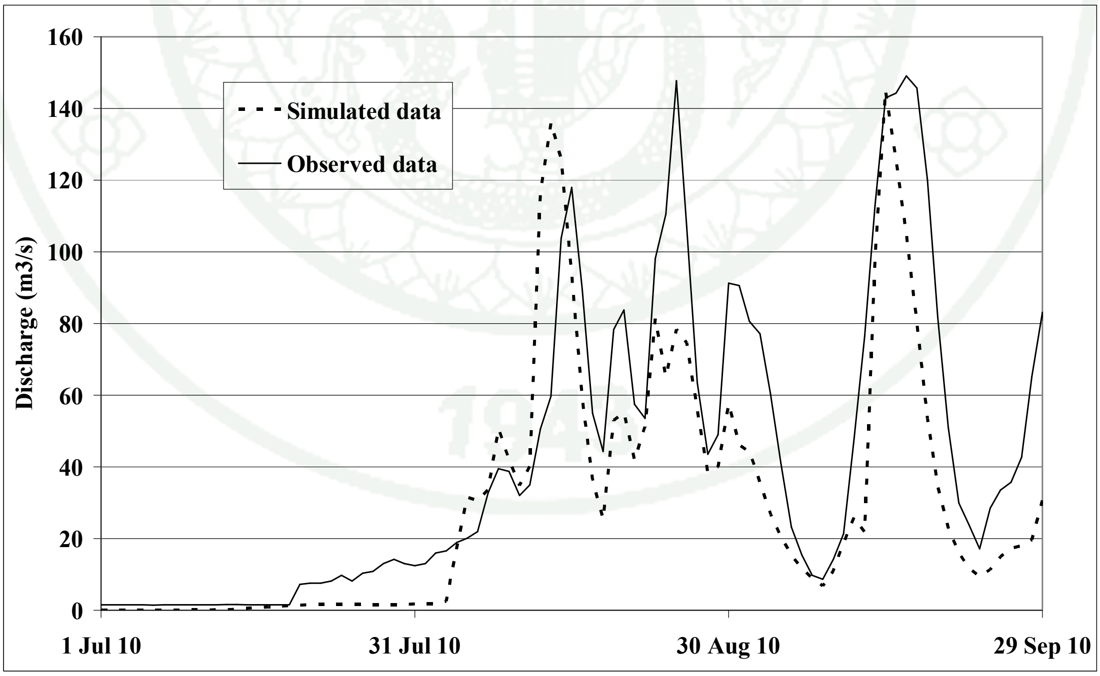

Figure 18 Simulated and observed flood hydrograph at the runoff station P.5 in 2010

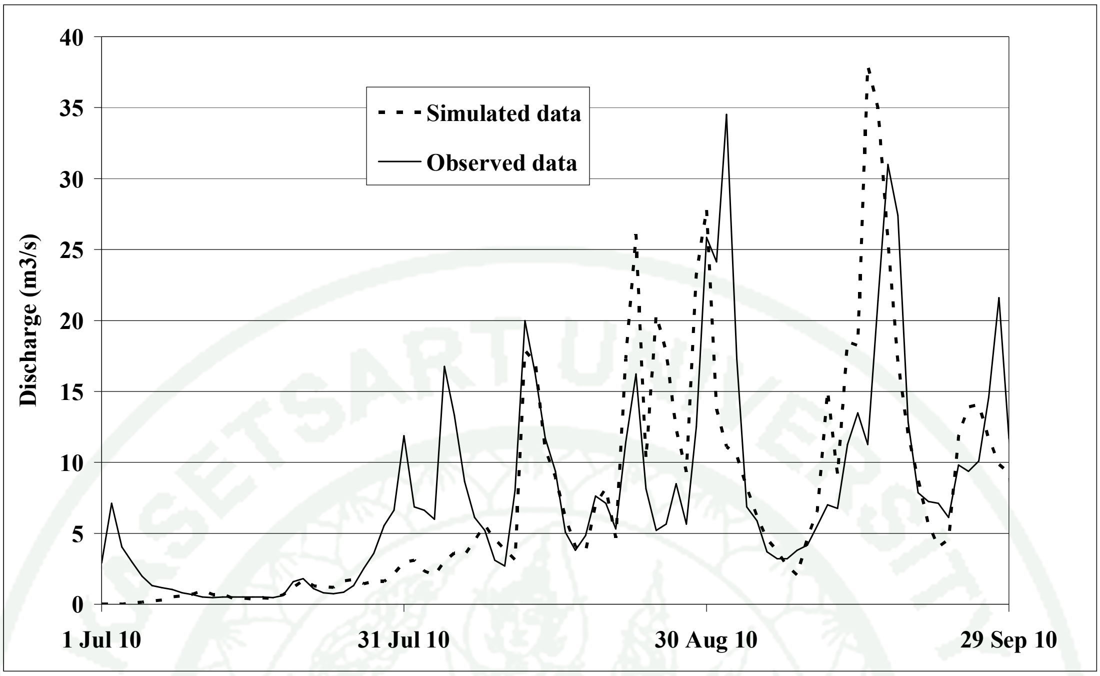

Figure 19 Simulated and observed flood hydrograph at the runoff station P.21 in 2010

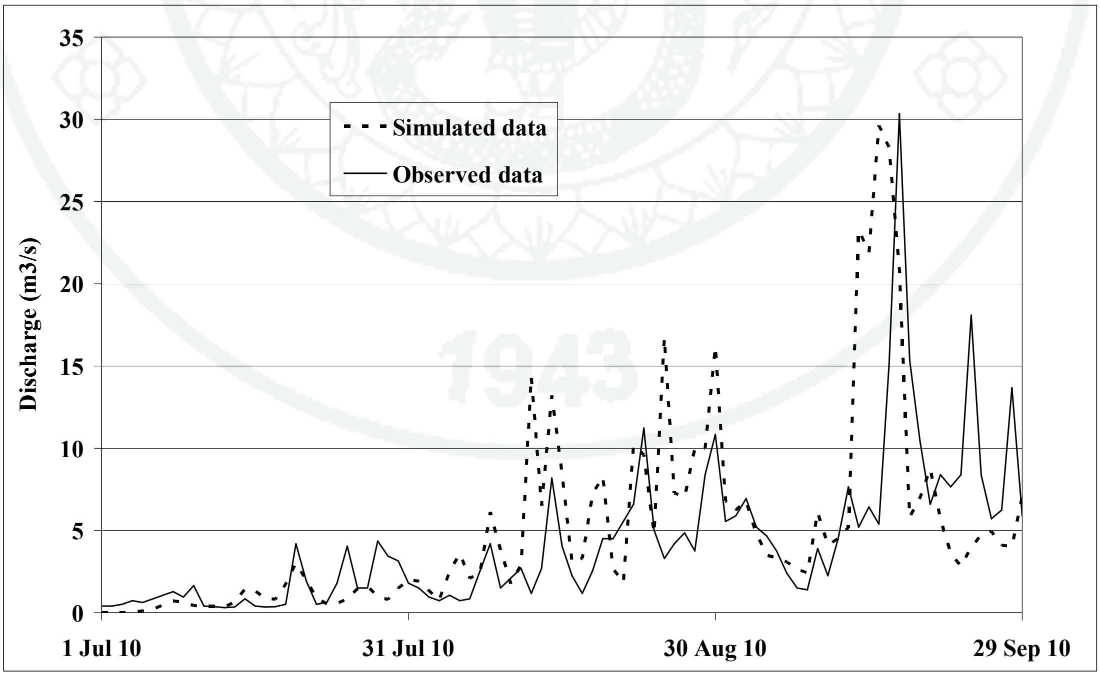

Figure 20 Simulated and observed flood hydrograph at the runoff station P.24A in 2010

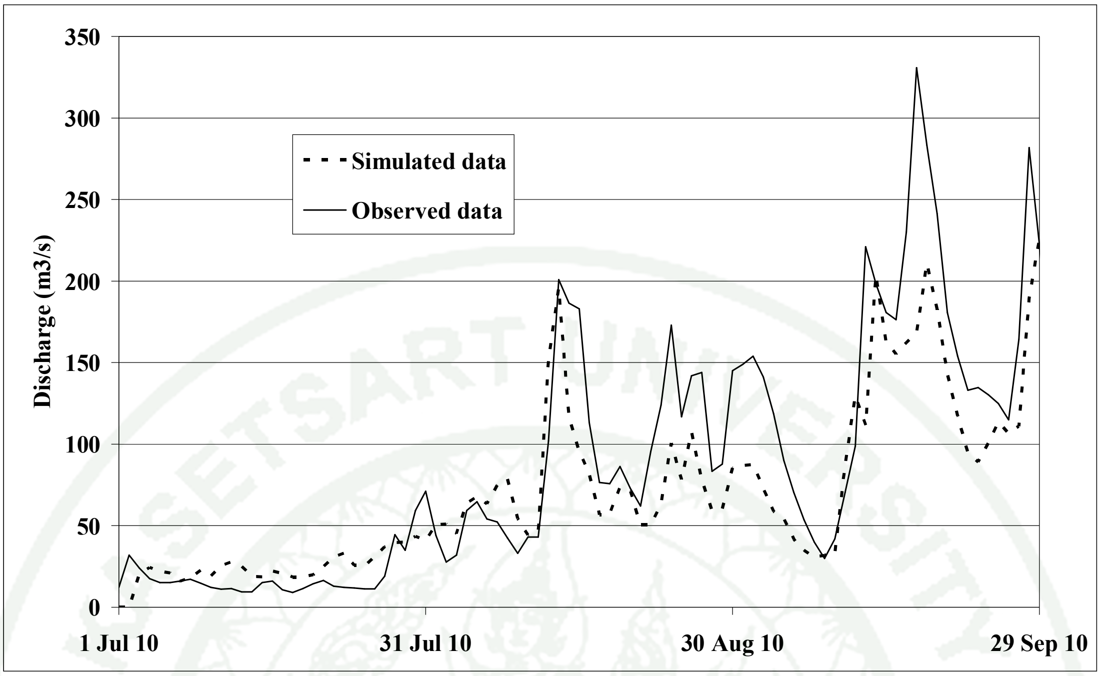

Figure 21 Simulated and observed flood hydrograph at the runoff station P.67 in 2010

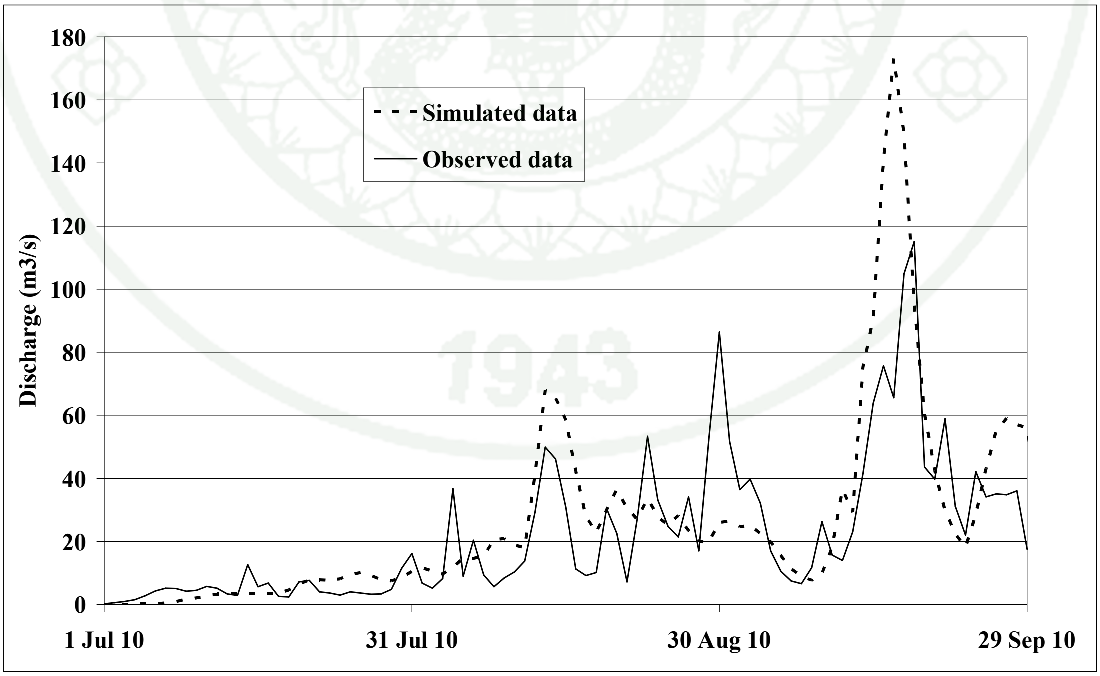

Figure 22 Simulated and observed flood hydrograph at the runoff station P.71 in 2010

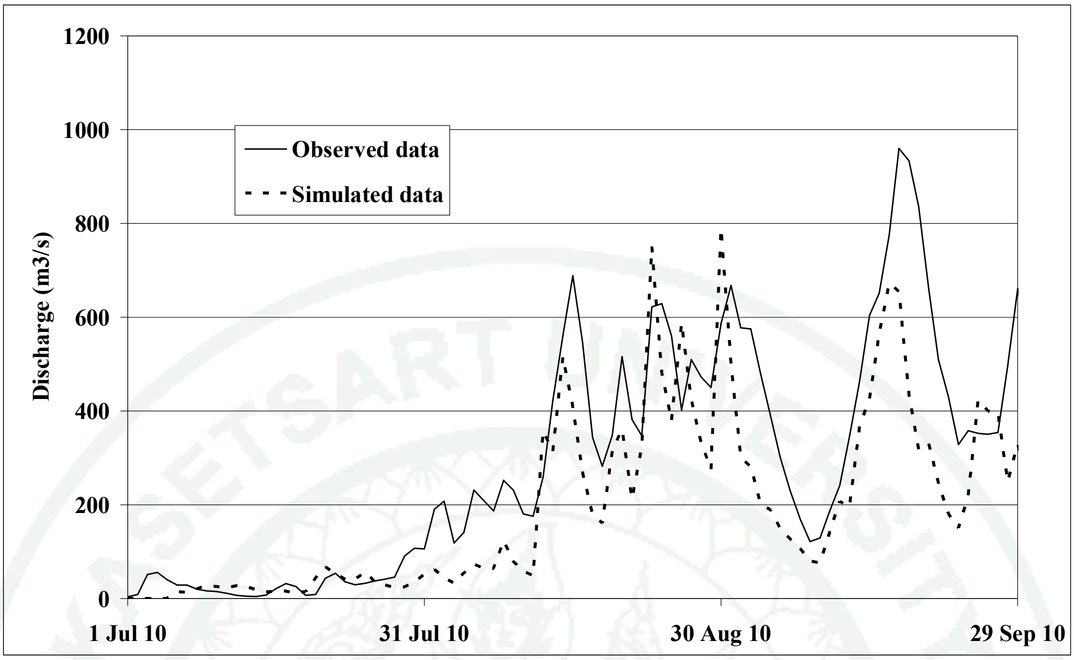

Figure 23 Simulated and observed flood hydrograph at the runoff station P.73 in 2010

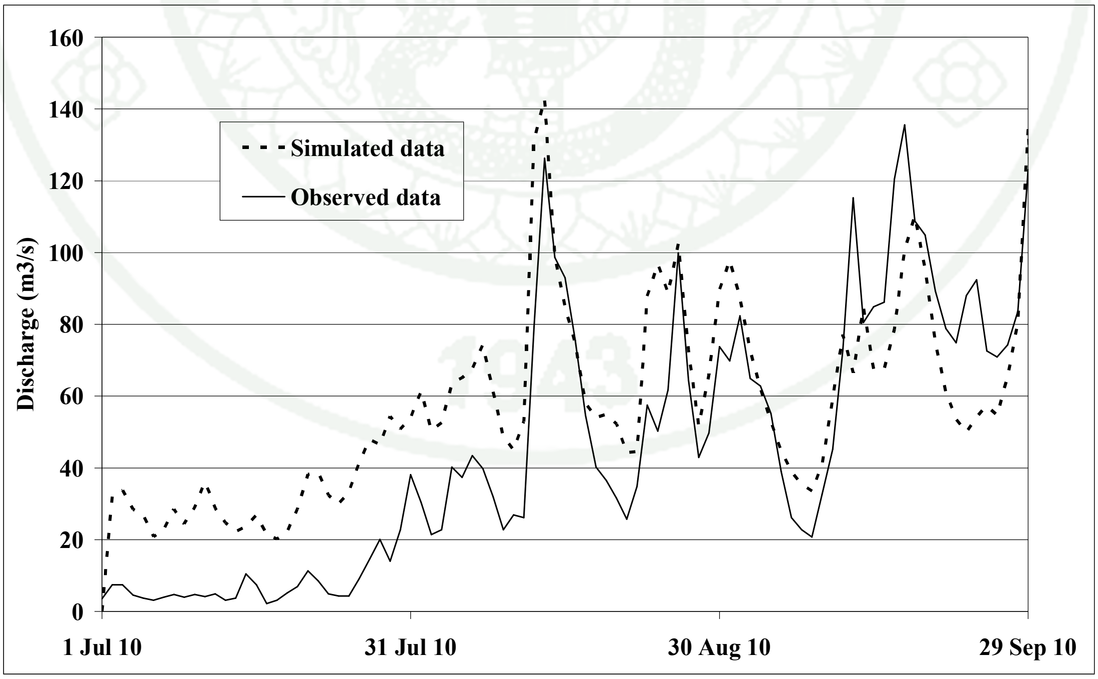

Figure 24 Simulated and observed flood hydrograph at the runoff station P.75 in 2010

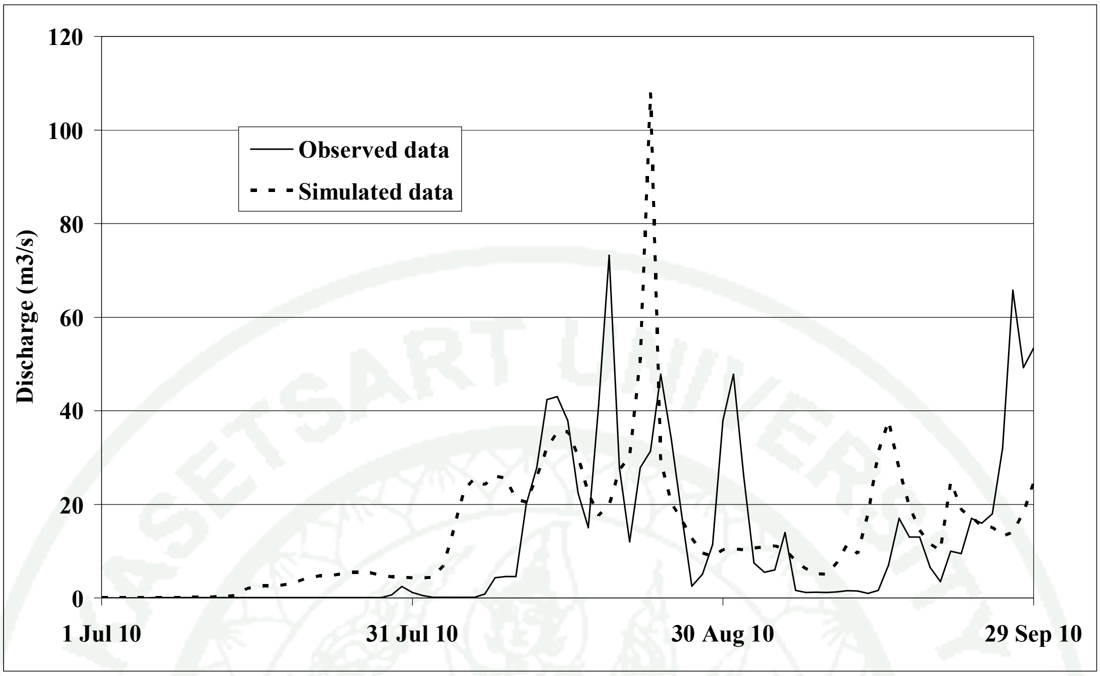

Figure 25 Simulated and observed flood hydrograph at the runoff station P.85 in 2010

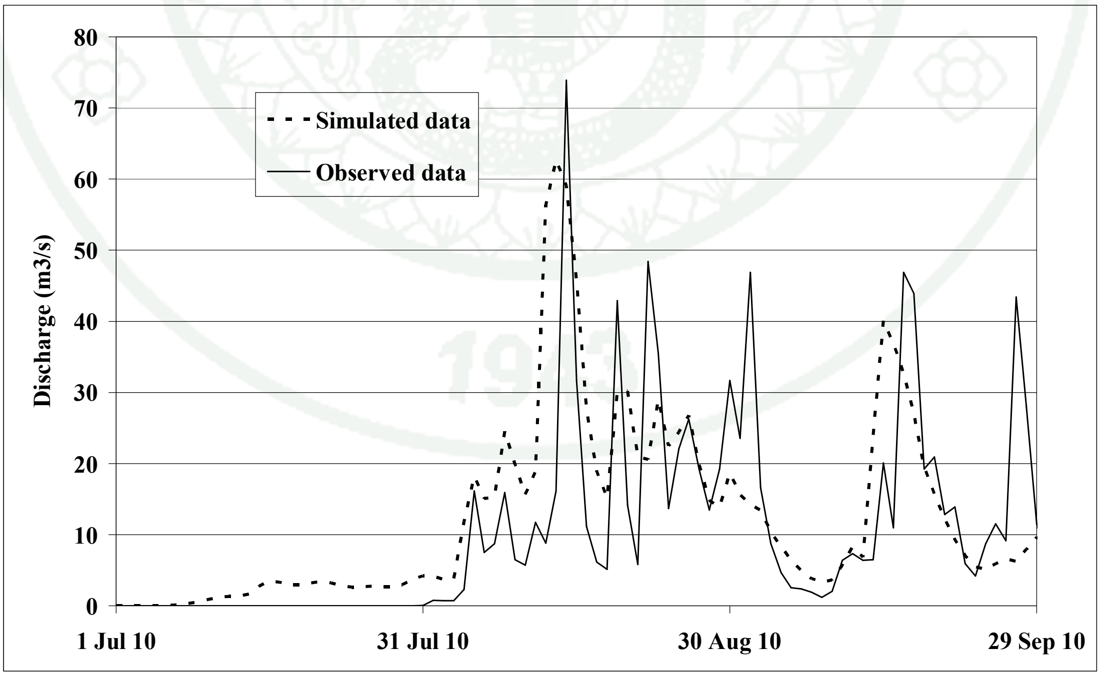

Figure 26 Simulated and observed flood hydrograph at the runoff station P.87 in 2010

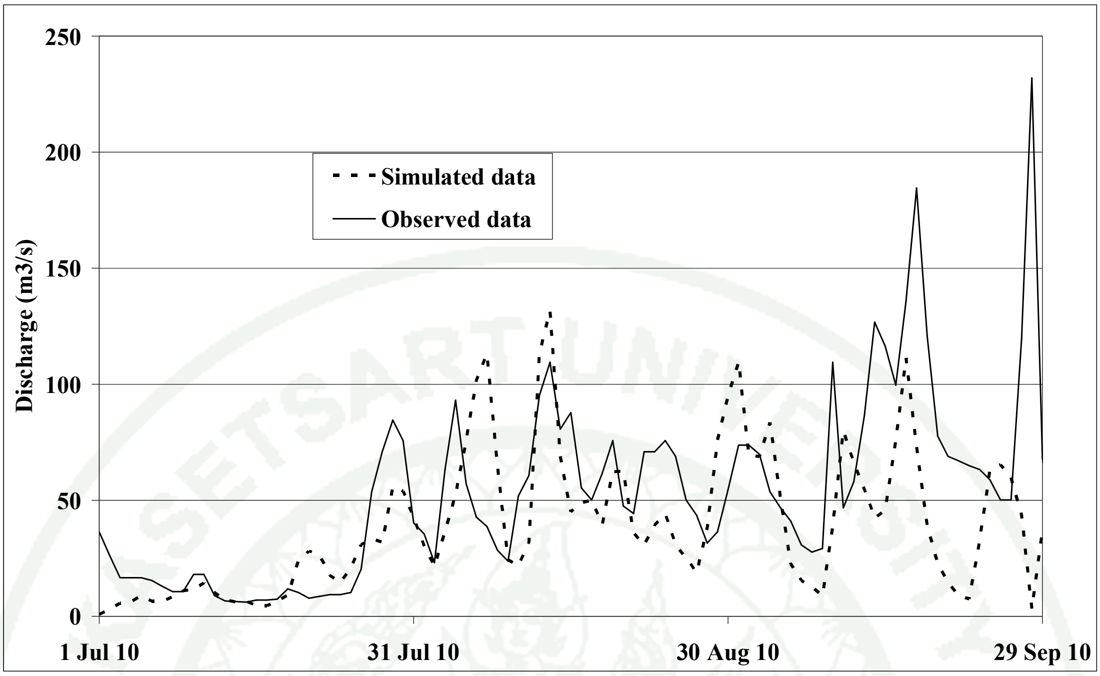

Figure 27 Simulated and observed flood hydrograph at the runoff station P.92 in 2010

The correlation statistics are shown in Table 7. It is found that the correlation coefficients (*r*) are in the range of 0.43 - 0.89. The efficiency index (EI) values are between 0.04 and 0.73, and the root mean square errors (RMSE) are between 5.26 and 156.01 m^3/s

Table 7 Comparison of approaches to channel discharge used in verification process

Rain gauged station	Correlation coefficient (r)	Efficiency Index (EI)	RMSE (m^3/s)
P.1	0.86	0.59	158.01
P.5	0.85	0.63	25.67
P.21	0.69	0.43	6.05
P.24A	0.54	0.22	5.26
P.67	0.89	0.73	39.08
P.71	0.78	0.22	20.21
P.73	0.75	0.20	73.38
P.75	0.84	0.60	22.93
P.85	0.48	0.07	16.49
P.87	0.65	0.41	10.99
P.92	0.43	0.04	40.55

Discussion

From model calibration, it is found that the suitable values of Manning coefficient (n) for computation of overland flow and channel flow in the Upper Ping river basin are about 0.6 and 0.25, respectively. Both parameters are obtained by trial-and-error to get the best-fitted solutions. For the overland flow model, the roughness coefficient (n) is set at 0.6 because most areas in the Upper Ping river basin are forests and farm lands. The runoff coefficients (C) of these areas are in the range of 0.1-0.6, depending on land use type. For overland flow model, since soil moisture is rather saturated after heavy rainfall, the runoff coefficient parameters in Table 6 are increased about 30-50%. These parameters (n and C) had some effect on water depth and water discharge. For channel flow model, it is found that the suitable values of roughness coefficient n are in the range of 0.1-0.25 depending on the type of channel bottom.

From correlation analysis, it is found that the values of correlation coefficient (*r*) at P.1, P.5 P.67 and P.75 are higher than 0.80. So, the simulation results at these stations are acceptable. At most stations, the EI values are between 0.2 and 0.6 which are generally considered as an acceptable level. The results obtained at stations P.85 and P.92 show low values of *r* and EI, indicating that there are significant differences between the simulation results and the observed data. The values of correlation coefficient r at stations P.1, P.5, P.67 and P.75 are higher than 0.8 indicating that the simulation results are good fitted with the observed data. For stations P.21, P.24A, P.71, P.73 and P.87, the correlation parameters are also within acceptable range.

CONCLUSION AND RECOMMENDATION

Conclusion

In this study, mathematical equations expressing overland flow and channel flow are used as basis equations in developing two-dimensional overland flow model and one-dimensional channel flow model which are used in flood forecasting. The finite element method with Galerkin's weighted residual technique is used in model development. The second-order Runge-Kutta method is applied to solve the set of differential equations obtained from finite element formulation. The important data required for these models are rainfall data, slope of the watershed areas and channels, land use patterns, channel cross-sections, and roughness coefficients.

The developed models are applied to the Upper Ping river basin. The obtained results are compared with the observed data at some available gauging stations. Correlation analysis shows that the simulation results are moderately fitted with the observed data. It is believed that this flood forecast model can be used as a tool to determine flood magnitude at various sections of the Upper Ping river.

Recommendation

The rainfall data should be collected at other stations so that more accurate flood hydrographs can be obtained from the model. More detailed investigation is needed to determine the suitable values of roughness coefficients used in the models. More up-to-date land use data are also needed. Along the river section where over flow often occur, the survey on channel cross-sections should be conducted. The GIS/RS should be applied together with the developed models.

LITERATURE CITED

Anderson, M.G. and P.D. Bates. 1994. Evaluating data constraints on two dimensional finite element models of floodplain flow. **Catena** 22 (1994): 1-15.

Arumpitakpun, A. 2006. **Forecasting of Flood levels of Ping river form station P. 67 to Nawarat bridge in Chiang Mai province by using hydrodynamic model**. M.S. Thesis. Chiang Mai University.

Bedient, P.B. and W.C. Huber. 2002. **Hydrology and Floodplain Analysis**. 3rd Edition. Prentice Hall, Inc. NJ.

Bethlahmy, N. 1967. The two-axis method: A new method to calculate average precipitation over a basin. **Hydro. Sci** 11 (3): 379-385.

Chagas P.F., S.H. Santos, C.F. Andrade, V. Ueta and R. Souza. 2010. Application of Mathematical Modeling to Study Flood Wave Behavior in Natural rivers as Function of Hydrualic and Hydrological Parameters of the Basin. **Hydrology Days** 2010: 114-120.

Chaskalovic, J. 2008. **Finite Element Methods for Engineering Sciences**. Springer-Verlag Berlin Heidelberg, Germany.

Connor, J.J. and C.A. Brebbia. 1976. **Finite Element Techniques for Fluid Flow**. Newnes - Butterworths, London.

Cohen, P.T. and R.E. Pearson. 1998. Communal irrigation, state, and capital in the Chiang Mai Valley (Northern Thailand): twentieth-century transformations **Journal of Southeast Asian Studies 29**. 86–110.

Gee M. and M.T. Tseng. 1997. **Unsteady Flow Model for Forecasting Missouri and Mississippi rivers.** US Army Crops of Engineers, CA.

Giammarco, P. Di, E. Todini and P. Lamberti. 1996. A conservative finite elements approach to overland flow: the control volume finite element formulation. **Journal of Hydrology** 175 (1996): 267-291:

Hinkelmann, R. 2005. **Efficient Numerical Methods and Information-Processing Techniques for Modeling Hydro-and Environmental Systems**. Springer-Verlag Berlin Heidelberg, Germany.

Homberger, G.M. and J.P. Wiberg. 2005. **Numerical Method in the Hydrological Sciences.** the American Geophysical Union, USA.

HYDROEUROPE team 7. 2008. **Hydrological Analysis Report Part 1**. Workspace 2008/2009 Available source: http://portail.unice.fr/jahia/Jahia/site/hydroeurope/lang/en/pid/11662, November 28, 2011.

Lastoria, B. 2008. Hydrological processes on the land surface: A survey of modeling approaches. **FORALPS Technical Report, 9**. Grafiche Futura s.r.l., Italy.

Lebel, L., P. Garden, N. Subsin, and S. Na Nan. 2009. Averted crises, contested transitions: water management in the Upper Ping River basin, northern Thailand, pp. 137-157. *In* D. Huitema and S.V. Meijerink, eds. **Water Policy Entrepreneurs: A Research Companion to Water Transition Around the Globe.** Edward Elgar Publishing, Massachusetts.

Lewatchanakul, K. 1996. **Hydrological Engineering.** Department of Civil Engineering, Faculty of Engineering, Rungsit University, Nakorn Prathom.

Logan, D.L. 2001**. A First Course in the Finite Element Method Using Algor^{TM}**. 2^{nd} Edition. Brooks/cole, USA.

MacArthur, R. and J.J. Devries. 1993. **Introduction and Application of Kinematic Wave Routing Techniques Using HEC-1**. US Army Crops of Engineers, Hydrologic Engineering Center, CA.

MathWorks Inc., 1996. **MATLAB Notebook User's Guide: Version 5**.

O'Connor A. J. **Introduction to MATLAB**. School of Science, Griffith University, Brisbane, Australia.

Office of Natural Resources and Environmental Policy and Planning (ONEP), Ministry of Natural Resources and Environment. 2005. **Developing Watershed Management Organizations in Pilot Sub-Basins of the Ping River Basin**.

Pfotenhauer, L. M.. 1994. Water Budgets and Water Regions: Planning and Managing Water Resources Development in Thailand. **TDRI Quarterly Review**. Vol.9: 14-23.

Puttaraksa, P., N. Sriwongsitanon and S. Lipiwattanakarn. 2005. Development of one dimensional implicit dynamic wave model. **KKU Engineering J**. Vol.32 No.1 : 31-48.

Puttaraksa, P. and N. Sriwongsitanon. 2009. Estimation of the URBS model for flood estimation of ungauged catchment in the upper Ping river basin, Thailand. **ScienceAsia** 35: 49-56.

Taesombat, W. and N. Sriwongsitanon. 2010. Flood Investigation in the Upper Ping River Basin Using Mathematical Models. **Kasetsart J.** (Nat Sci.) 44: 152-166.

Tabuenca, P., J. Villa, J. Cardona and A. Samartin. 1997. Finite element simulation of dispersion in the Bay of Santander. **Advance in Engineering Software** 28 : 313-332.

Vieuux, B.E. and J.E. Vieux. 2005. **Vflo™ : A Real-Time Distributed Hydrologic Model**. Vieux & Associates, Inc., Norman, OK.

Zhou, Y., H. Tang and X. Liu. 2006. A split-characteristic finite element model for 1-D unsteady flows. **Journal of Hydrodynamics** 19 (1): 54-61.

APPENDICES

Appendix A

Roughness Coefficient for Overland Flow

and Runoff Coefficient for Channel Flow

Appendix Table A1 Effective Resistance Parameters for Overland Flow

Surface	N Value
Asphalt/Concrete	0.05-0.15
Bare Packed Soil Free Stone	0.10
Fallow-No residue	0.008-0.012
Convential Tillage-No Residual	0.06-0.12
Convential Tillage-With Residual	0.16-0.22
Chisel Plow-No Residual	0.06-0.12
Chisel Plow-With Residual	0.10-0.16
Fall Disking-With Residual	0.30-0.50
No-Till-No Residual	0.04-0.10
No Till(20-40% residual cover)	0.07-0.17
No Till(60-100% residual cover)	0.17-0.47
Sparse Rangeland with Debris:	
0 % Cover	0.09-0.34
20% Cover	0.05-0.25
Sparse Vegetation	0.053-0.13
Short Grass Prarie	0.10-0.20
Poor Grass Cover on Moderately Rough	0.30
Bare Surface	
Light Turf	0.20
Average Grass Cover	0.4
Dense Turf	0.17-0.80
Dense Grass	0.17-0.80
Bermuda Grass	0.30-0.48
Dense Shrubby and Forest Litter	0.4

Appendix Table A2 Roughness Coefficient (Manning's n)

Surface	Best	Good	Fair	Bad
Uncoated cast-iron pipe	0.012	0.013	0.014	0.015
Coated cast-iron-pipe	0.011	0.012	0.013	
Commercial wrought-iron pipe, black	0.012	0.013	0.014	0.015
Commercial wrought-iron pipe, galvanized	0.013	0.014	0.015	0.017
Riveted and spiral steel pipe	0.013	0.015	0.017	
Common clay drainage tile	0.011	0.012	0.014	0.017
Neat cement surfaces	0.010	0.011	0.012	0.013
Cement mortar surfaces	0.011	0.012	0.013	0.015
Concrete pipe	0.012	0.013	0.015	0.016
Concrete-lined channel	0.012	0.014	0.016	0.018
Cement-rubble surface	0.017	0.020	0.025	0.030
Dry-rubble surface	0.025	0.030	0.033	0.035
Canals and ditches:				
Earth, straight and uniform	0.017	0.020	0.225	0.025
Rock cuts, smooth and uniform	0.025	0.030	0.033	0.035
Rock cuts, jagged and irregular	0.035	0.040	0.045	
Winding sluggish canals	0.0225	0.025	0.028	0.030
Dredged earth channel	0.025	0.028	0.030	0.033
Canals with rough stony beds, weeds on earth banks	0.025	0.030	0.035	0.040
Earth bottom, rubble sides	0.028	0.030	0.033	0.035
Natural stream channels:				
1. Clean, straight bank, full stage, no rifts or deep pools	0.025	0.028	0.030	0.033
2. Same as#1, but some weeds and stones	0.030	0.033	0.035	0.040
3. Winding, some pools and shoals, clean	0.033	0.035	0.040	0.045
4. Same as#3, Lower stages, more ineffective slope and sections	0.040	0.045	0.050	0.055

Appendix Table A2 (Continued)

Surface	Best	Good	Fair	Bad
5. Same as#3, some weeds and stones	0.035	0.040	0.045	0.050
6. Same as#4, stony sections	0.045	0.050	0.055	0.060
7. Sluggish river reaches, rather weedy or with very deep pools	0.050	0.060	0.070	0.080
8. Very weedy reaches	0.075	0.100	0.125	0.150

Appendix Table A3 Runoff Coefficient (C)

Land Use	C	Land Use	C
Business:		***Lawns:***	
Downtown areas	0.70 - 0.95	Sandy soil, flat, 2%	0.05 - 0.10
Neighborhood areas	0.50 - 0.70	Sandy soil, avg., 2-7%	0.10 - 0.15
		Sandy soil, steep, 7%	0.15 - 0.20
		Heavy soil, flat, 2%	0.13 - 0.17
		Heavy soil, avg., 2-7%	0.18 - 0.22
		Heavy soil, steep, 7%	0.25 - 0.35
Residential:		***Agricultural land:***	
Single-family areas	0.30 - 0.50	*Bare packed soil*	
Multi units, detached	0.40 - 0.60	*Smooth	0.30 - 0.60
Munti units, attached	0.60 - 0.75	*Rough	0.20 - 0.50
Suburban	0.25 - 0.40	*Cultivated rows*	
		*Heavy soil, no crop	0.30 - 0.60
		*Heavy soil, with crop	0.20 - 0.50
		*Sandy soil, no crop	0.20 - 0.40
		*Sandy soil, with crop	0.10 - 0.25
		Pasture	
		*Heavy soil	0.15 - 0.45
		*Sandy soil	0.05 - 0.25
		Woodlands	0.05 - 0.25
Industrial:		*Streets:*	
Light areas	0.50 - 0.80	Asphaltic	0.70 - 0.95
Heavy areas	0.60 - 0.90	Concrete	0.80 - 0.95
		Brick	0.70 - 0.85
Parks, cemeteries	0.10 - 0.25	Unimproved areas	0.10 - 0.30
Playgrounds	0.20 - 0.35	Drives and walks	0.75 - 0.85
Railroad yard areas	0.20 - 0.40	Roofs	0.75 - 0.95

Appendix B

Channel Cross-sections

Appendix table B1 Cross-sectional channel in P.1, P.5, P.21, P.24A and P.67 station

P.1 station		P.5 station		P.21 station		P.24A station		P.67 station	
X	level	X	level	X	level	X	level	X	level
-50	305.521	-50	295.124	-50	325.068	-50	277.926	-50	324.876
-40	305.721	-40	295.246	-40	325.083	-40	277.971	-40	325.171
-30	306.036	-30	295.384	-30	325.093	-30	278.268	-30	325.474
-20	306.416	-20	295.499	-20	325.150	-20	278.733	-20	325.786
-10	306.938	-10	295.622	-10	325.203	-10	279.436	-10	326.053
0	307.73	0	295.792	0	325.166	0	280.196	0	326.328
0	304.183	0	294.606	0	324.308	0	277.571	0	325.165
2	304.175	2	294.189	2	324.209	2	277.389	2	323.697
4	303.996	4	293.226	4	324.053	3	277.02	4	323.094
6	303.908	6	292.717	6	323.127	4	276.08	6	321.869
8	303.943	8	292.418	8	322.466	6	275.762	8	320.834
9	303.288	10	292.464	10	322.535	8	275.692	10	319.781
10	302.938	12	292.208	12	322.548	10	275.652	12	318.759
12	302.578	14	291.802	14	322.572	12	275.652	14	317.677
14	302.216	16	291.58	16	322.512	14	275.332	16	317.198
15	302.101	18	290.764	18	322.085	16	275.492	17	317.229
15	301.123	20	290.204	20	321.895	18	275.642	17	316.284
16	301.093	22	290.174	22	321.750	20	275.94	18	315.842
18	300.793	24	289.864	24	321.780	22	275.925	20	315.812
20	300.523	26	289.274	26	320.311	24	275.692	22	315.762
22	300.583	28	289.184	28	319.841	26	275.532	24	315.582
24	300.603	30	289.524	30	319.891	28	275.542	26	315.052
26	300.743	32	290.304	32	320.191	30	276.185	28	314.932
28	301.023	34	290.314	34	320.921	31	276.905	30	314.432
30	301.443	36	290.264	36	320.861	31	280.082	32	314.522
32	301.343	38	290.164	38	320.801	40	279.813	34	314.012
34	300.483	40	289.944	40	320.751	50	279.423	36	314.252
36	300.133	42	289.754	42	320.571	60	279.138	38	314.042
38	300.043	44	289.694	44	320.431	70	278.973	40	314.412
40	299.773	46	289.434	46	320.671	80	278.863	42	316.544
42	299.793	48	289.294	48	321.886			44	317.029
44	300.093	50	289.494	50	322.129			46	316.799
46	299.703	52	289.854	52	322.591			48	316.734
48	299.733	54	290.014	54	323.407			50	316.499
50	299.533	56	289.824	56	323.882			52	316.654
52	299.443	58	289.914	56	325.165			54	316.829
54	299.553	60	289.504	66	325.097			56	316.504
56	299.823	62	289.394	76	325.010			58	315.902

Appendix table B1 (Continued)

P.1 station		P.5 station		P.21 station		P.24A station		P.67 station	
X	level	X	level	X	level	X	level	X	level
58	300.143	64	289.304	86	324.995			60	315.662
60	299.683	66	289.304	96	324.968			62	315.682
62	299.663	68	289.544	106	324.966			64	315.722
64	299.373	70	289.894					66	315.732
66	299.683	72	290.314					68	315.142
68	300.453	74	290.774					70	314.572
70	301.393	76	291.830					72	314.392
72	301.053	78	293.275					74	314.822
74	300.143	80	294.426					76	315.082
76	299.773	82	294.436					78	315.742
78	299.13	84	294.925					80	317.125
80	299.273	86	295.015					82	317.351
82	299.143	88	295.385					84	317.417
84	299.173	90	295.652					86	317.954
86	299.203	90	295.800					88	319.527
88	299.293	100	295.275					90	320.796
90	299.713	110	295.212					92	321.105
92	300.143	120	295.130					94	323.298
94	301.303	130	295.030					96	323.355
95	301.593	140	294.900					98	323.797
96	302.213							100	325.108
98	302.618							100	326.2
100	302.868							110	325.863
100	307.635							120	325.443
110	307.108							130	325.102
120	306.658							140	324.698
130	306.238							150	324.418
140	306.073								
150	305.923								

Appendix table B2 Cross-sectional channel in P.71, P.73, P.75, P.85 and P.92 station

P.71 station		P.73 station		P.75 station		P.85 station		P.92 station	
X	level	X	level	X	level	X	level	X	level
-50	289.16	-50	267.584	-50	344.37	-50	294.786	-50	448.982
-40	289.225	-40	267.579	-40	344.478	-40	294.796	-40	448.862
-30	289.365	-30	267.584	-30	344.635	-30	294.886	-30	448.317
-20	289.54	-20	267.604	-20	344.842	-20	294.966	-20	447.887
-10	289.794	-10	267.606	-10	345.064	-10	295.222	-10	447.582
0	290.762	0	267.726	0	345.12	0	295.371	0	447.415
0	288.823	0	267.052	0	344.595	0	294.064	0	446.239
1	287.747	5	267.166	2	343.053	2	293.446	2	445.387
2	287.242	10	267.119	4	342.313	3	292.951	4	444.888
3	286.707	15	266.939	5	342.018	4	292.275	6	444.655
4	286.122	20	266.624	10	341.843	5	291.8	8	444.64
5	285.567	25	265.837	15	341.818	6	291.385	10	444.505
6	285.072	30	265.742	20	341.758	6	290.935	12	444.315
8	284.289	35	264.394	25	341.634	7	290.505	14	444.105
10	284.079	40	261.122	30	340.959	10	289.437	16	443.975
12	284.019	45	260.841	35	340.414	12	288.767	18	443.307
14	284.129	50	260.141	40	339.919	14	288.367	20	441.933
16	284.549	55	260.601	45	339.599	16	288.317	22	440.674
18	283.649	60	260.041	50	339.574	18	288.557	24	440.654
20	282.799	65	260.281	55	339.449	20	289.077	26	440.604
22	282.549	70	259.901	60	339.359	22	288.617	28	440.714
24	282.769	75	259.811	65	339.424	24	288.697	30	440.674
26	283.499	80	260.221	70	339.434	26	288.937	32	440.624
28	284.479	85	260.561	75	339.354	28	289.157	34	440.454
30	284.679	90	261.117	80	339.156	30	289.547	36	441.114
32	284.619	95	261.158	85	338.828	32	289.617	38	440.744
34	284.099	100	261.143	95	337.691	34	290.047	40	440.404
36	285.217	105	261.176	100	338.041	36	290.167	42	439.954
37	285.845	110	261.101	105	337.271	38	290.157	44	439.944
38	286.957	115	261.194	110	336.841	40	289.617	46	440.064
40	288.385	120	261.515	115	337.211	42	289.627	48	440.424
41	288.965	125	261.631	116	337.941	44	290.017	50	440.954
42	289.001	130	260.856	117	338.676	45	290.563	52	440.804
43	289.248	135	260.726	118	339.391	46	291.34	54	440.704
44	289.691	140	261.836	119	340.191	47	291.995	56	440.304
45	290.419	145	261.801	125	340.554	48	293.078	58	440.104

Appendix table B2 (Continued)

P.71 station		P.73 station		P.75 station		P.85 station		P.92 station	
X	level	X	level	X	level	X	level	X	level
55	289.891	150	262.286	130	340.489	49	293.729	60	440.484
65	289.174	155	262.136	135	340.449	50	294.096	62	440.794
75	288.935	160	262.056	140	340.624	50	295.348	64	441.583
85	288.914	165	261.941	145	340.674	60	295.179	66	442.578
95	288.904	170	262.414	150	340.604	70	294.921	68	443.55
		175	262.776	155	340.679	80	294.713	70	443.831
		180	263.202	160	340.729	90	294.818	72	443.454
		185	263.224	165	340.789	100	295.098	74	443.986
		190	263.496	170	340.794			76	444.418
		195	263.754	175	340.944			78	444.501
		200	264.234	180	340.814			80	444.518
		205	264.142	185	341.024			82	444.806
		210	264.292	190	341.184			84	446.086
		215	264.43	195	341.054			86	446.191
		220	264.769	200	341.194			86	447.311
		225	265.244	205	341.127			90	447.216
		230	265.855	210	341.099			100	447.428
		235	266.585	215	341.024			110	447.571
		240	267.131	220	340.989			120	447.846
		240	268.025	225	340.969			130	448.481
		250	267.57	230	340.946			140	448.961
		260	267.413	235	340.996				
		270	267.382	240	340.656				
		280	267.443	245	340.646				
		290	267.548	250	340.761				
				255	340.671				
				260	340.876				
				265	341.376				
				270	341.401				
				275	342.056				
				280	344.464				
				280	345.136				
				290	344.994				
				300	344.866				
				310	344.714				
				320	344.554				
				330	344.469				

Appendix C

Rainfall data at rain gauged station

(327501, 327201, 300201, 300202, 329201, 328201, 328202 and 376203)

Appendix Table C1 Rainfall, in millimeter per hour, July - September 2010 at Doi Ang Kang station, Chiang mai (327202)

Time / Date	1:00	4:00	7:00	10:00	13:00	16:00	19:00	22:00	Total
1/7/2010	-	-	18.3	0.9	0	5.2	1.3	-	25.7
2/7/2010	-	-	0.4	0	11.3	7.7	0	-	19.4
3/7/2010	-	-	0	0.3	0	0.7	0	-	1
4/7/2010	-	-	0	0	0	0	0	-	-
5/7/2010	-	-	0	0	0	0	0	-	-
6/7/2010	-	-	0	0	0	0	0	-	-
7/7/2010	-	-	15.7	0	0	0	0	-	15.7
8/7/2010	-	-	14.8	0	0	7.5	6.7	-	29
9/7/2010	-	-	1.2	0	0	0	1.3	-	2.5
10/7/2010	-	-	0.7	0	0	9.5	0.5	-	10.7
11/7/2010	-	-	0	0	0	0	0	-	-
12/7/2010	-	-	0	0	0	0	0	-	-
13/7/2010	-	-	0	0	0	0	0	-	-
14/7/2010	-	-	3.2	6.6	3.2	0.1	0	-	13.1
15/7/2010	-	-	0	0	0	0	0	-	-
16/7/2010	-	-	0	0	0	0	0	-	-
17/7/2010	-	-	0	0	10.1	0	0	-	10.1
18/7/2010	-	-	8.9	5.8	0.2	0	0.4	-	15.3
19/7/2010	-	-	7.5	0.5	0.1	0.7	15.8	-	24.6
20/7/2010	-	-	50.5	0	0	0	0	-	50.5
21/7/2010	-	-	0	0	0	0	0	-	-
22/7/2010	-	-	5.1	2.1	0.6	1.5	0	-	9.3
23/7/2010	-	-	0.6	0.2	0.3	2	0.4	-	3.5
24/7/2010	-	-	12.8	5	4.3	0.2	3.6	-	25.9
25/7/2010	-	-	30.2	0.3	2.8	19.2	2.5	-	55
26/7/2010	-	-	1	0	0	1.8	0	-	2.8
27/7/2010	-	-	24.1	2.7	0	0	0	-	26.8
28/7/2010	-	-	6.5	0	3.1	31.2	47.6	-	88.4
29/7/2010	-	-	2.1	0	1	15.2	5.9	-	24.2
30/7/2010	-	-	1	0	0	2.3	4.4	-	7.7
31/7/2010	-	-	29	0	0	0.5	0	-	29.5
1/8/2010	-	-	1.2	0	0	0	0	-	1.2
2/8/2010	-	-	0	0	0	0	0	-	-
3/8/2010	-	-	31	0.4	0.4	1.1	7.6	-	40.5
4/8/2010	-	-	0.4	0	0	2.5	14.4	-	17.3
5/8/2010	-	-	16.3	0	0	0	4	-	20.3
6/8/2010	-	-	2.5	23.5	25.5	1	0	-	52.5
7/8/2010	-	-	0.2	0.5	0.2	0	0	-	0.9
8/8/2010	-	-	0	0	0	0	0	-	-

Appendix Table C1 (Continued)

Time / Date	1:00	4:00	7:00	10:00	13:00	16:00	19:00	22:00	Total
9/8/2010	-	-	0	1	0	5.4	0	-	6.4
10/8/2010	-	-	0	0.3	1.3	5.6	3.2	-	10.4
11/8/2010	-	-	10.9	3.7	2.5	3.6	2.6	-	23.3
12/8/2010	-	-	46	1.5	0	5.1	2.7	-	55.3
13/8/2010	-	-	0	0	1.3	5.5	0.4	-	7.2
14/8/2010	-	-	0.9	0.1	0.4	0	0.5	-	1.9
15/8/2010	-	-	8.9	0	0	9.3	5.4	-	23.6
16/8/2010	-	-	7	0	2	0.4	0	-	9.4
17/8/2010	-	-	6.9	0	4	2.5	0.4	-	13.8
18/8/2010	-	-	1.9	0.3	1.6	0.8	11.3	-	15.9
19/8/2010	-	-	19	0.2	0	0	0	-	19.2
20/8/2010	-	-	1	0	0	0	3	-	4
21/8/2010	-	-	0	0	0	2.6	2.5	-	5.1
22/8/2010	-	-	1	0.7	7.6	0	0.6	-	9.9
23/8/2010	-	-	7.6	7.5	1.5	0	0	-	16.6
24/8/2010	-	-	0.2	0	0	0	0	-	0.2
25/8/2010	-	-	0	0	1.5	1.5	4	-	7
26/8/2010	-	-	0.6	0	0.2	0	0	-	0.8
27/8/2010	-	-	2.5	0.6	2	0.4	0	-	5.5
28/8/2010	-	-	4.6	22.9	10.8	1.3	0	-	39.6
29/8/2010	-	-	9	0	0	15	0	-	24
30/8/2010	-	-	0	3.9	0.9	28.7	11.1	-	44.6
31/8/2010	-	-	1.1	0	0	0	1.7	-	2.8
1/9/2010	-	-	0	6.1	0	0	0	-	6.1
2/9/2010	-	-	34.3	0	0	0	0	-	34.3
3/9/2010	-	-	6.5	2.3	0	0	0	-	8.8
4/9/2010	-	-	0	0	0.1	0.3	0	-	0.4
5/9/2010	-	-	0	0	0	0	0	-	-
6/9/2010	-	-	0	0	2	1.8	0	-	3.8
7/9/2010	-	-	0	0	0.4	0	0.2	-	0.6
8/9/2010	-	-	0	0	0	0	0	-	-
9/9/2010	-	-	22.8	2.4	21.5	4	0	-	50.7
10/9/2010	-	-	0	0	1.2	3.4	0	-	4.6
11/9/2010	-	-	5.5	1	0	0	0	-	6.5
12/9/2010	-	-	2.6	0	0	0.3	0.3	-	3.2
13/9/2010	-	-	13.7	0	0.3	0	0	-	14
14/9/2010	-	-	9.7	0.2	0	1.7	2.2	-	13.8
15/9/2010	-	-	4	0.4	29.1	0.9	0.8	-	35.2
16/9/2010	-	-	4.8	1.1	0.4	0	0	-	6.3
17/9/2010	-	-	6	0.2	0	0	0	-	6.2
18/9/2010	-	-	0.2	0	0	0	0	-	0.2

Appendix Table C1 (Continued)

Time / Date	1:00	4:00	7:00	10:00	13:00	16:00	19:00	22:00	Total
19/9/2010	-	-	0	0	0	0	0	-	-
20/9/2010	-	-	0	0	0	0	0	-	-
21/9/2010	-	-	0	0	0	0	3.1	-	3.1
22/9/2010	-	-	0	0	0	0	0	-	-
23/9/2010	-	-	31.3	5	0	0	0	-	36.3
24/9/2010	-	-	0	6.1	0	11.3	0	-	17.4
25/9/2010	-	-	0	0	0.2	5.8	1.7	-	7.7
26/9/2010	-	-	8	0	0	2	0	-	10
27/9/2010	-	-	0	0	0	0	0.3	-	0.3
28/9/2010	-	-	12.5	0	0	4.7	0.3	-	17.5
29/9/2010	-	-	0	0	0	0	0	-	-
30/9/2010	-	-	1.4	0	0	0	0	-	1.4

Appendix Table C2 Rainfall, in millimeter per hour, July - September 2010 at Chiang mai station (327501)

Date \ Time	1:00	4:00	7:00	10:00	13:00	16:00	19:00	22:00	Total
1/7/2010	0	0	0.8	0.4	0	0	0	0	1.2
2/7/2010	1.2	0	0	0	0	0	0	0	1.2
3/7/2010	0	0	0	0	0	0	7.1	0.7	7.8
4/7/2010	T	0	0	0	0	0	0	0	T
5/7/2010	0	0	0	0	0	0	0	0	-
6/7/2010	0	0	0	0	0	0	0	T	T
7/7/2010	9.3	0.2	0	0	0	0	0	0	9.5
8/7/2010	0	0	0	0	0	2.8	0	0	2.8
9/7/2010	0	0	0	0	0	3.4	0	0	3.4
10/7/2010	0	0	0	0	0	0	0	5	5
11/7/2010	0	0	0	0	0	0	0	0	-
12/7/2010	0	0	0	0	0	0.2	0	0	0.2
13/7/2010	0	0	0	0	0	0	0	0	-
14/7/2010	0	0	2.6	0.2	0	0	0	0.2	3
15/7/2010	0	0	0	0	0	0	0	0	-
16/7/2010	0	0	0	0	0	0	0	0	-
17/7/2010	0	0	0	0	0	0.7	0	0.6	1.3
18/7/2010	0	0	0	0	T	6.7	3.6	0.3	10.6
19/7/2010	0.6	0.2	T	0	0	0	0	4.4	5.2
20/7/2010	5.4	0.5	T	0	0	0	0	0	5.9
21/7/2010	0	0	0	0	0	0	0	0	-
22/7/2010	0	0	0	0.8	0.9	1.4	0.3	0.3	3.7
23/7/2010	0	0	0	0	0	3.4	0	0	3.4
24/7/2010	0	0	0	0	0	3.4	8.1	0.5	12
25/7/2010	0	0	0	0	0	0	0.4	0	0.4
26/7/2010	0	0	0	0	0	0	0	0	-
27/7/2010	0	0	1.7	0	0	2.4	0.2	1.9	6.2
28/7/2010	0	0	0	0	0	0	0	0	-
29/7/2010	1.5	1.8	0	2.3	0	5.4	0	4.7	15.7
30/7/2010	0	0	0	0	0.7	0	0	12.5	13.2
31/7/2010	1.6	0.2	0	0	0	0	1.8	0	3.6
1/8/2010	0	0	0	0	0	0	0	0	-
2/8/2010	T	0.1	0	0	0	0	0	0	0.1
3/8/2010	0	0	10.1	4.2	0.8	0	0	7.8	22.9
4/8/2010	5.7	0.3	0	0	0	0	0.4	3.8	10.2
5/8/2010	2.5	0	0	0	0.6	3.4	0.6	1.1	8.2
6/8/2010	0.5	0	0	0	4.2	0.2	0	0	4.9
7/8/2010	T	2.4	13.1	17.3	0.9	0	0	2	35.7
8/8/2010	0	0	0	0	0	0	0	0.5	0.5

Appendix Table C2 (Continued)

Time / Date	1:00	4:00	7:00	10:00	13:00	16:00	19:00	22:00	Total
9/8/2010	2.8	0	0	0	0	0.3	T	0	3.1
10/8/2010	0	0	0.3	0.3	0	1.9	0	0.1	2.6
11/8/2010	0.6	0.4	1.5	2.7	0	0	0	62.9	68.1
12/8/2010	52.5	1.8	0.2	0	0.8	0	0	28.3	83.6
13/8/2010	12.6	0	0	0	0	2.8	1.8	0	17.2
14/8/2010	3.5	7	12.6	T	0	0	0	0	23.1
15/8/2010	0	0	0	0	0	0	0	0	-
16/8/2010	0	0	0	0	0	0	0	0	-
17/8/2010	0	0	0.5	0	0	0.3	0.7	0.4	1.9
18/8/2010	0.3	0.7	1.7	0.2	0	10.3	4	0.5	17.7
19/8/2010	18.8	12.2	0.4	0	0	0	0	0	31.4
20/8/2010	0	0	0	0	0	0	0	0	-
21/8/2010	0	0	0	0	0.4	1.8	0	T	2.2
22/8/2010	0	0	8.5	31.9	0	1.9	0	0	42.3
23/8/2010	0	0	0	0.3	0	T	T	0	0.3
24/8/2010	0	0	0	0	0	0	0	0	-
25/8/2010	0.6	24.5	3.5	1.6	T	0	0	0.5	30.7
26/8/2010	T	0	T	0	0	0	6.3	0.4	6.7
27/8/2010	0	0	0	0	0	0	0	0	-
28/8/2010	0	0	0	0	0.4	3.3	0	0	3.7
29/8/2010	0	0	9.4	30	0.3	0	0	6.5	46.2
30/8/2010	0.3	0	0	0.4	0	0	1	0	1.7
31/8/2010	0	0	0	0	T	0.4	T	0.9	1.3
1/9/2010	4.3	0	0	0	0	0	0	0	4.3
2/9/2010	0.7	0	0	0	0	0	0	0.2	0.9
3/9/2010	0	2.6	0	0	0	0	T	0	2.6
4/9/2010	0	0	0	0	0	0	0	0	-
5/9/2010	0	0	0	0	0	0	0	0	-
6/9/2010	0	0	0	0	0	0	0	0	-
7/9/2010	0	0	0	0	0	0	0	0	-
8/9/2010	0	0	0	0	0	0	0	0	-
9/9/2010	7.2	1.4	2	1.1	0.6	0.3	0	0	12.6
10/9/2010	0.2	0.3	0	0	0	0.7	0	0	1.2
11/9/2010	16	7.7	1.3	0	0	0	0	0	25
12/9/2010	0	0	0	0	0	0	T	17.8	17.8
13/9/2010	4.3	1	0	0	0	0	1	6	12.3
14/9/2010	3.6	0.7	0	0	0	0	8.2	19.9	32.4
15/9/2010	1.8	0.2	0.6	0.3	4	1.9	0.7	2.2	11.7
16/9/2010	8.7	1	8	5.6	0	0	0	3	26.3
17/9/2010	0	0	0	0.8	0	0	0	0	0.8
18/9/2010	3.9	0	0.3	0	0	0	0	0	4.2

Appendix Table C2 (Continued)

Time / Date	1:00	4:00	7:00	10:00	13:00	16:00	19:00	22:00	Total
19/9/2010	0	0	0	0	0	0	0	0	-
20/9/2010	0	0	0	0	0	0	0	0	-
21/9/2010	0	0	0	0	0	0	0	0	-
22/9/2010	0	0	0	0	0	0	0	0	-
23/9/2010	2.5	1.7	0	0	0	0	0	8.4	12.6
24/9/2010	6.6	0	0.4	0	0	4.8	2.2	0	14
25/9/2010	0	0	0	0	0	0	0	11.3	11.3
26/9/2010	0	0	0	0	0	0	0.7	0.5	1.2
27/9/2010	0	0	0	0	0	0	T	6.3	6.3
28/9/2010	2.4	0.6	0	0	0	0	0	0	3
29/9/2010	0	0	0	0	0	0	0	0	-
30/9/2010	0	0	0	0	0	0	0	0	-

Appendix Table C3 Rainfall, in millimeter per hour, July - September 2010 at Maehongson station (300201)

Date \ Time	1:00	4:00	7:00	10:00	13:00	16:00	19:00	22:00	Total
1/7/2010	12.5	0	2.2	0	0	0	0	0	14.7
2/7/2010	0	6	0.4	0	4.5	0	0	0	10.9
3/7/2010	0	0	0	0	0	13.2	0.1	4.1	17.4
4/7/2010	8.9	0	0	0	0	1	1.7	0	11.6
5/7/2010	8.3	0.2	0	0	0	0	0	0	8.5
6/7/2010	0	0	0	0	0	0	0	0	-
7/7/2010	0	0	0	0	0	0	0	0	-
8/7/2010	0	0	0	0	0	0	3.4	0	3.4
9/7/2010	0	0	0	0	0	T	42.7	0.6	43.3
10/7/2010	0	0	0	0	0	0	0	0	-
11/7/2010	0	0	0	0	0	0	0	3.6	3.6
12/7/2010	0.7	0	0	0	0	0	0	0	0.7
13/7/2010	0	0	0	0	0	0	4.5	0	4.5
14/7/2010	0	0	0	0	0	0	0	0	-
15/7/2010	6.8	0	0	0	0	0	T	0	6.8
16/7/2010	0	0	0	0	0	0	0	0	-
17/7/2010	0	0	0	0	0	0	0	0	-
18/7/2010	4.2	2.6	0.6	0	T	0.1	2.6	5.5	15.6
19/7/2010	4.3	2.6	1	0.5	0	0.5	0	0.1	9
20/7/2010	0	2	0	0	0	3	0	0	5
21/7/2010	0	0	0	1	0	0	5.9	0	6.9
22/7/2010	0	0	0	0	0.1	0.9	T	T	1
23/7/2010	7.4	0	0	0	0	0.1	0	7.1	14.6
24/7/2010	1.9	3.2	0	0.5	0	1.7	5.8	0.2	13.3
25/7/2010	1	0.1	0.1	0	0.5	0	0.2	0.2	2.1
26/7/2010	0	0	0	0	0	3.1	0.5	0	3.6
27/7/2010	1.1	4.4	0.1	0	0	2	0	1.5	9.1
28/7/2010	0.4	3.2	2.8	0	0	12.7	1.3	0.5	20.9
29/7/2010	0	0	0.5	0	T	8	0.3	44	52.8
30/7/2010	0.5	0.1	T	0.1	0	0	5.4	12.4	18.5
31/7/2010	4.3	0.2	0	0	0	0	0	4.3	8.8
1/8/2010	0.5	1	0.5	0	0	0	0	0	2
2/8/2010	0	0	0	0	0	2.1	0	1.8	3.9
3/8/2010	14.6	0	0.2	2	0.8	0	1.8	2.1	21.5
4/8/2010	0.2	0	0	0	0	T	1.4	0.3	1.9
5/8/2010	1.6	T	0	0	0.2	0	T	1.1	2.9
6/8/2010	0.4	0	0	0	2.3	0.5	T	31.3	34.5
7/8/2010	2.2	0.3	1	0	0	25.3	2.3	0	31.1
8/8/2010	0	0	0	0	0	0	0	0	-

Appendix Table C3 (Continued)

Date \ Time	1:00	4:00	7:00	10:00	13:00	16:00	19:00	22:00	Total
9/8/2010	3.8	0	0	0	0	0	0.1	0	3.9
10/8/2010	0	0	0	0	0	0	0	0	-
11/8/2010	0.4	T	0	0.6	T	T	0.1	11.8	12.9
12/8/2010	4.5	2	1.1	0	T	0	0	2.2	9.8
13/8/2010	4.6	0.1	0.1	0	0	0	0	1	5.8
14/8/2010	1.8	0.2	2.5	0.5	0.1	0	0	0	5.1
15/8/2010	0	0	0	0	0	0	0	1.4	1.4
16/8/2010	0.2	0	0	0	0	0	0	0.4	0.6
17/8/2010	2.3	0	0	0.2	0.1	7	3.6	3	16.2
18/8/2010	2.6	1.4	0.4	0.5	0	0	0	8.8	13.7
19/8/2010	3.3	0	0	0	0	0	0	0	3.3
20/8/2010	0	0	0	0	0	0	0	0	-
21/8/2010	0	0	0	0	0	0.1	0.7	0	0.8
22/8/2010	43	1.2	0.1	0.7	1.2	0	0.1	0.8	47.1
23/8/2010	1.3	0	0	T	0	5.7	0	0	7
24/8/2010	0	0	0	0	0	0	T	1	1
25/8/2010	0	0	0	0.2	T	0	0.1	1.1	1.4
26/8/2010	0.1	T	0	0	0	0	T	0	0.1
27/8/2010	0	0	0	0	0.2	0	0	0	0.2
28/8/2010	0	7.8	87	0.2	1.6	0.6	0	3.9	101.1
29/8/2010	0	2.4	1.8	1.4	1.6	9.8	1.8	5.3	24.1
30/8/2010	0.5	0	0	0	0	0	18.3	1	19.8
31/8/2010	0	0	0.1	0.1	0	0	0	0	0.2
1/9/2010	0	0	0	0	0	0	0	0.8	0.8
2/9/2010	4.5	0	0	0	0	2	T	0	6.5
3/9/2010	0	0	0	0	T	0.3	0.1	0	0.4
4/9/2010	0	0	0	0	0	0	0	0	-
5/9/2010	0	0	0	0	0	0	0	0	-
6/9/2010	0	0	0	0	0	0	T	0	T
7/9/2010	0	0	0	0	0	0	0	0	-
8/9/2010	0	0	0	0	0	0	0	T	T
9/9/2010	0.9	2.5	0.5	7.1	0.9	0.5	0	0	12.4
10/9/2010	0	0	1	2.3	1.6	0	0	2.5	7.4
11/9/2010	5.5	5	0.5	0	0	T	0	3.1	14.1
12/9/2010	0.3	0	0	0	0.4	1.2	3.8	0.4	6.1
13/9/2010	2	0.4	T	0	T	0.3	0.7	0.5	3.9
14/9/2010	0	0	0	0	0	0	0.2	0.4	0.6
15/9/2010	2.8	0.2	0.2	1.2	0	0	1.2	0.1	5.7
16/9/2010	0.1	0	0	0	0	0	0	0.7	0.8
17/9/2010	29.9	5.8	0.6	0.2	0	0	T	T	36.5
18/9/2010	0	0	0.2	0	0	0.4	2.7	0.1	3.4

Appendix Table C3 (Continued)

Time / Date	1:00	4:00	7:00	10:00	13:00	16:00	19:00	22:00	Total
19/9/2010	0	0	0	0	0	0	0	0	-
20/9/2010	0	0	0	0	0	0	0	0	-
21/9/2010	0	0	0	0	0	0	1.7	0.5	2.2
22/9/2010	0	0	T	0.1	0	0	0	0.5	0.6
23/9/2010	0	0	0	0	0	0	0	0	-
24/9/2010	0	0	1	T	0.1	2.5	7.2	1	11.8
25/9/2010	0	0	0	0	0	0	0	20.7	20.7
26/9/2010	2.3	0	0	0	0	0	0	2.5	4.8
27/9/2010	2.8	0	0	0	0	0	0	8	10.8
28/9/2010	8.6	2.9	0	0	0	0	4.1	0.9	16.5
29/9/2010	0	0.3	0	0.2	0	0	0	0	0.5
30/9/2010	0	0	0	T	0	0	0	1.6	1.6

Appendix Table C4 Rainfall, in millimeter per hour, July - September 2010 at Maesariang station, Maehongson (300202)

Time / Date	1:00	4:00	7:00	10:00	13:00	16:00	19:00	22:00	Total
1/7/2010	0	0	0	0	0	0	2.5	0.5	3
2/7/2010	0	0.3	8.5	0.3	0	0	0	0	9.1
3/7/2010	0	0	0	0	T	4.4	0.1	1.4	5.9
4/7/2010	0	0	0	0	0	7.8	0	33.8	41.6
5/7/2010	0.9	0	0	0	0	3.4	0	0	4.3
6/7/2010	0	0	0	0	0	0	0	0	-
7/7/2010	0	0	0	0	0	0	0	0	-
8/7/2010	0	0	0	0	0	0	0	0	-
9/7/2010	0	0	0	0	4.4	0	24.4	2.5	31.3
10/7/2010	0	0	0	0	0	0	0	0	-
11/7/2010	0	0	0	0	0	0	5.2	0.3	5.5
12/7/2010	0	0	0	0	0.2	1.8	0	0	2
13/7/2010	0	0	0	0	0	0	2.2	0	2.2
14/7/2010	0	0	0	0	0	0	0.2	14.8	15
15/7/2010	0	0	1.6	0	0	0	0	0	1.6
16/7/2010	9	1.7	0	0	0	0	0	0	10.7
17/7/2010	0	0	0	0	0	0	0	0	-
18/7/2010	0	0.4	1.5	0	0.3	0.2	0	0	2.4
19/7/2010	0	0.3	0.8	0	0	0	1	0	2.1
20/7/2010	0	0.2	0	0	0	T	1.2	0	1.4
21/7/2010	0	0	0	0	0.4	0	0	0	0.4
22/7/2010	0	0	0	0.2	2.2	3	1.8	1.2	8.4
23/7/2010	0	0	0	0	0.2	18.6	0	6.4	25.2
24/7/2010	2.3	0	0	0	2.7	0	20	2	27
25/7/2010	3.3	0	0	3.2	0	0.7	0	0	7.2
26/7/2010	1.9	0	0	0	0	0	0	0	1.9
27/7/2010	0	1	0	0	0	0	2.5	2.3	5.8
28/7/2010	0.3	1.8	0	0	0	4	0.4	0.4	6.9
29/7/2010	4	0	0	0	0	0	1.5	0	5.5
30/7/2010	0	0	1	0	0	0	4.5	4.2	9.7
31/7/2010	0	0	0	0	0	0	0	0	-
1/8/2010	0	0	0	0	0	0	0	0	-
2/8/2010	0	0	0	0	0	0.9	0	0.6	1.5
3/8/2010	0	0	0	0	0	0	0	2	2
4/8/2010	0	0	1.2	1.3	0	5	0.3	1.6	9.4
5/8/2010	0	0	0	0	0	0	0	0	-
6/8/2010	0	0	0	0.2	0	0	16.3	5	21.5
7/8/2010	0	0	0	0.6	T	0	0	0	0.6
8/8/2010	0	0	0	0	0	0.7	0	0	0.7

Appendix Table C4 (Continued)

Time / Date	1:00	4:00	7:00	10:00	13:00	16:00	19:00	22:00	Total
9/8/2010	0	0	0	0	0	0	0	0	-
10/8/2010	0	0	0	0	0	0	0	0.8	0.8
11/8/2010	2	1.8	1	0	0.2	0	2.1	0	7.1
12/8/2010	0	0	0.3	0	8	0	0	0.1	8.4
13/8/2010	0.1	1.8	0	0	0	0	0	0	1.9
14/8/2010	0.9	1.9	4.5	2	0.3	0	T	0	9.6
15/8/2010	0	0	0	0	0	0	0	0	-
16/8/2010	0	0	0	0	0.5	16.8	7.8	0	25.1
17/8/2010	0	0.4	0.4	1.8	0	1.7	0.2	T	4.5
18/8/2010	0.3	0	0.2	0	0	0	13.5	9.5	23.5
19/8/2010	1	0.3	0	0	0	0	0	0	1.3
20/8/2010	0	0	0	0	0	0	0	0	-
21/8/2010	0	2.2	0	0	0	0	0	0	2.2
22/8/2010	0	4.4	10	1.6	0	0	13.6	46.2	75.8
23/8/2010	1.4	0	0	0	0	0	3	0	4.4
24/8/2010	0	0	0	0	0	0	0	0.8	0.8
25/8/2010	1	1.8	1	0	T	1.4	0	0	5.2
26/8/2010	0	0.2	T	0.2	0	0.4	0	0	0.8
27/8/2010	0	0	0	0	0	0	0	0	-
28/8/2010	0	T	0.4	0	0	1	6.8	0.2	8.4
29/8/2010	T	0	0	0	0	0.4	0.8	0.4	1.6
30/8/2010	0.6	0	0	0	0	1.8	0	0	2.4
31/8/2010	0	0	0	0.4	0	11.8	3.6	0	15.8
1/9/2010	0	0	0	0	0	0	26	10.6	36.6
2/9/2010	0	0	0	0	0	0	9.2	0.4	9.6
3/9/2010	0	2.4	0	0	0	0	0.1	8.9	11.4
4/9/2010	0.9	0	0	0	0	0	0.4	0	1.3
5/9/2010	0	0	0	0	0	3.8	0	0	3.8
6/9/2010	0	0	0.5	0	0	0	0	0	0.5
7/9/2010	0.2	0	0	0	0	0	0	0	0.2
8/9/2010	0	0	0	0	0	0	0	2	2
9/9/2010	0	0	20.5	4.2	0	0	0	0	24.7
10/9/2010	0	0	0	0	0.8	3	0	2	5.8
11/9/2010	37.6	12	0	0	0	3.8	1.6	0	55
12/9/2010	0	0	0.4	0	0	0	0	T	0.4
13/9/2010	0.6	0	0	0	0.2	0	0	1	1.8
14/9/2010	0.2	2.6	0.4	0.2	0	0	0	0	3.4
15/9/2010	0	0	0	0	0	9.8	5.2	0	15
16/9/2010	0	0	0	0	0	0	1.4	9	10.4
17/9/2010	22.8	5	0	0	0	0	0	0	27.8
18/9/2010	0	0	0	0	0	0	0	0.2	0.2

Appendix Table C4 (Continued)

Time / Date	1:00	4:00	7:00	10:00	13:00	16:00	19:00	22:00	Total
19/9/2010	5.6	0	0	0	0	0	0.6	0	6.2
20/9/2010	0	0	0	0	0	0	0	9.7	9.7
21/9/2010	0.8	0	0	0	0	0	14.4	5.2	20.4
22/9/2010	0	0	0	0	0	0	0	0	-
23/9/2010	0	0	0	0	0	0	0	0.3	0.3
24/9/2010	0	0	0	0	0	0	0	0	-
25/9/2010	0	0	0	0	0	0	5.3	0	5.3
26/9/2010	0	0	0	0	0	0	0.3	1.1	1.4
27/9/2010	0	0	0	0	0	1	0	0.1	1.1
28/9/2010	0.5	0	0	0	0	0	0	0	0.5
29/9/2010	0	0	0	0	0	0	24.8	0	24.8
30/9/2010	0	0	0	0	0	0	4.7	0	4.7

Appendix Table C5 Rainfall, in millimeter per hour, July - September 2010 at Lamphun station (329201)

Date \ Time	1:00	4:00	7:00	10:00	13:00	16:00	19:00	22:00	Total
1/7/2010	0	0	2	0	0	0	0	0	2
2/7/2010	0	0	0	0	0	0	0	0	-
3/7/2010	0	0	0	0	0.2	0	0	0	0.2
4/7/2010	0.1	0	0	0	0	0	0	0	0.1
5/7/2010	0	0	0	0	0	0	0	0	-
6/7/2010	0	0	0	0	0	0	12.1	4.9	17
7/7/2010	0.2	0	0	0	0	0	0	0	0.2
8/7/2010	0	0	0	0	0	0	0	0	-
9/7/2010	0	0	0	0	0	0	0	0	-
10/7/2010	0	0	0	0	0	0	8.2	1.2	9.4
11/7/2010	0	0	0	0	0	0	0	0	-
12/7/2010	0	0	0	0	0	0	0	0	-
13/7/2010	0	0	0	0	0	0	0	0	-
14/7/2010	0	12.2	39.3	0	0	0	T	1.5	53
15/7/2010	T	0	0	0	0	0	0	0	T
16/7/2010	0	0	0	0	0	0	0	0	-
17/7/2010	0	0	0	0	0	0	0	0.2	0.2
18/7/2010	0.1	0	0	0	0	1.1	1.2	0.1	2.5
19/7/2010	0.1	0	0	0	0	0	0	3.8	3.9
20/7/2010	6.3	0	0	0	0	0	1.2	0.4	7.9
21/7/2010	0	0	0	0	0	0	0	0	-
22/7/2010	0	0	0	0	0	0.8	0	0	0.8
23/7/2010	0	0	0	0	0	0	0	0	-
24/7/2010	0	0	0	0.9	0	0	1.4	0	2.3
25/7/2010	0.5	0	0	0	0	0	0	0	0.5
26/7/2010	0	0	0	0	0	0.2	2.4	0	2.6
27/7/2010	0	0	0	0	0	2.6	0.8	1.8	5.2
28/7/2010	0	0	0	0	0.4	1.5	0.9	1.7	4.5
29/7/2010	15.4	0.9	0	0	0	0.3	0	0.1	16.7
30/7/2010	0.3	0	0	0	T	0	0	0	0.3
31/7/2010	0	0	0	0	0	0	0	0	-
1/8/2010	0	0	0	0	0	0	0	0	-
2/8/2010	0	0	0	0	0	0	0	0	-
3/8/2010	0	0	11.8	3.6	0.4	0	10.2	35.5	61.5
4/8/2010	3	0.6	2.3	0.1	0	0	0	2.9	8.9
5/8/2010	0.4	0	0	0	0	0	0	0.4	0.8
6/8/2010	0.3	0	0	T	0.5	T	0	0	0.8
7/8/2010	0	T	5.6	23.8	0.4	0	19.6	2.3	51.7
8/8/2010	0	0	0	0	0	0	0	0	-

Appendix Table C5 (Continued)

Time / Date	1:00	4:00	7:00	10:00	13:00	16:00	19:00	22:00	Total
9/8/2010	0	0	0	0	0	0	0	0	-
10/8/2010	0	0	0	25.4	0.3	12.3	3.9	5.2	47.1
11/8/2010	1.2	0.1	0	0	0	0	0	62.5	63.8
12/8/2010	3.3	0	0	0	0	5.5	T	4.7	13.5
13/8/2010	0	0	0	0	0	0	0	2.8	2.8
14/8/2010	44.8	14.7	10.6	0	0	0	0	0	70.1
15/8/2010	0	0	0	0	0	0	0	0	-
16/8/2010	0	0	0	0	0	0	0	0	-
17/8/2010	0	0	0	0	0	0	0	0.4	0.4
18/8/2010	0.6	1.3	0.2	0	0	0.6	53.3	1.5	57.5
19/8/2010	12.9	2.3	0	0	0	0	0	0	15.2
20/8/2010	0	0	0	0	0	0	0	0	-
21/8/2010	3.5	0	0	0	2.7	0.2	0	0	6.4
22/8/2010	0	0	31.2	12	0	0.4	2.7	0	46.3
23/8/2010	0	0	0.6	3.7	0	6.3	0	0	10.6
24/8/2010	0	0	0	0	0	0	0	0	-
25/8/2010	35.4	7.8	0.6	0.7	T	0.1	0	0.1	44.7
26/8/2010	0	0	0	0	0	0	0	0.8	0.8
27/8/2010	1.8	0.4	0	0	0	0	0	0	2.2
28/8/2010	0	0	0	0	0	8.3	0.4	T	8.7
29/8/2010	0	0	0	8.5	1.5	0	0	0	10
30/8/2010	1.6	0	0	0	0	0	0	0	1.6
31/8/2010	0	0	0	0	0	0	0	15.8	15.8
1/9/2010	5.9	0	0	0	0	0	0	0	5.9
2/9/2010	0	0	0	0	1.2	0	0	0.4	1.6
3/9/2010	0	0	0	0	0	0	0	0	-
4/9/2010	0	0	0	0	0	0	0	0.4	0.4
5/9/2010	0	0	0	0	0	0	0	0	-
6/9/2010	0	0	0	0	0	0	0	0	-
7/9/2010	0	0	0	0	0	0	0	0	-
8/9/2010	0	0	0	0	0	0	0	0	-
9/9/2010	25.6	0.2	0	0.8	T	0	0	0	26.6
10/9/2010	0	0.2	0.1	0	0	0	0	0	0.3
11/9/2010	0	9.2	0	0	0	T	1.5	1	11.7
12/9/2010	0	0	0	0	0	0	0	81.5	81.5
13/9/2010	4.6	0.8	0	0	0	0	38.8	12.9	57.1
14/9/2010	2.4	0	0	0	T	0	0	3.6	6
15/9/2010	0.6	0.4	T	0.3	2	0.2	0.3	2.3	6.1
16/9/2010	5.4	2.8	2.6	0.1	0	0	0	0	10.9
17/9/2010	0	0	0	0	0	0	0	0	-
18/9/2010	0	0	0	0	0	0	0	0	-

Appendix Table C5 (Continued)

Time / Date	1:00	4:00	7:00	10:00	13:00	16:00	19:00	22:00	Total
19/9/2010	0	0	0	0	0	0	0	0	-
20/9/2010	0	0	0	0	0	0	0	0	-
21/9/2010	0	0	0	0	0	0.8	0	0	0.8
22/9/2010	0	0	0	0	0	0	0	0	-
23/9/2010	0	0	0	0	0	0	T	1.3	1.3
24/9/2010	1	0	0	0	0	0	0.6	0	1.6
25/9/2010	0	0	0	0	0	0	0	2.3	2.3
26/9/2010	0.2	0	0	0	0	0	T	0.5	0.7
27/9/2010	0.2	0	0	0	0	0	21.8	6.2	28.2
28/9/2010	4.8	0	0	0	0	0	0	0	4.8
29/9/2010	0	0	0	0	0	0	0	1.8	1.8
30/9/2010	0.2	0	0	0	0	0	0	0	0.2

Appendix Table C6 Rainfall, in millimeter per hour,July - September 2010 at Bhumibol Dam station, Tak (376203)

Time / Date	1:00	4:00	7:00	10:00	13:00	16:00	19:00	22:00	Total
1/7/2010	0	0	1.2	0	0	0	9.8	1.3	12.3
2/7/2010	0	0	7	20.8	0.1	0	0	0	27.9
3/7/2010	0	0	0	4.7	0	0	0.4	15.2	20.3
4/7/2010	4.8	0.1	0	0	0	0	0	0	4.9
5/7/2010	0	0	0	0	0	0	0	0	-
6/7/2010	0	0	0	0	0	0	0	0	-
7/7/2010	0	0	0	0	0	0	0	0	-
8/7/2010	0	0	0	0	0	0	0	0	-
9/7/2010	0	0	0	0	0	0	0	0	-
10/7/2010	0	0	0	0	0	0	0	0	-
11/7/2010	0	0	0	0	0	0	0	0	-
12/7/2010	0	0	0	0	0	0	0	0	-
13/7/2010	0	0	0	0	0	0	0	5.8	5.8
14/7/2010	0.6	0	0	0	0	0	0	0.2	0.8
15/7/2010	0	0	0	0	0	0	0	7.2	7.2
16/7/2010	T	0	0	0	0	0	0	0	T
17/7/2010	0	0	0	0	0	0	0	0	-
18/7/2010	0	0	0	0	0	0.3	0	0.1	0.4
19/7/2010	0.7	2.6	0.3	T	0	T	34.1	T	37.7
20/7/2010	0	0	0	0	0	0.5	17.5	T	18
21/7/2010	0	0	0	0	T	T	0	0	0
22/7/2010	0	0	0	0	0	0	T	0.2	0.2
23/7/2010	0	0	0	0	0	0	0	0.8	0.8
24/7/2010	0.4	5.5	5.6	0.5	T	0	0	0	12
25/7/2010	0	0	0	0	0	0	0	0	-
26/7/2010	0	0	0	0	0	0	0	0	-
27/7/2010	0	0	0	0	0	2.2	T	0	2.2
28/7/2010	0	3	1.7	0	0	0	0	2	6.7
29/7/2010	1.4	0.4	0.4	0	0.2	0	0	0	2.4
30/7/2010	0	0	2	6.2	0	0	0	0	8.2
31/7/2010	0	0	0	0	0	0	0	0	-
1/8/2010	0	0	0	0	0	0	0	0	-
2/8/2010	0	0	0	0	T	0.2	0	0.2	0.4
3/8/2010	1.4	0	0	0.3	0	0	0	0	1.7
4/8/2010	0.1	0.3	1	0.1	T	0	T	0	1.5
5/8/2010	0	0	0	0	0	0	0	0	-
6/8/2010	0	0	0	0	T	0.5	0.5	0.1	1.1
7/8/2010	0	0	0	0	0	0	0	0	-
8/8/2010	0	0	0	0	0	0	0	0	-

Appendix Table C6 (Continued)

Time / Date	1:00	4:00	7:00	10:00	13:00	16:00	19:00	22:00	Total
9/8/2010	0	0	0	0	0	0	0	0	-
10/8/2010	0	0	0	0	0	0	0	0	-
11/8/2010	0	0	0	0	0	0	0	0	-
12/8/2010	4.1	1.6	0.2	0.1	0.1	12.8	3.2	0	22.1
13/8/2010	0.1	T	0	0	0	0.4	T	1.9	2.4
14/8/2010	9	2.2	0.2	0	0	0	0	0	11.4
15/8/2010	0	0	0	0	T	0	0	0	T
16/8/2010	0	0	0	0	0	0	0	0	-
17/8/2010	0	0	0.5	T	T	T	0	0	0.5
18/8/2010	0	0	0	0	0	0	1	35	36
19/8/2010	12.5	3.6	0	0	0	0	0	0	16.1
20/8/2010	0	0	0	0	0	0	0	0	-
21/8/2010	0	0	0.1	0.7	0.6	0	0	0	1.4
22/8/2010	0	T	10	1.8	0	0	0	0	11.8
23/8/2010	0	0	0	0	0	T	0	0	T
24/8/2010	0	0	0	0	0	0	0	0	-
25/8/2010	0	2.1	2.9	0.1	T	T	T	T	5.1
26/8/2010	0	0	0	0	0	0	0	0	-
27/8/2010	0	0	0	0	0	0	0	0	-
28/8/2010	0	0	0	0	0	0	0.4	3.6	4
29/8/2010	1.2	0	0.3	T	0	0	0	0	1.5
30/8/2010	0	0	0	0	0	0	0	0	-
31/8/2010	0	0	0	0	0	0.6	0	0	0.6
1/9/2010	0	0	0	0	0	0	6	0	6
2/9/2010	0	0	0	0	0	0	0	T	T
3/9/2010	T	0	9.6	0	0	0	0	0	9.6
4/9/2010	0	0	0	0	0	0	0	0	-
5/9/2010	0	0	0	0	0	0	0	0	-
6/9/2010	0	0	0	0	0	0	0	0	-
7/9/2010	0	0	0	0	0	0	0	0	-
8/9/2010	0	0	0	0	0	0	T	0	T
9/9/2010	0	0.2	1.2	T	T	0	1.8	T	3.2
10/9/2010	T	T	0.2	0	0.1	0	0	1.2	1.5
11/9/2010	4.5	0.6	0.2	0	0	1.6	0.2	0.1	7.2
12/9/2010	0.8	0	0	0	0	0	0	0	0.8
13/9/2010	0	0	0	0	0.6	T	0.1	6.3	7
14/9/2010	T	T	0.2	0	0	0	0	0	0.2
15/9/2010	0	0	0.2	T	0.5	T	0.2	T	0.9
16/9/2010	T	T	0.5	T	0.5	0	1.1	0	2.1
17/9/2010	0	0	0	0	0	0	0	0.2	0.2
18/9/2010	0	0	0	0	0	0	1.3	0.5	1.8

Appendix Table C6 (Continued)

Time / Date	1:00	4:00	7:00	10:00	13:00	16:00	19:00	22:00	Total
19/9/2010	0	0	0.5	9.5	0	0	0	0	10
20/9/2010	0	0	0	0	0	0	0	0	-
21/9/2010	0	0	0	0	0	26.8	0	0	26.8
22/9/2010	0	0	0	0	0	0	19.3	T	19.3
23/9/2010	0	0	0	0	0	T	0	0	T
24/9/2010	0	0	0	0	0.3	0	7.6	0	7.9
25/9/2010	0	0	0	0	T	0	0	0	T
26/9/2010	0	0	0	0	0	0	2.7	T	2.7
27/9/2010	0	0	0	1.4	1.6	0	0	2.6	5.6
28/9/2010	0	0	0	0	0	0	2.9	0	2.9
29/9/2010	0	0	0	0	1.3	1.5	0	0	2.8
30/9/2010	0	0	0	0	0	0	0	0	-

Appendix Table C7 Rainfall, in millimeter per hour, July - September 2010 at Tern station, Lampang (328202)

Date \ Time	1:00	4:00	7:00	10:00	13:00	16:00	19:00	22:00	Total
1/7/2010	-	-	7.6	0.2	0	0	0	-	7.8
2/7/2010	-	-	4.2	6.7	0.1	0	0	-	11
3/7/2010	-	-	1.2	0	0	3	7.6	-	11.8
4/7/2010	-	-	7	0	0	0	0	-	7
5/7/2010	-	-	2.1	0	0	0	0	-	2.1
6/7/2010	-	-	0	0	0	0	0	-	-
7/7/2010	-	-	0	0	0	0	0	-	-
8/7/2010	-	-	0	0	0	0	0	-	-
9/7/2010	-	-	8.5	0	0	0	0	-	8.5
10/7/2010	-	-	0	0	0	0	2.5	-	2.5
11/7/2010	-	-	0	0	0	0	0	-	-
12/7/2010	-	-	0	0	0	0	5.8	-	5.8
13/7/2010	-	-	0	0	0	0	0	-	-
14/7/2010	-	-	15.1	0	0	0	4.2	-	19.3
15/7/2010	-	-	2.5	0	0	4.3	0	-	6.8
16/7/2010	-	-	0	0	0	0	0	-	-
17/7/2010	-	-	0	0	0	0	0	-	-
18/7/2010	-	-	0	0	0	0	T	-	T
19/7/2010	-	-	1.3	0	0	0	33.5	-	34.8
20/7/2010	-	-	8.4	0	0	0	0.6	-	9
21/7/2010	-	-	1.7	0.1	0	0	0	-	1.8
22/7/2010	-	-	0	0	0	0	0	-	-
23/7/2010	-	-	0	0	0	0	3	-	3
24/7/2010	-	-	0	0	0	0	0	-	-
25/7/2010	-	-	0	0	0	0	0	-	-
26/7/2010	-	-	0	0	0	0	0	-	-
27/7/2010	-	-	0	0	0	0	0	-	-
28/7/2010	-	-	3.7	0	0	0.6	3.1	-	7.4
29/7/2010	-	-	26.5	0	0	0	0.7	-	27.2
30/7/2010	-	-	0	0	0	5.5	0.1	-	5.6
31/7/2010	-	-	0	0	0	0	0	-	-
1/8/2010	-	-	0	0	0	0	0	-	-
2/8/2010	-	-	0	0	23.5	0	0	-	23.5
3/8/2010	-	-	2	2.5	0	0	0	-	4.5
4/8/2010	-	-	9.7	0	0	0	0	-	9.7
5/8/2010	-	-	0	0	0	1.5	1.2	-	2.7
6/8/2010	-	-	0	0	0.5	0	0	-	0.5
7/8/2010	-	-	2.9	0	0	1.4	0	-	4.3
8/8/2010	-	-	0	0	0	0.2	0.3	-	0.5

Appendix Table C7 (Continued)

Time / Date	1:00	4:00	7:00	10:00	13:00	16:00	19:00	22:00	Total
9/8/2010	-	-	0	0	0	0	0	-	-
10/8/2010	-	-	0.6	0	0	0	0	-	0.6
11/8/2010	-	-	4.7	0	0	0	0	-	4.7
12/8/2010	-	-	19.6	0	2.8	0	0	-	22.4
13/8/2010	-	-	0	0	0	0	0	-	-
14/8/2010	-	-	5.1	0	0	0	0	-	5.1
15/8/2010	-	-	0	0	0	0	0	-	-
16/8/2010	-	-	0	0	0	0	0	-	-
17/8/2010	-	-	3.1	0.1	0	0	0	-	3.2
18/8/2010	-	-	3.8	0.4	0	0	0	-	4.2
19/8/2010	-	-	31.6	0	0	0	0	-	31.6
20/8/2010	-	-	0	0	0	0	0	-	-
21/8/2010	-	-	0	2.4	27.3	0	0	-	29.7
22/8/2010	-	-	126.8	0	0	1.1	3.2	-	131.1
23/8/2010	-	-	5.5	0.2	0	T	0	-	5.7
24/8/2010	-	-	0	0	0	0	0	-	-
25/8/2010	-	-	8.5	1.1	0.2	2.8	0.5	-	13.1
26/8/2010	-	-	0.8	0.1	0	0	0	-	0.9
27/8/2010	-	-	0	0	0	0	0	-	-
28/8/2010	-	-	0	0	0	3.7	6.1	-	9.8
29/8/2010	-	-	15.9	0	0	0	0	-	15.9
30/8/2010	-	-	0	0	0	0	0	-	-
31/8/2010	-	-	0	0	0	0	0	-	-
1/9/2010	-	-	4	0	0	1.7	6.9	-	12.6
2/9/2010	-	-	2.5	0	0.6	1	0	-	4.1
3/9/2010	-	-	36.3	0	0	0	0	-	36.3
4/9/2010	-	-	0	0	0	0	0	-	-
5/9/2010	-	-	0	0	0	0	0	-	-
6/9/2010	-	-	0	0	0	0	0	-	-
7/9/2010	-	-	0	0	0	0	0	-	-
8/9/2010	-	-	0	0	0	0	0	-	-
9/9/2010	-	-	33.9	0	0	25.5	2	-	61.4
10/9/2010	-	-	0	0	0	0	18.4	-	18.4
11/9/2010	-	-	19.1	0	0	0	0	-	19.1
12/9/2010	-	-	31.6	0.1	0	0	0	-	31.7
13/9/2010	-	-	0	0	0	0	8	-	8
14/9/2010	-	-	11.8	0	0.4	0	0	-	12.2
15/9/2010	-	-	0.7	0.2	0	0	0	-	0.9
16/9/2010	-	-	1.1	0	0	0	0	-	1.1
17/9/2010	-	-	2.1	0	0	0	0	-	2.1
18/9/2010	-	-	6.1	2.6	0	13	0	-	21.7

Appendix Table C7 (Continued)

Time / Date	1:00	4:00	7:00	10:00	13:00	16:00	19:00	22:00	Total
19/9/2010	-	-	0	0	0	0	0	-	-
20/9/2010	-	-	0	0	0	0	0	-	-
21/9/2010	-	-	0	0	0	0	0	-	-
22/9/2010	-	-	0	0	0	0	0	-	-
23/9/2010	-	-	3.9	0	0	0	3.5	-	7.4
24/9/2010	-	-	3.1	0	0	0	0	-	3.1
25/9/2010	-	-	0	0	0	0	0	-	-
26/9/2010	-	-	0	0	0	0	0	-	-
27/9/2010	-	-	14.1	0	0	0	0	-	14.1
28/9/2010	-	-	1.8	0	0	7.6	0	-	9.4
29/9/2010	-	-	0	0	0	5.6	0.2	-	5.8
30/9/2010	-	-	0	0	0	0	0.5	-	0.5

Appendix Table C8 Rainfall, in millimeter per hour, July - September 2010 at Lampang station (328201)

Date \ Time	1:00	4:00	7:00	10:00	13:00	16:00	19:00	22:00	Total
1/7/2010	0	1.2	5.7	1.7	0	0	0	0	8.6
2/7/2010	0	0	0	0	0	0	0	0	-
3/7/2010	0	0	0	0	0	0	0	0.8	0.8
4/7/2010	2.1	0	0	0	0	0	0	0	2.1
5/7/2010	0	0	0	0	0	0	0	0	-
6/7/2010	0	0	0	0	0	0	0	0	-
7/7/2010	0	0	0	0	0	0	0	0	-
8/7/2010	0	0	0	0	0	0	0	0	-
9/7/2010	7.4	0.4	0	0	0	0	0	0	7.8
10/7/2010	0	0	0	0	0	0	0	0	-
11/7/2010	0	0	0	0	0	0	0	0	-
12/7/2010	0	0	0	0	0	0	0	0	-
13/7/2010	0	0	0	0	0	0	0	0	-
14/7/2010	0	0	0	2.5	0	0	0	0	2.5
15/7/2010	0	0	0	0	1.8	0	0	0	1.8
16/7/2010	0	0.6	0	0	0	0	0	0	0.6
17/7/2010	0	0	0	0	0	0	0	0	-
18/7/2010	0	0	0	0	0.2	0.8	12.5	2	15.5
19/7/2010	0	2.5	0	0	0	0.2	0	10	12.7
20/7/2010	2.2	T	0.3	0	0	0	2	1.2	5.7
21/7/2010	1.2	0	0	0	0	0	0	0	1.2
22/7/2010	0	0	0	0	0	0	0	0	-
23/7/2010	0	0	0	0	0	0	0	0	-
24/7/2010	0	0	0	0	0	8.2	1.5	0	9.7
25/7/2010	0	0	0	0	0	0	0	0	-
26/7/2010	0	0	0	0	0	0	0	0	-
27/7/2010	0	0	0	0	0	2.7	0.3	3.4	6.4
28/7/2010	0	0	0	2.5	T	5	0	1.4	8.9
29/7/2010	15.5	1.3	0.2	0	0	0	0	1.2	18.2
30/7/2010	0	0	0	0	0	0	0	0	-
31/7/2010	0	0	0	0	0	0	0	0	-
1/8/2010	1.3	2.6	0	0	0	0	0	0	3.9
2/8/2010	0	0	T	0	0.5	2.2	3	0	5.7
3/8/2010	0	3.8	12.2	2	0.5	0	0	2.1	20.6
4/8/2010	0.3	0	0	0	0	0	0	0.5	0.8
5/8/2010	0.4	0	0	0	0	0	8.3	2.2	10.9
6/8/2010	0.5	1.5	0	3.2	4.7	0	0	0	9.9
7/8/2010	0	0	0	0	0	0	0	0	-
8/8/2010	0	0	0	0	0	1.2	0	0	1.2

Appendix Table C8 (Continued)

Time / Date	1:00	4:00	7:00	10:00	13:00	16:00	19:00	22:00	Total
9/8/2010	0	0	0	0	0	0	0	0	-
10/8/2010	0.8	1.7	0.3	0.1	T	0	0.2	21.5	24.6
11/8/2010	0.3	0	0	0	0	0	0	0	0.3
12/8/2010	0	2	0	0	0	0	0	4	6
13/8/2010	0	0	0	0	0	0	0	0.2	0.2
14/8/2010	13.3	6.8	0	0	0	0	0	0	20.1
15/8/2010	0.4	0	0	0	0	0	0	0	0.4
16/8/2010	0	0	0	0	0	0	0	0	-
17/8/2010	0	0	0	0.8	0.3	0	0	0	1.1
18/8/2010	0	0	0	0	0	0	0	0	-
19/8/2010	2	15.8	0.1	0	0	0	0	0	17.9
20/8/2010	0	0	0	0	0	0	0	0	-
21/8/2010	0	0	0	2.9	7	0	0	0.5	10.4
22/8/2010	1	14.5	0	0.6	0	0	0	0	16.1
23/8/2010	0	1.5	0.7	0	0.4	8	0	0	10.6
24/8/2010	0	0	0	0	0	0	1.2	0	1.2
25/8/2010	9.6	0.8	1.7	3.5	2.5	0.2	0	0	18.3
26/8/2010	0	0	0.9	0	0	0	0.6	2	3.5
27/8/2010	3.4	2.8	0	0	0	0	0	0	6.2
28/8/2010	0	0	0	0	1.8	12.2	T	0.2	14.2
29/8/2010	0	0	2	12.4	3.5	0	15.3	0	33.2
30/8/2010	0	0	0	0.2	0	0	13.8	0	14
31/8/2010	0	0	0	0	0	0	0	32.3	32.3
1/9/2010	1.9	0	0	0	0	3.7	0	0	5.6
2/9/2010	0	0	0	0	0	0	0	0	-
3/9/2010	0	0	0	0	0	0	0	0	-
4/9/2010	0	0	0	0	0	0	0	0	-
5/9/2010	0	0	0	0	0	0	0	0	-
6/9/2010	0	0	0	0	0	0	0	0	-
7/9/2010	0	0	0	0	0	0	0	0	-
8/9/2010	0	0	0	0	0	0	0	0	-
9/9/2010	0	2	2.4	0.2	0	0	0	0	4.6
10/9/2010	0	0	0	0	0	0	0.2	0	0.2
11/9/2010	0	3	3	0	12.8	0	0	0	18.8
12/9/2010	3.3	0	0	0	0	0	0	0	3.3
13/9/2010	0	0	0	0	0	0	25.8	7	32.8
14/9/2010	0	0	0	0	2	1.9	0	0	3.9
15/9/2010	2.8	1.4	2.5	1.9	3	0.1	0	0	11.7
16/9/2010	2	0.4	0.5	0	0	0	0.5	0.7	4.1
17/9/2010	0.3	0.1	0	0	0	0	0	0	0.4
18/9/2010	0	0	0	0	0	0	0	0	-

Appendix Table C8 (Continued)

Time / Date	1:00	4:00	7:00	10:00	13:00	16:00	19:00	22:00	Total
19/9/2010	0	0	0	0	0	0	0	0	-
20/9/2010	0	0	0	0	0	0	0	0	-
21/9/2010	0	0	0	0	0	0	0	0	-
22/9/2010	0	0	0	0	0	0	0	0	-
23/9/2010	0	0	0	0	0	0	0	0	-
24/9/2010	0	0	0.3	0.1	0	0	1.5	0	1.9
25/9/2010	0	0	0	0	0	0	4.4	0	4.4
26/9/2010	0	0	0	0	0	0	18.5	11	29.5
27/9/2010	2.5	0.2	T	0.2	0	0	0	0	2.9
28/9/2010	0	0.4	0	0	0	0	0	0	0.4
29/9/2010	0	0	0	0	0	0	0	0	-
30/9/2010	0	0	0	0	0	0	0	0	-

Appendix D

Runoff Data at P.1, P.5, P21, P.24A, P67, P.21, P.73, P.75, P85, P.87 and P.92 Stations

Appendix Table D1 Discharge, in cubic meter per second, at P.1 Station from April 1st, 2010 to March 31st, 2011

Date	Apr	May	Jun	Jul	Aug	Sep	Oct	Nov	Dec	Jan	Feb	Mar
1	2.92	2.00	8.60	13.00	72.00	167.5	127.4	84.00	27.50	8.60	7.40	8.60
2	2.92	2.30	9.20	43.10	52.20	158.0	104.4	73.50	23.60	8.60	8.60	9.80
3	2.40	2.70	13.00	40.50	58.70	131.0	90.00	66.00	19.00	9.80	8.60	9.80
4	2.10	2.00	19.00	39.20	88.50	104.4	76.50	54.80	17.00	8.60	8.00	8.60
5	2.50	1.24	21.00	31.40	91.60	87.00	70.50	52.20	16.00	9.20	8.60	7.40
6	2.40	5.60	13.00	22.30	78.00	70.50	67.50	53.50	15.00	9.20	8.00	5.60
7	2.30	20.00	9.80	23.60	67.50	54.80	57.40	50.90	18.00	8.60	6.80	7.40
8	2.20	18.00	8.60	24.90	70.50	47.00	67.50	50.90	16.00	9.20	7.40	8.00
9	2.20	12.00	13.00	26.20	50.90	50.90	84.00	49.60	15.00	7.40	6.80	8.00
10	2.30	11.00	18.00	23.60	49.60	87.00	72.00	49.60	15.00	8.00	6.20	8.60
11	3.16	14.00	18.00	17.00	64.50	99.60	64.50	45.70	13.00	12.00	4.60	9.80
12	2.92	16.00	21.00	16.00	129.2	178.9	60.00	44.40	15.00	14.00	5.00	11.00
13	2.92	18.00	26.20	14.00	190.3	240.1	60.00	40.50	16.00	12.00	4.60	12.00
14	3.04	19.00	23.60	11.00	221.2	192.2	64.50	39.20	14.00	11.00	4.60	11.00
15	2.70	21.00	19.00	19.00	194.1	196.0	72.00	41.80	14.00	10.40	4.60	13.00
16	2.60	21.00	14.00	24.90	127.4	257.3	75.00	44.40	14.00	9.20	4.60	17.00
17	2.70	20.00	13.00	16.00	88.50	370.2	76.50	39.20	16.00	8.00	4.20	31.40
18	2.70	19.00	13.00	10.40	85.50	367.8	58.70	37.90	21.00	7.40	4.20	37.90
19	2.60	16.00	14.00	12.00	102.8	294.8	57.40	47.00	17.00	8.00	3.80	30.10
20	2.50	18.00	14.00	23.60	96.40	200.2	114.0	52.20	16.00	10.40	3.80	19.00
21	2.30	18.00	14.00	32.70	64.50	171.3	177.0	50.90	14.00	6.20	3.40	17.00
22	2.30	20.00	19.00	24.90	129.2	150.8	167.5	49.60	13.00	5.60	3.40	19.00
23	2.10	20.00	23.60	20.00	190.3	132.8	132.8	35.30	11.00	6.20	3.00	17.00
24	1.90	15.00	21.00	19.00	221.2	149.0	107.6	35.30	12.00	6.80	3.80	15.00
25	1.80	14.00	18.00	22.30	194.1	147.2	87.00	41.80	11.00	6.80	5.60	16.00
26	2.50	15.00	15.00	26.20	127.4	129.2	75.00	39.20	10.40	6.80	7.40	15.00
27	2.10	9.80	15.00	35.30	88.50	132.8	87.00	36.60	10.40	6.20	8.00	17.00
28	2.20	9.20	13.00	64.50	85.50	270.2	88.50	34.00	10.40	5.00	8.60	17.00
29	2.30	6.80	11.00	53.50	102.8	292.5	88.50	32.70	9.80	5.00		17.00
30	2.10	7.40	9.80	54.80	96.40	192.2	114.0	34.00	9.20	9.20		16.00
31		8.60		93.20	158.0		117.2		8.60	7.40		16.00
Total	73.68	402.6	468.4	898.1	3437	5123	2761.	1406	457.9	260.8	163.6	456.00
Mean	2.46	12.99	15.61	28.97	110.8	170.7	89.09	46.89	14.77	8.41	5.84	14.71
Max	3.16	21.00	26.20	93.20	221.2	370.2	177.0	84.00	27.50	14.00	8.60	37.90
Min	1.80	1.24	8.60	10.40	49.60	47.00	57.40	32.70	8.60	5.00	3.00	5.60

Appendix Table D2 Discharge, in cubic meter per second, at P.5 Station from April 1st, 2010 to March 31st, 2011

Date	Apr	May	Jun	Jul	Aug	Sep	Oct	Nov	Dec	Jan	Feb	Mar
1	1.40	0.69	1.44	1.52	13.00	80.63	42.70	23.78	2.87	0.68	1.19	0.62
2	1.44	0.78	1.50	1.52	15.95	77.13	30.60	20.12	2.68	0.64	1.31	0.64
3	1.54	1.08	1.50	1.52	16.54	60.25	22.56	20.12	2.30	0.76	1.10	0.52
4	1.54	1.54	1.52	1.50	18.90	41.10	16.54	15.36	2.03	0.80	1.10	0.36
5	1.58	1.60	1.56	1.48	20.12	23.17	14.77	14.77	1.37	0.80	1.19	0.40
6	1.60	1.60	1.60	1.44	21.95	15.36	14.18	14.18	1.22	0.80	1.16	0.39
7	1.50	1.58	1.58	1.54	32.75	9.76	13.00	12.46	1.22	0.80	0.89	0.30
8	1.46	1.52	1.54	1.54	39.50	8.68	13.59	10.30	1.37	0.78	0.68	0.09
9	1.48	1.40	1.50	1.54	38.75	14.18	14.77	9.76	1.25	0.64	0.68	0.28
10	1.44	1.40	1.52	1.54	32.00	21.34	15.95	7.60	1.25	0.86	0.92	0.52
11	1.40	1.38	1.50	1.54	35.00	48.00	17.72	7.60	1.22	1.10	0.98	0.76
12	1.34	1.28	1.54	1.54	50.50	76.55	19.51	6.58	1.31	0.80	1.49	1.10
13	1.20	1.11	1.52	1.56	59.70	112.8	25.00	5.90	1.49	0.86	2.21	0.83
14	1.20	1.05	1.44	1.58	103.7	142.9	32.00	5.22	4.20	0.83	1.07	0.68
15	1.20	1.08	1.42	1.54	118.0	144.3	32.75	7.26	4.20	0.98	0.74	0.64
16	1.20	1.24	1.50	1.54	89.38	149.0	33.50	6.92	5.56	1.13	0.64	0.98
17	1.11	1.40	1.46	1.54	55.00	145.6	32.00	7.60	4.54	0.70	0.58	7.60
18	0.85	1.40	1.48	1.54	44.30	120.0	27.10	7.60	6.24	0.58	0.50	11.92
19	0.96	1.40	1.52	1.52	78.28	81.88	25.00	8.14	6.24	0.68	0.48	13.59
20	1.24	1.48	1.52	7.26	83.75	51.00	44.30	8.68	5.22	1.22	0.54	14.18
21	1.16	1.48	1.50	7.60	57.50	29.90	95.00	7.26	4.20	1.76	0.39	10.84
22	0.98	1.50	1.56	7.60	53.50	23.78	106.3	9.22	4.88	1.49	0.36	9.76
23	0.67	1.42	1.56	8.14	98.12	17.13	80.63	10.30	3.25	1.31	0.52	6.24
24	0.71	1.46	1.54	9.76	110.8	28.50	57.00	9.22	3.25	1.13	0.64	1.52
25	1.05	1.46	1.54	8.14	147.7	33.50	33.50	8.68	1.58	0.70	0.80	1.48
26	1.17	1.46	1.50	10.30	106.9	35.75	27.80	8.14	1.22	0.66	0.72	1.50
27	0.98	1.44	1.50	10.84	63.55	42.70	21.95	8.68	1.40	0.56	0.56	1.22
28	0.78	1.42	1.50	13.00	43.50	65.20	17.13	7.26	0.98	0.58	0.54	1.26
29	0.74	1.48	1.54	14.18	49.00	83.13	21.95	6.92	0.74	0.62		1.40
30	0.71	1.50	1.54	13.00	91.25	60.25	30.60	6.58	0.86	0.76		1.42
31		1.50		12.46	90.63		29.90		1.16	1.19		1.46
Total	35.63	42.13	45.44	151.3	1879	1843	1009	302.2	81.30	27.20	23.98	94.50
Mean	1.19	1.36	1.51	4.88	60.63	61.46	32.56	10.07	2.62	0.88	0.86	3.05
Max	1.60	1.60	1.60	14.18	147.7	149.0	106.3	23.78	6.24	1.76	2.21	14.18
Min	0.67	0.69	1.42	1.44	13.00	8.68	13.00	5.22	0.74	0.56	0.36	0.09

Appendix Table D3 Discharge, in cubic meter per second, at P.21 Station from April 1st, 2010 to March 31st, 2011

Date	Apr	May	Jun	Jul	Aug	Sep	Oct	Nov	Dec	Jan	Feb	Mar
1	0.68	0.26	2.90	2.90	6.87	34.53	5.20	6.12	2.34	0.80	0.41	0.12
2	0.50	1.31	7.12	7.12	6.63	17.30	4.28	4.62	1.80	0.98	0.41	0.08
3	0.50	2.52	4.04	4.04	6.00	6.87	3.81	4.62	1.66	1.31	0.38	0.10
4	0.47	1.24	3.00	3.00	16.76	5.89	3.93	5.77	1.59	1.04	0.44	0.12
5	0.44	0.68	1.98	1.98	13.32	3.70	3.93	5.31	1.52	0.74	0.41	0.18
6	0.47	0.47	1.31	1.31	8.64	3.20	3.40	4.39	1.45	0.74	0.38	0.18
7	0.41	0.41	1.17	1.17	6.12	3.20	3.10	4.16	1.45	0.74	0.35	0.12
8	0.41	0.38	1.04	1.04	5.20	3.81	5.31	4.28	1.45	0.68	0.26	0.12
9	0.35	0.29	0.80	0.80	3.10	4.16	4.85	4.04	1.45	0.68	0.20	0.10
10	0.35	0.26	0.68	0.68	2.70	5.54	6.63	3.40	1.45	0.80	0.23	0.12
11	0.38	0.29	0.50	0.50	8.00	7.00	5.08	3.20	1.45	1.04	0.23	0.14
12	0.35	0.23	0.47	0.47	20.00	6.75	4.50	3.00	1.52	1.59	0.20	0.14
13	0.35	0.20	0.50	0.50	16.22	11.26	5.66	2.90	1.59	1.17	0.16	0.10
14	0.35	0.26	0.50	0.50	11.72	13.48	9.66	3.00	1.38	1.04	0.18	0.10
15	0.35	0.29	0.50	0.50	9.37	11.26	7.87	2.80	1.17	0.98	0.10	0.14
16	0.35	0.29	0.50	0.50	5.08	21.40	7.25	3.20	1.04	0.92	0.10	0.41
17	0.38	0.26	0.50	0.50	3.81	31.00	6.50	3.10	1.04	0.74	0.10	3.40
18	0.32	0.29	0.47	0.47	4.85	27.40	6.00	2.43	1.52	0.50	0.10	7.25
19	0.29	0.29	0.62	0.62	7.63	12.84	7.12	2.43	1.38	0.80	0.10	4.16
20	0.29	0.29	1.59	1.59	7.12	7.87	17.84	2.34	1.04	0.68	0.08	1.66
21	0.29	0.26	0.26	1.80	5.31	7.25	29.20	2.34	0.80	0.50	0.08	1.10
22	0.26	0.56	0.50	1.10	11.40	7.12	16.22	2.25	0.56	0.50	0.10	0.74
23	0.16	0.86	0.47	0.80	16.22	6.12	9.23	2.25	0.62	0.47	0.10	0.68
24	0.16	0.35	0.98	0.74	8.13	9.81	8.64	1.89	1.04	0.35	0.14	0.56
25	0.16	0.29	1.45	0.86	5.20	9.37	7.12	1.98	0.80	0.35	0.56	0.62
26	0.14	0.32	1.52	1.31	5.66	10.10	6.87	1.89	0.68	0.32	0.80	0.62
27	0.23	0.32	0.92	2.52	8.50	14.60	7.38	1.89	0.62	0.35	0.86	0.62
28	0.32	0.35	0.68	3.60	5.66	21.60	6.00	1.89	0.50	0.35	0.50	0.62
29	0.26	0.29	0.62	5.54	12.52	11.72	6.37	1.89	0.56	0.41		0.56
30	0.23	0.23	0.74	6.63	25.86	6.50	8.25	1.89	0.56	0.44		0.74
31		0.26		11.88	24.13		7.63		0.68	0.62		0.62
Total	10.20	14.60	38.33	66.97	297.7	342.6	234.8	95.27	36.71	22.63	7.96	26.22
Mean	0.34	0.47	1.28	2.16	9.60	11.42	7.58	3.18	1.18	0.73	0.28	0.85
Max	0.68	2.52	7.12	11.88	25.86	34.53	29.20	6.12	2.34	1.59	0.86	7.25
Min	0.14	0.20	0.26	0.47	2.70	3.20	3.10	1.89	0.50	0.32	0.08	0.08

Appendix Table D4 Discharge, in cubic meter per second, at P.24A Station from April 1st, 2010 to March 31st, 2011

Date	Apr	May	Jun	Jul	Aug	Sep	Oct	Nov	Dec	Jan	Feb	Mar
1	0.38	0.84	0.40	0.40	1.50	5.90	4.05	5.20	2.25	0.38	0.32	0.24
2	0.36	0.95	0.36	0.40	0.95	6.95	4.67	4.85	2.10	0.38	0.30	0.26
3	0.34	2.10	0.34	0.51	0.73	5.20	5.90	4.50	1.50	0.36	0.32	0.24
4	0.34	1.65	5.38	0.73	1.06	4.67	3.15	4.67	1.17	0.34	0.32	0.26
5	0.26	1.28	2.70	0.62	0.73	3.75	2.70	4.50	1.06	0.36	0.32	0.26
6	0.34	0.73	1.06	0.84	0.84	2.40	2.40	4.20	0.95	0.36	0.30	0.26
7	0.62	0.62	0.40	1.06	2.55	1.50	6.60	3.60	1.28	0.36	0.28	0.26
8	1.50	0.40	0.36	1.28	4.20	1.39	12.85	3.30	0.95	0.36	0.28	0.24
9	1.28	0.40	0.36	0.95	1.50	3.90	5.90	3.00	0.51	0.36	0.28	0.24
10	1.17	0.62	0.36	1.65	2.10	2.25	8.00	3.00	0.62	0.36	0.28	0.24
11	1.06	0.40	0.40	0.40	2.70	4.50	4.05	3.00	0.73	0.62	0.26	0.38
12	1.06	0.36	0.38	0.36	1.17	7.65	3.15	3.45	1.50	1.06	0.28	0.32
13	0.95	0.36	0.51	0.32	2.70	5.20	5.90	3.75	1.50	0.95	0.28	0.40
14	0.84	0.38	0.38	0.34	8.19	6.43	34.94	3.45	0.73	0.62	0.28	0.36
15	0.73	0.34	0.36	0.84	4.05	5.38	18.52	3.45	0.62	0.40	0.28	0.34
16	1.06	0.36	0.36	0.40	2.25	15.16	15.16	3.45	1.17	0.62	0.28	0.95
17	0.95	0.40	0.36	0.34	1.17	30.35	8.76	3.45	1.39	0.51	0.28	3.00
18	0.73	0.38	0.36	0.36	2.55	15.37	12.43	3.60	1.65	0.34	0.28	8.19
19	0.51	0.40	0.40	0.51	4.50	10.47	28.92	3.30	1.50	0.34	0.28	22.85
20	1.06	0.36	0.51	4.20	4.50	6.60	114.6	3.15	1.95	0.34	0.28	11.42
21	0.95	0.34	0.40	1.95	5.55	8.38	127.5	3.15	1.80	0.34	0.24	0.51
22	0.84	0.32	0.62	0.51	6.60	7.65	46.63	3.00	1.50	0.34	0.22	0.36
23	0.62	0.30	1.28	0.62	11.23	8.38	23.12	3.00	1.50	0.34	0.24	0.32
24	0.73	0.28	5.38	1.80	5.02	18.10	16.84	2.85	1.06	0.34	0.24	0.36
25	0.84	0.38	1.39	4.05	3.30	8.38	12.43	2.70	0.51	0.34	0.24	0.32
26	0.95	0.38	0.51	1.50	4.20	5.72	10.09	2.70	0.40	0.34	0.24	0.36
27	1.28	0.40	0.40	1.50	4.85	6.25	8.76	2.70	0.40	0.34	0.24	0.62
28	0.95	0.38	0.36	4.35	3.75	13.69	6.25	2.70	0.40	0.32	0.24	0.95
29	0.40	0.36	0.36	3.45	8.38	5.90	6.07	2.55	0.40	0.32		0.34
30	0.62	0.34	0.34	3.15	10.85	4.85	6.43	2.40	0.40	0.32		0.34
31		0.38		1.80	5.55		5.55		0.40	0.32		0.32
Total	23.72	17.19	26.78	41.19	119.2	232.3	572.4	102.6	33.90	13.08	7.68	55.51
Mean	0.79	0.55	0.89	1.33	3.85	7.74	18.47	3.42	1.09	0.42	0.27	1.79
Max	1.50	2.10	5.38	4.35	11.23	30.35	127.5	5.20	2.25	1.06	0.32	22.85
Min	0.26	0.28	0.34	0.32	0.73	1.39	2.40	2.40	0.40	0.32	0.22	0.24

Appendix Table D5 Discharge, in cubic meter per second, at P.67 Station from April 1st, 2010 to March 31st, 2011

Date	Apr	May	Jun	Jul	Aug	Sep	Oct	Nov	Dec	Jan	Feb	Mar
1	18.25	11.00	9.75	12.25	44.00	154.0	113.2	61.35	23.60	10.00	8.25	7.75
2	18.60	12.25	9.75	32.00	27.65	141.1	91.60	58.75	17.90	10.25	7.50	8.50
3	18.25	11.00	12.25	24.05	32.00	118.6	78.00	50.30	18.25	10.00	7.50	8.25
4	18.95	7.25	14.75	17.55	59.40	90.00	68.50	40.00	15.45	9.75	6.75	8.00
5	18.95	8.00	12.50	15.10	64.60	70.45	60.70	39.50	14.75	9.50	6.00	8.00
6	18.25	14.05	10.75	15.10	54.20	53.55	49.00	41.50	14.05	8.50	5.50	8.00
7	17.90	15.45	10.25	16.15	52.25	40.00	46.50	40.00	14.05	9.00	5.50	7.75
8	17.90	12.75	11.25	17.20	42.50	30.00	52.90	39.00	14.05	8.75	5.00	8.50
9	17.90	11.50	12.50	14.75	33.00	42.00	70.45	39.00	13.35	9.25	4.75	9.25
10	18.95	11.75	14.40	12.25	43.00	70.45	55.50	38.00	13.00	9.00	4.25	9.25
11	20.45	13.00	14.40	11.00	43.00	98.80	45.50	35.50	13.00	10.00	4.00	10.00
12	21.35	14.05	16.15	11.50	102.0	221.0	42.50	34.50	13.00	12.25	4.75	10.00
13	21.35	15.80	18.95	9.50	200.8	198.4	46.00	33.50	13.70	12.50	4.25	10.25
14	22.70	15.80	14.75	9.50	186.4	180.7	45.50	36.00	13.70	10.75	4.00	11.25
15	23.15	15.80	12.75	15.10	182.9	176.3	53.55	35.50	13.35	10.25	4.50	12.25
16	23.60	15.80	12.00	16.15	113.2	230.1	56.15	34.50	13.00	9.75	4.00	15.45
17	23.60	14.40	12.75	10.75	76.50	330.8	52.25	31.50	15.10	8.50	4.00	19.65
18	22.25	14.05	13.70	9.00	75.75	283.3	41.50	33.00	16.15	8.00	4.25	17.20
19	18.95	16.15	13.70	11.50	86.25	241.2	45.50	42.50	13.00	7.25	4.25	14.05
20	18.25	15.45	14.40	14.40	73.05	180.7	102.8	44.00	11.00	6.75	3.50	11.50
21	17.90	17.20	14.40	16.50	62.00	154.0	130.3	43.50	11.00	7.00	3.25	14.05
22	17.20	17.55	18.60	13.00	95.60	133.0	131.2	38.00	10.75	7.75	3.75	14.75
23	15.80	14.75	22.70	12.25	124.0	134.8	105.2	25.40	10.00	8.00	3.50	14.05
24	13.35	14.40	14.40	11.75	173.0	130.3	78.00	30.00	10.00	8.25	4.50	13.35
25	11.50	13.35	12.50	11.25	116.8	124.9	64.60	32.00	10.00	7.50	5.75	12.50
26	12.00	12.00	12.50	11.25	142.0	115.0	56.15	29.00	10.25	6.00	6.50	13.00
27	12.50	10.50	11.00	18.95	144.0	164.2	71.75	28.55	10.00	6.00	6.75	14.05
28	12.50	8.50	10.75	44.50	83.25	281.8	69.80	28.10	10.00	5.75	7.00	14.40
29	12.25	8.50	9.75	35.00	87.75	222.3	65.90	28.55	9.75	6.25		14.40
30	12.00	9.50	9.50	59.40	145.0	154.0	88.50	27.65	9.75	6.50		14.05
31		10.00		71.10	149.0		79.50		10.00	7.75		14.05
Total	536.5	401.5	397.8	599.7	2914	4565	2158	1118	404.9	266.7	143.5	367.50
Mean	17.89	12.95	13.26	19.35	94.03	152.2	69.63	37.29	13.06	8.60	5.13	11.85
Max	23.60	17.55	22.70	71.10	200.8	330.8	131.2	61.35	23.60	12.50	8.25	19.65
Min	11.50	7.25	9.50	9.00	27.65	30.00	41.50	25.40	9.75	5.75	3.25	7.75

Appendix Table D6 Discharge, in cubic meter per second, at P.71 Station from April 1st, 2010 to March 31st, 2011

Date	Apr	May	Jun	Jul	Aug	Sep	Oct	Nov	Dec	Jan	Feb	Mar
1	-	-	1.28	0.20	6.80	36.38	17.85	21.70	6.80	4.59	4.17	0.50
2	-	-	1.68	0.56	5.17	39.75	13.31	21.15	7.50	4.59	2.70	0.49
3	-	-	1.68	0.96	8.26	32.15	11.70	23.08	9.40	4.59	3.00	0.49
4	-	-	1.36	1.52	36.70	17.03	10.09	21.43	9.40	5.03	3.00	0.49
5	-	-	1.68	2.80	9.02	10.55	8.83	17.85	9.21	6.28	2.90	0.48
6	-	-	3.39	4.30	20.33	7.50	7.33	17.58	8.64	6.10	2.50	0.43
7	-	-	2.20	5.17	9.40	6.63	7.33	16.75	8.07	6.45	2.20	0.46
8	-	-	1.02	5.03	5.61	11.70	7.15	15.93	7.50	6.28	0.84	0.49
9	-	-	0.60	4.17	8.45	26.30	7.33	15.10	7.50	6.10	0.60	0.49
10	-	-	0.84	4.45	10.32	15.65	11.24	14.28	7.50	6.10	0.60	0.50
11	-	-	1.02	5.75	13.77	14.00	11.24	13.54	7.50	6.28	0.40	0.49
12	-	-	1.84	5.17	29.23	23.08	11.47	12.85	7.50	6.28	0.40	0.52
13	-	-	5.61	3.39	49.88	41.50	14.55	12.16	7.50	6.28	0.40	0.52
14	-	-	1.20	2.90	46.13	63.90	37.35	13.08	7.50	6.45	0.40	0.53
15	-	-	0.84	12.62	30.85	75.75	33.78	13.77	7.33	6.45	0.55	0.52
16	-	-	0.84	5.61	11.24	65.60	40.45	12.16	7.50	6.45	0.57	0.56
17	-	-	0.84	6.80	9.21	104.8	20.60	11.24	7.33	6.63	0.57	8.26
18	-	-	0.84	2.60	10.09	115.1	17.03	12.16	7.15	6.98	0.57	17.58
19	-	-	0.84	2.40	30.53	43.60	29.23	12.39	7.15	6.10	0.57	11.47
20	-	-	0.72	7.15	22.53	39.75	109.2	11.70	6.98	5.75	0.57	10.09
21	-	-	0.28	7.69	7.15	58.90	217.8	11.70	6.80	5.75	0.57	5.46
22	-	-	0.36	4.04	27.28	31.18	207.1	11.24	6.80	5.75	0.53	0.63
23	-	-	2.20	3.65	53.30	21.98	138.6	11.24	6.80	5.75	0.52	0.60
24	-	-	9.86	3.00	33.13	42.20	76.65	11.01	6.10	5.75	0.49	0.62
25	-	-	3.65	4.04	24.73	34.10	46.88	8.64	5.46	5.75	0.49	0.57
26	-	-	2.70	3.65	21.43	35.08	35.08	9.02	4.74	5.61	0.49	0.57
27	-	-	1.44	3.26	34.10	34.75	29.55	9.02	5.32	5.17	0.49	0.60
28	-	-	0.84	3.39	17.03	36.05	26.95	9.40	5.61	5.46	0.49	0.63
29	-	-	0.56	4.74	53.30	17.58	25.33	8.45	5.46	5.46		0.66
30	-	-	0.18	11.47	86.40	19.50	24.18	6.45	5.17	4.88		0.70
31	-	-		16.20	51.75		23.35		4.74	4.30		0.72
Total	-	-	52.39	148.6	783.1	1122	1278	406.0	217.9	179.3	31.58	67.12
Mean	-	-	1.75	4.80	25.26	37.40	41.25	13.54	7.03	5.79	1.13	2.17
Max	-	-	9.86	16.20	86.40	115.1	217.8	23.08	9.40	6.98	4.17	17.58
Min	-	-	0.18	0.20	5.17	6.63	7.15	6.45	4.74	4.30	0.40	0.43

Appendix Table D7 Discharge, in cubic meter per second, at P.73 Station from April 1st, 2010 to March 31st, 2011

Date	Apr	May	Jun	Jul	Aug	Sep	Oct	Nov	Dec	Jan	Feb	Mar
1	6.20	0.47	0.70	3.60	190.5	577.2	444.0	295.2	78.00	18.15	7.00	5.80
2	8.20	0.60	0.47	9.00	207.5	575.0	319.3	241.5	76.60	18.15	7.00	4.65
3	3.60	0.90	0.35	51.40	118.6	480.0	257.2	210.9	72.40	18.15	7.40	7.80
4	6.20	1.00	0.44	55.60	141.0	390.0	219.4	182.0	65.40	16.05	8.20	19.20
5	3.25	3.60	3.25	40.20	231.3	300.8	193.9	159.6	57.00	15.00	27.60	31.80
6	1.20	6.20	3.95	28.65	209.2	229.6	167.6	158.0	55.60	13.20	13.80	38.80
7	1.40	5.00	2.90	28.65	187.1	169.2	154.8	151.6	54.20	13.20	5.80	14.40
8	2.90	3.95	0.50	20.25	251.8	121.5	158.0	141.0	51.40	13.20	5.80	11.40
9	3.25	1.00	2.90	16.05	231.3	129.0	177.2	138.0	45.80	12.00	7.40	7.80
10	3.25	0.47	3.60	15.00	180.4	187.1	219.4	136.5	45.80	17.10	12.60	7.00
11	3.25	0.41	3.25	11.40	175.6	241.5	187.1	133.5	43.00	11.40	6.60	8.20
12	2.55	0.20	4.30	6.60	259.0	345.2	162.8	124.5	43.00	20.25	3.95	7.40
13	1.10	0.18	3.95	5.00	422.0	462.0	161.2	117.2	43.00	21.30	3.95	7.80
14	0.80	0.60	8.20	4.30	559.6	603.6	262.6	107.4	38.80	22.35	3.95	9.00
15	1.00	1.20	10.80	7.80	688.5	651.7	345.2	106.0	38.80	19.20	3.95	17.10
16	5.00	0.35	8.20	21.30	546.4	775.5	362.0	103.2	37.40	14.40	3.95	28.65
17	5.80	0.32	5.80	31.80	343.3	959.8	326.7	107.4	37.40	13.20	3.95	66.80
18	6.20	0.44	3.95	25.50	282.4	933.8	287.8	104.6	40.20	12.60	3.60	99.00
19	6.20	7.00	2.55	7.00	348.9	825.5	269.8	101.8	55.60	9.60	3.25	92.00
20	5.40	5.80	2.55	9.00	516.0	660.9	486.0	106.0	59.80	8.60	3.60	76.60
21	4.30	2.20	2.90	43.00	382.0	510.0	1163	118.6	57.00	8.60	2.90	48.60
22	1.85	1.00	3.60	54.20	347.0	430.0	1384	121.5	47.20	8.60	5.40	43.00
23	3.95	1.85	7.40	36.00	621.8	328.5	1372	115.8	44.40	8.60	7.00	43.00
24	3.95	2.55	29.70	29.70	628.7	358.1	1060	103.2	37.40	8.60	7.00	32.85
25	1.85	1.85	26.55	32.85	559.6	352.6	644.8	103.2	37.40	8.60	7.00	20.25
26	1.40	1.85	20.25	37.40	402.0	350.7	474.0	96.20	34.95	7.80	7.00	20.25
27	1.20	2.20	23.40	41.60	510.0	354.4	394.0	87.80	31.80	5.40	6.20	23.40
28	0.50	3.25	5.40	45.80	472.0	496.0	341.5	85.00	23.40	5.00	6.20	26.55
29	0.60	2.55	4.30	90.60	450.0	660.9	311.9	83.60	20.25	7.00		26.55
30	0.50	1.40	5.40	107.4	586.0	546.4	310.0	79.40	18.15	7.00		28.65
31		1.00		106.0	667.8		317.4		18.15	6.60		25.50
Total	96.85	61.39	201.5	1022	11717	14006	12935	3920	1409	388.9	192.0	899.80
Mean	3.23	1.98	6.72	32.99	377.9	466.8	417.2	130.6	45.46	12.55	6.86	29.03
Max	8.20	7.00	29.70	107.4	688.5	959.8	1384	295.2	78.00	22.35	27.60	99.00
Min	0.50	0.18	0.35	3.60	118.6	121.5	154.8	79.40	18.15	5.00	2.90	4.65

Appendix Table D8 Discharge, in cubic meter per second, at P.75 Station from April 1st, 2010 to March 31st, 2011

Date	Apr	May	Jun	Jul	Aug	Sep	Oct	Nov	Dec	Jan	Feb	Mar
1	18.36	17.00	7.15	3.55	30.35	82.37	25.34	50.74	13.10	13.70	8.25	12.80
2	15.80	18.36	6.60	7.42	21.42	64.92	45.20	40.70	12.80	13.40	7.98	13.10
3	8.80	14.90	6.60	7.42	22.78	62.78	42.05	38.14	12.50	11.30	7.98	13.40
4	6.88	7.15	6.88	4.52	40.25	55.10	42.05	36.48	12.50	7.98	7.70	12.80
5	6.88	8.80	5.11	3.75	37.31	38.97	48.80	35.23	12.20	7.98	7.42	12.80
6	6.60	13.40	0.87	3.16	43.40	26.11	33.16	33.99	12.20	7.98	7.42	12.50
7	6.33	9.35	1.60	3.94	39.80	22.78	31.12	33.16	11.90	7.70	7.15	12.80
8	6.60	4.92	5.77	4.72	31.91	20.74	32.33	33.16	11.60	7.15	7.42	14.90
9	6.33	5.31	6.33	3.94	22.78	32.74	38.14	32.33	11.60	7.15	7.70	15.50
10	9.90	11.60	6.05	4.72	26.88	45.20	33.58	27.65	11.30	7.15	7.42	15.20
11	23.46	21.76	5.50	4.14	26.11	73.15	32.33	20.74	10.45	8.80	7.15	15.20
12	23.12	22.78	5.31	4.92	79.37	115.2	30.73	20.06	10.73	10.73	6.88	14.90
13	23.46	23.12	5.31	3.16	126.3	80.50	29.19	22.10	11.30	9.08	6.60	15.20
14	24.18	22.78	4.92	3.75	98.63	84.87	29.57	29.57	10.73	7.98	6.60	15.80
15	24.18	23.12	5.11	10.45	93.00	86.12	33.16	29.57	10.45	7.70	6.60	17.68
16	23.80	23.12	5.50	7.42	75.42	120.4	39.39	28.81	13.10	7.15	6.88	19.04
17	23.80	15.50	4.14	2.18	54.62	135.5	36.07	28.04	15.50	7.15	6.88	24.18
18	19.04	2.77	1.50	3.16	40.25	108.7	31.50	27.65	10.45	6.88	6.60	18.02
19	8.53	6.05	1.39	5.11	36.48	104.8	34.40	31.12	10.45	6.88	6.60	14.60
20	7.70	6.05	1.50	6.88	31.50	89.25	65.99	47.90	10.18	6.88	6.60	13.40
21	7.70	6.33	1.60	11.30	25.73	78.81	57.53	40.25	9.90	6.88	6.60	22.10
22	4.92	6.05	1.79	8.53	34.82	74.85	59.57	24.18	9.90	6.60	6.88	21.08
23	5.11	4.92	1.99	4.92	57.53	88.00	68.67	15.80	9.35	6.33	8.25	20.74
24	2.18	6.05	2.96	4.33	50.26	92.38	48.35	26.49	9.08	6.05	9.90	19.38
25	9.63	7.98	4.33	4.33	61.71	72.59	39.80	19.72	9.08	6.05	9.90	19.04
26	16.40	12.80	2.96	9.08	99.88	70.89	40.70	14.60	8.53	6.05	9.35	19.38
27	16.70	10.18	2.77	14.60	64.38	74.28	57.53	14.30	8.53	6.05	9.35	19.72
28	17.34	8.53	2.58	20.06	42.95	83.63	55.59	14.00	8.53	8.25	9.35	20.40
29	17.34	8.80	1.99	14.00	49.77	123.0	58.50	14.60	9.08	8.25		18.36
30	17.00	9.08	1.99	22.78	73.72	62.24	63.85	13.40	8.80	8.25		19.72
31		8.80		38.14	69.76		58.50		10.18	8.25		20.06
Total	408.0	367.3	118.1	250.3	1609	2271	1342	844.4	336.0	247.7	213.4	523.80
Mean	13.60	11.85	3.94	8.08	51.91	75.71	43.31	28.15	10.84	7.99	7.62	16.90
Max	24.18	23.12	7.15	38.14	126.3	135.5	68.67	50.74	15.50	13.70	9.90	24.18
Min	2.18	2.77	0.87	2.18	21.42	20.74	25.34	13.40	8.53	6.05	6.60	12.50

Appendix Table D9 Discharge, in cubic meter per second, at P.85 Station from April 1st, 2010 to March 31st, 2011

Date	Apr	May	Jun	Jul	Aug	Sep	Oct	Nov	Dec	Jan	Feb	Mar
1	0.04	0.04	0.02	0.02	0.49	26.00	27.80	14.00	1.09	4.12	1.37	0.63
2	0.04	0.04	0.02	0.02	0.15	7.50	20.60	2.46	1.04	4.34	1.66	0.63
3	0.04	0.04	0.02	0.02	0.15	5.50	8.50	2.11	1.04	4.34	1.85	0.63
4	0.04	0.04	0.02	0.02	0.15	6.00	9.50	2.46	1.04	3.90	1.62	0.63
5	0.04	0.04	0.02	0.03	0.15	14.00	12.00	3.02	1.02	3.90	1.41	0.63
6	0.04	0.04	0.02	0.05	0.15	1.62	8.00	2.20	0.86	3.90	1.41	0.51
7	0.04	0.04	0.02	0.05	0.86	1.18	5.50	1.80	0.81	3.90	1.41	0.33
8	0.04	0.04	0.02	0.05	4.34	1.20	4.34	1.71	0.72	3.68	1.20	0.23
9	0.04	0.04	0.02	0.05	4.56	1.16	4.34	1.64	0.97	3.46	0.95	0.23
10	0.04	0.04	0.02	0.05	4.56	1.27	4.34	1.80	2.46	3.46	1.02	0.28
11	0.04	0.04	0.02	0.05	20.00	1.53	3.90	7.50	1.62	3.46	1.25	2.11
12	0.04	0.04	0.02	0.05	27.80	1.46	2.54	8.50	0.70	3.46	1.46	0.59
13	0.04	0.02	0.02	0.05	42.40	0.97	3.24	8.50	1.76	3.46	1.16	0.63
14	0.04	0.02	0.02	0.05	43.05	1.62	36.55	10.00	2.11	3.46	0.90	0.63
15	0.04	0.03	0.02	0.05	37.85	7.00	60.50	11.00	2.54	3.24	0.85	0.63
16	0.04	0.02	0.02	0.05	22.40	17.00	57.60	8.50	2.63	2.54	0.85	0.63
17	0.04	0.02	0.02	0.05	15.00	13.00	57.60	8.50	4.34	2.46	0.85	0.51
18	0.04	0.02	0.02	0.05	41.10	13.00	37.85	8.50	7.00	2.37	0.85	1.39
19	0.04	0.02	0.02	0.05	73.25	6.50	32.00	8.50	6.50	2.46	0.90	4.84
20	0.04	0.02	0.02	0.05	27.80	3.46	90.87	8.50	7.00	2.20	1.00	6.94
21	0.04	0.02	0.02	0.05	12.00	10.00	321.	8.50	6.00	1.89	0.63	6.10
22	0.04	0.02	0.02	0.05	27.80	9.50	407.2	8.50	5.00	1.57	0.63	5.26
23	0.04	0.02	0.02	0.05	31.40	17.00	321.2	8.50	4.34	1.41	0.59	3.51
24	0.04	0.02	0.02	0.05	47.80	16.00	219.3	3.68	4.34	1.55	0.39	3.26
25	0.04	0.02	0.02	0.05	33.95	18.00	107.5	1.43	4.34	1.85	0.63	3.26
26	0.04	0.02	0.02	0.05	18.00	32.00	69.50	1.37	4.34	1.87	0.55	3.26
27	0.04	0.02	0.02	0.05	2.54	65.75	53.40	1.23	4.34	1.64	0.47	3.26
28	0.04	0.02	0.02	0.05	5.00	49.20	41.75	1.18	3.90	1.25	0.63	3.26
29	0.04	0.02	0.02	0.65	22.40	53.40	29.60	1.18	3.24	1.62		3.26
30	0.04	0.02	0.02	2.46	37.85	45.00	31.40	1.13	2.54	1.80		3.26
31		0.02		1.16	47.80		25.40		2.54	1.73		2.77
Total	1.20	0.87	0.60	5.53	652.7	446.8	2115	157.9	92.17	86.29	28.49	64.09
Mean	0.04	0.03	0.02	0.18	21.06	14.89	68.23	5.26	2.97	2.78	1.02	2.07
Max	0.04	0.04	0.02	2.46	73.25	65.75	407.2	14.00	7.00	4.34	1.85	6.94
Min	0.04	0.02	0.02	0.02	0.15	0.97	2.54	1.13	0.70	1.25	0.39	0.23

Appendix Table D10 Discharge, in cubic meter per second, at P.87 Station from April 1st, 2010 to March 31st, 2011

Date	Apr	May	Jun	Jul	Aug	Sep	Oct	Nov	Dec	Jan	Feb	Mar
1	0.00	0.00	0.00	0.00	0.77	46.90	5.24	1.98	0.10	0.10	0.09	0.08
2	0.00	0.00	0.00	0.00	0.72	16.60	3.10	1.61	0.10	0.10	0.07	0.08
3	0.00	0.00	0.00	0.00	0.72	8.74	2.45	1.19	0.09	0.10	0.07	0.08
4	0.00	0.00	0.00	0.00	2.36	4.66	1.91	1.10	0.07	0.10	0.07	0.08
5	0.00	0.00	0.00	0.00	16.15	2.54	1.46	0.96	0.04	0.10	0.07	0.08
6	0.00	0.00	0.00	0.00	7.48	2.36	0.77	0.96	0.08	0.10	0.07	0.08
7	0.00	0.00	0.00	0.00	8.74	1.91	0.23	0.96	0.04	0.10	0.07	0.08
8	0.00	0.00	0.00	0.00	15.93	1.19	0.09	0.96	0.03	0.10	0.07	0.07
9	0.00	0.00	0.00	0.00	6.50	2.04	0.03	0.96	0.04	0.10	0.08	0.07
10	0.00	0.00	0.00	0.00	5.70	6.39	0.01	1.05	0.09	0.10	0.09	0.07
11	0.00	0.00	0.00	0.00	11.71	7.34	0.01	1.10	0.10	0.10	0.09	0.08
12	0.00	0.00	0.00	0.00	8.60	6.39	0.01	0.96	0.10	0.10	0.09	0.09
13	0.00	0.00	0.00	0.00	16.15	6.50	0.01	1.00	0.10	0.10	0.08	0.10
14	0.00	0.00	0.00	0.00	73.90	20.06	1.51	1.05	0.10	0.10	0.08	0.10
15	0.00	0.00	0.00	0.00	31.68	10.96	2.30	0.91	0.10	0.10	0.08	0.10
16	0.00	0.00	0.00	0.00	11.15	46.90	7.20	0.86	0.10	0.10	0.09	0.13
17	0.00	0.00	0.00	0.00	6.16	43.90	4.31	0.72	0.10	0.10	0.08	0.09
18	0.00	0.00	0.00	0.00	5.12	19.21	2.30	0.72	0.10	0.10	0.08	0.13
19	0.00	0.00	0.00	0.00	42.90	20.92	2.73	0.68	0.10	0.10	0.08	0.10
20	0.00	0.00	0.00	0.00	14.13	12.82	31.26	0.68	0.10	0.10	0.08	0.10
21	0.00	0.00	0.00	0.00	5.81	13.90	86.50	0.72	0.10	0.10	0.08	0.10
22	0.00	0.00	0.00	0.00	48.40	5.93	40.40	0.54	0.10	0.10	0.08	0.10
23	0.00	0.00	0.00	0.00	35.46	4.20	24.90	0.26	0.10	0.10	0.08	0.10
24	0.00	0.00	0.00	0.00	13.67	8.74	10.59	0.23	0.10	0.10	0.08	0.10
25	0.00	0.00	0.00	0.00	22.06	11.52	6.50	0.18	0.10	0.10	0.08	0.09
26	0.00	0.00	0.00	0.00	26.26	9.16	4.78	0.18	0.10	0.10	0.08	0.09
27	0.00	0.00	0.00	0.00	19.21	43.40	3.74	0.18	0.10	0.10	0.08	0.09
28	0.00	0.00	0.00	0.00	13.45	27.96	3.00	0.18	0.10	0.10	0.08	0.09
29	0.00	0.00	0.00	0.00	19.21	11.52	2.45	0.15	0.10	0.10		0.09
30	0.00	0.00	0.00	0.00	31.68	6.64	2.30	0.15	0.10	0.10		0.09
31		0.00		0.04	23.54		2.04		0.10	0.10		0.09
Total	0.00	0.00	0.00	0.04	545.3	431.3	254.1	23.18	2.78	3.10	2.22	2.82
Mean	0.00	0.00	0.00	0.00	17.59	14.38	8.20	0.77	0.09	0.10	0.08	0.09
Max	0.00	0.00	0.00	0.04	73.90	46.90	86.50	1.98	0.10	0.10	0.09	0.13
Min	0.00	0.00	0.00	0.00	0.72	1.19	0.01	0.15	0.03	0.10	0.07	0.07

Appendix Table D11 Discharge, in cubic meter per second, at P.92 Station from April 1st, 2010 to March 31st, 2011

Date	Apr	May	Jun	Jul	Aug	Sep	Oct	Nov	Dec	Jan	Feb	Mar
1	3.92	2.46	3.03	36.30	35.50	73.78	53.63	23.80	10.60	6.60	4.00	3.62
2	3.60	3.22	3.03	26.11	23.08	69.88	52.75	23.80	10.60	6.60	4.00	3.05
3	3.22	3.60	3.03	16.60	63.25	53.63	47.50	25.34	10.60	6.60	4.00	3.05
4	3.22	4.56	3.03	16.60	93.10	46.70	45.10	23.80	10.60	6.60	4.00	3.05
5	3.22	4.24	3.03	16.60	57.13	41.10	39.50	23.80	10.60	6.60	4.00	3.05
6	3.22	3.60	3.22	15.40	42.70	30.73	40.30	22.36	10.60	6.60	4.00	2.67
7	2.84	3.22	3.22	13.00	38.70	27.65	55.38	23.80	10.60	6.60	4.52	2.10
8	3.03	3.22	3.22	10.60	28.42	29.19	72.80	23.80	11.20	6.60	4.00	2.10
9	3.03	3.22	3.22	10.60	23.80	109.4	47.50	20.20	10.60	6.60	4.00	2.29
10	2.65	3.22	3.22	18.04	51.88	46.70	47.50	16.60	10.60	6.60	4.00	2.48
11	1.70	3.22	3.22	18.04	60.63	58.00	43.50	16.60	10.60	6.60	3.81	2.48
12	1.70	3.22	3.22	9.00	95.25	86.65	36.30	16.60	10.60	6.60	3.81	2.29
13	1.70	3.22	3.22	6.60	109.4	126.7	37.90	16.60	10.60	6.60	3.81	2.29
14	1.70	3.22	3.22	6.34	80.60	116.3	33.10	16.60	10.60	6.60	3.81	3.05
15	1.70	3.22	3.41	6.08	87.73	99.55	31.50	16.60	10.60	6.60	3.81	5.04
16	1.70	3.22	3.41	7.00	55.38	135.9	51.00	16.60	10.20	6.60	3.81	9.80
17	1.70	3.22	3.41	7.00	50.13	184.5	29.96	16.60	9.80	6.60	3.81	16.60
18	1.70	3.22	3.41	7.40	61.50	120.9	23.80	16.60	9.40	6.60	3.81	16.60
19	1.70	3.22	3.41	11.80	75.73	77.68	27.65	16.60	9.00	6.60	3.81	6.60
20	1.70	3.22	6.34	10.20	47.50	68.90	69.88	16.60	8.60	6.60	3.81	5.82
21	1.70	3.03	3.22	7.80	44.30	66.95	99.55	16.60	8.60	6.60	3.62	3.81
22	1.70	3.03	3.22	8.60	70.85	65.00	70.85	15.40	8.60	6.60	3.62	3.24
23	1.70	3.03	3.22	9.40	70.85	63.25	57.13	12.40	8.60	6.60	3.62	2.67
24	1.89	3.03	3.22	9.40	75.73	58.88	44.30	10.60	8.60	6.34	3.62	2.10
25	1.70	3.03	3.22	10.20	68.90	50.13	37.10	10.60	8.60	5.82	3.62	2.10
26	1.70	3.03	3.22	20.20	50.13	50.13	38.70	10.60	8.60	5.56	3.62	2.67
27	1.70	3.03	3.41	53.63	43.50	119.8	44.30	10.60	8.60	5.04	3.62	4.00
28	1.70	3.03	7.80	70.85	31.50	232.8	40.30	10.60	7.80	4.52	3.62	4.78
29	1.70	2.84	11.20	84.50	36.30	67.93	48.38	10.60	6.60	4.26		4.52
30	1.70	2.84	20.20	75.73	54.50	49.25	45.90	10.60	6.60	4.00		4.26
31		2.84		40.30	73.78		32.30		6.60	4.00		4.00
Total	66.14	99.52	129.4	659.9	1801	2428	1445	511.9	294.4	191.3	107.5	136.18
Mean	2.20	3.21	4.32	21.29	58.12	80.94	46.62	17.06	9.50	6.17	3.84	4.39
Max	3.92	4.56	20.20	84.50	109.4	232.8	99.55	25.34	11.20	6.60	4.52	16.60
Min	1.70	2.46	3.03	6.08	23.08	27.65	23.80	10.60	6.60	4.00	3.62	2.10

CIRRICULUM VITAE

NAME : Miss Atchara Komsai

BIRTH DATE : October 27, 1984

BIRTH PLACE : Lampang, Thailand

EDUCATION :

YEAR	**INSTITUTE**	**DEGREE/DIPLOMA**
2006	Chiang Mai Univ.	B.Sc.(Biotechnology)

POSITION/TITLE : Technical Service Representative III

WORK PLACE : Nalco Industrial Service (Thailand) Co., Ltd.